Electron Probe Micro-Analysis

Nilanjan Chatterjee, Ph.D.
Principal Research Scientist

Electron Microprobe Facility
Department of Earth, Atmospheric and Planetary Sciences
Massachusetts Institute of Technology

Uses of the EPMA

Spot mode operation **for quantitative analysis:**

- Micron-scale, complete chemical analysis

  Be to U (10-50 ppm under favorable conditions)

Raster mode operation **for high resolution imaging:**

- Back-scattered electron: *composition and topography*
- Secondary electron: *topography*
- X-ray map: *spatial distribution of elements*
- Cathodoluminescence: *trace elements, defects*

JXA-8200 scheme

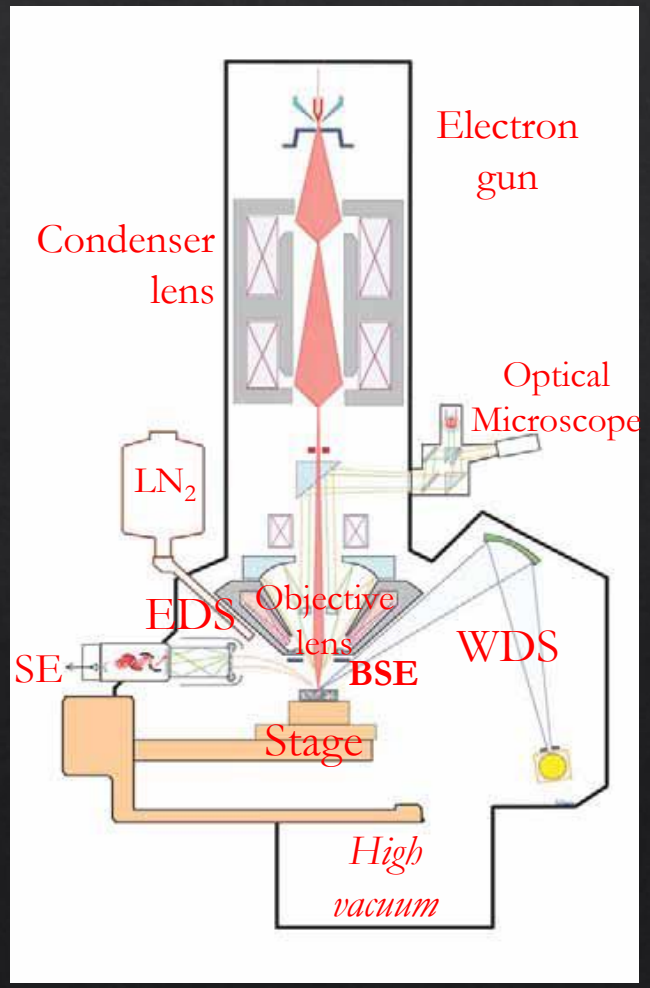

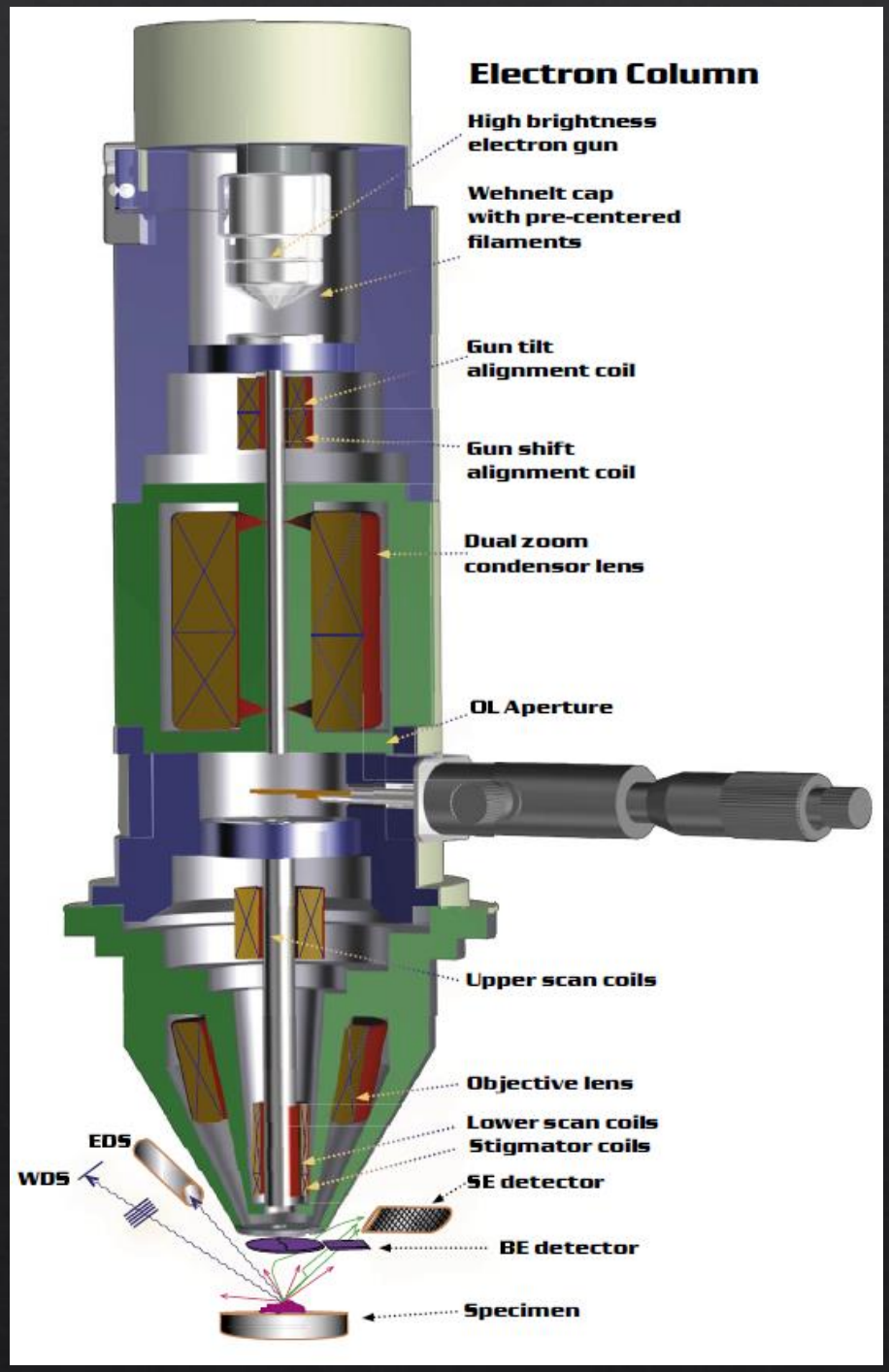

Electron emitting source: Tungsten hairpin

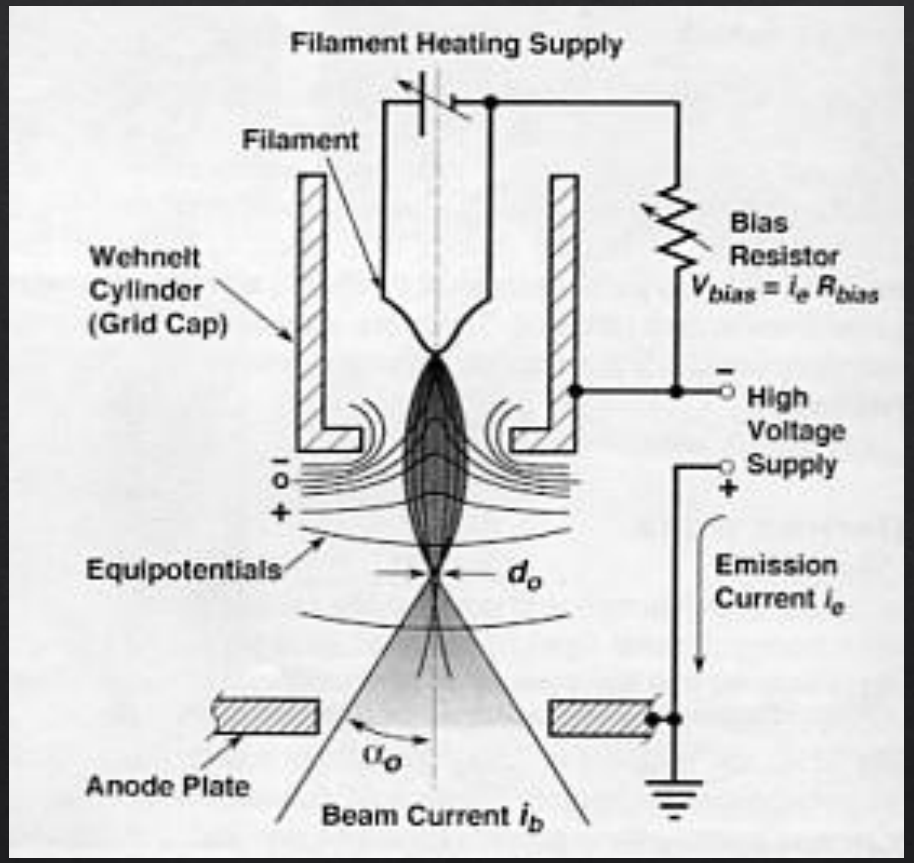

Self-biased thermionic electron gun

- **Cathode: Filament** *at negative potential*

  Tungsten has a high melting point and a low work-function energy barrier; heated by filament current, i_f, until electrons overcome the barrier

- **Wehnelt Cylinder** *at a slightly higher negative potential than the filament because of the Bias Resistor*

  Bias voltage (V_{bias}) automatically adjusts with changes in i_e to stabilize emission; the grid cap also focuses the electron beam

- **Anode: Plate** *at ground potential*

  Potential difference (accelerating voltage, V_0) causes electron emission (current, i_e)

Electron probe parameters

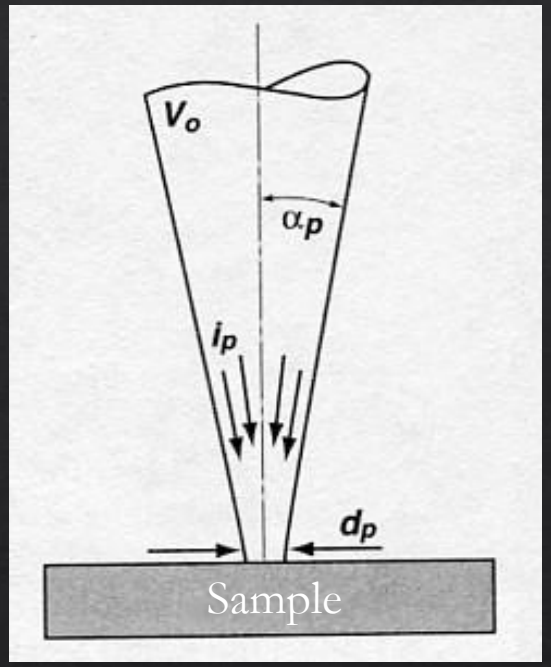

Accelerating voltage, V_0
(V_0 of 15 kV generates electron beam with 15 keV energy)

Final beam current, or probe current, i_p
Final beam diameter, or probe diameter, d_p
Final beam convergence angle, or probe convergence angle, α_p

Filament saturation

Probe current, i_p

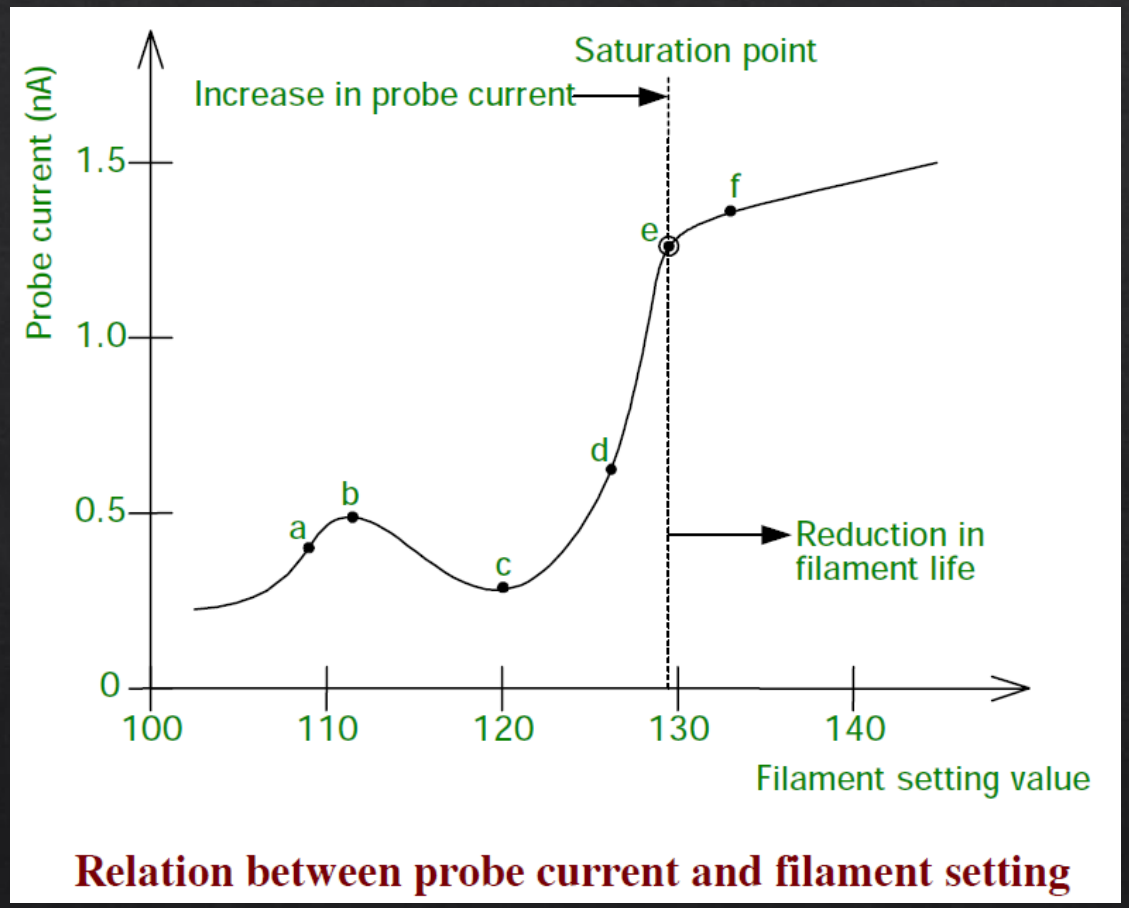

Filament current, i_f

Electron probe diameter

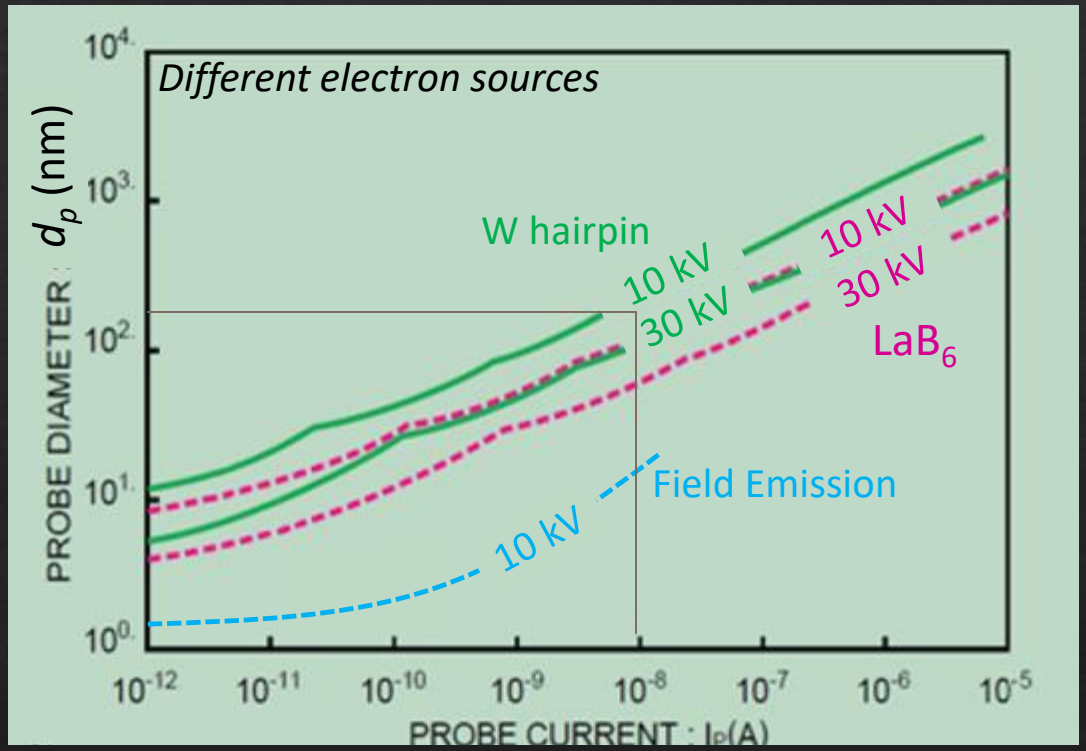

Probe diameter decreases with

- *decrease in Probe current*
- *increase in Accelerating voltage*
- *W > LaB6 > Field Emission source*

Higher probe current improves signal but results in poorer image resolution

d_p ≈100 nm at 10 nA and 15 kV with a Tungsten hairpin source

Electron probe diameter

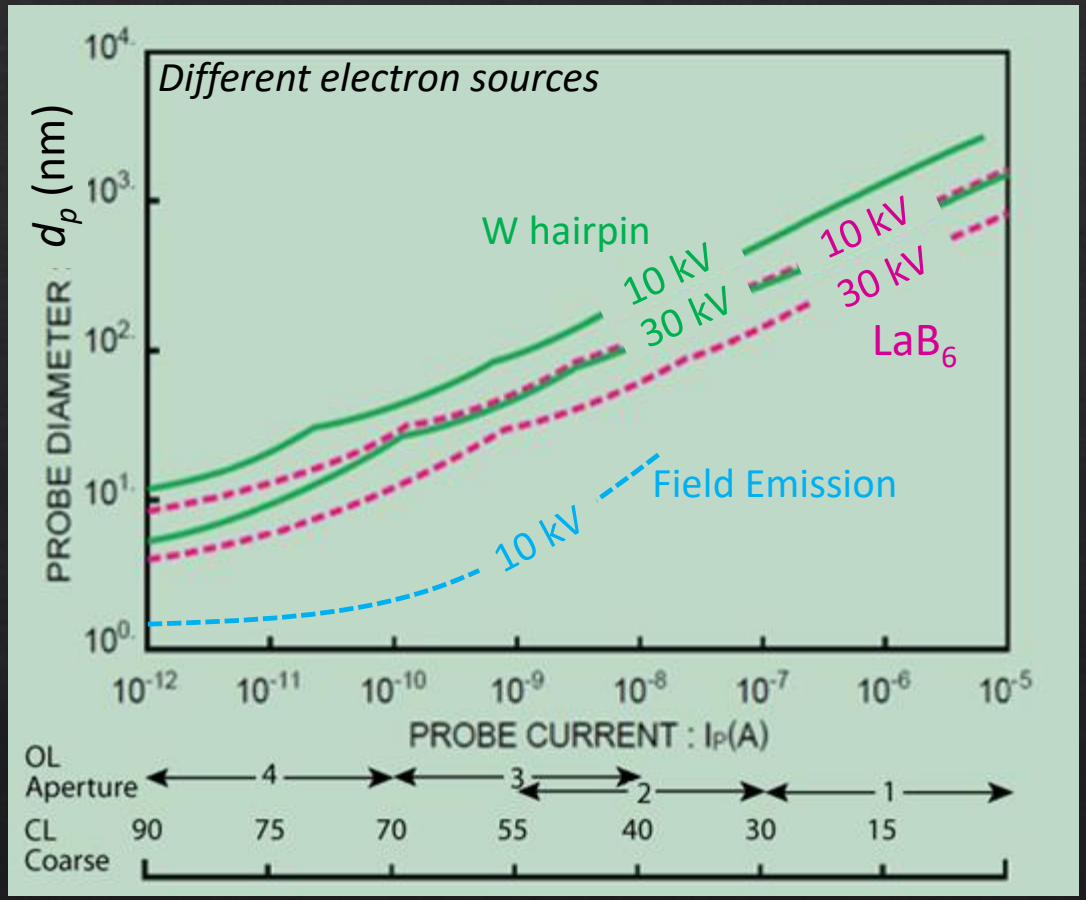

Probe current can be changed by adjusting the condenser lens (CL) current and the objective lens (OL) aperture settings

OL aperture control on probe diameter and current

Table 4.1 Selection of OL apertures

Scale (OL aperture No.)	Aperture diameter (μm)	Indication coefficient: Probe diameter*	Probe current range (Acc. voltage: 25 kV)	Purpose of use
4	70	Approx. 0.3	10^{-10} A or less	High resolution SEM LDF mode; large depth of focus.
3	130	Approx. 0.5	10^{-10} to 10^{-8} A	
2	170	Approx. 0.7	10^{-8} to 10^{-7} A	
1	240	1	10^{-7} to 10^{-5} A	Higher current X-ray microanalysis.

* The value (other than 0) indicated in the Control window is an approximate probe diameter when OL aperture No. 1 is selected. When an aperture other than No. 1 is used, multiply the indicated probe diameter by the probe diameter indication coefficient to obtain the approximate value. The actual probe diameter can be determined from the diameter of a disk-shaped luminescent pattern of ZrO_2 displayed on the OM monitor of the workstation.

- *Actual diameter = diameter in control window X indication coefficient*
- *Use ZrO_2 and 25 kV to determine probe diameter, which depends on the material and increases sharply with accelerating voltage*

Electron gun brightness

$$\text{Brightness, } \beta = \frac{current}{(area)(solid\ angle)} = \frac{i_b}{\left(\pi\left(\frac{d}{2}\right)^2\right)(\pi\alpha^2)}\ A/cm^2 sr$$

i_b : beam current
d : beam diameter
α : beam convergence angle

Higher beam current and smaller diameter results in greater brightness

Maximum brightness can be achieved by correctly setting the

gun bias voltage and filament-to-grid cap distance

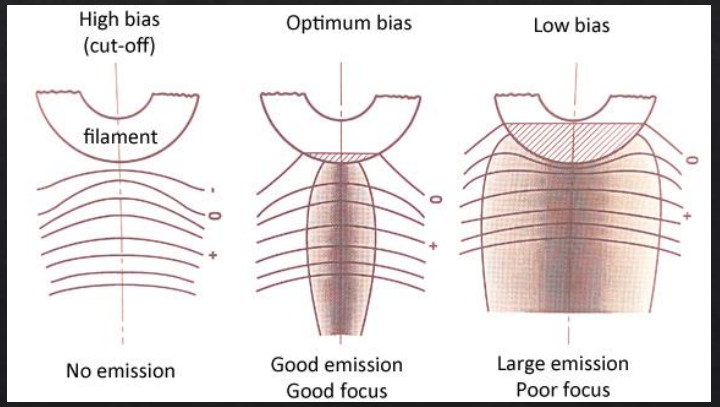

Low bias: high emission but large d, hence low β

High bias (cut-off): no emission

Optimum bias and filament-grid cap distance: good emission and small d, hence high β

Comparison of electron emitting sources

Source	Brightness, β at initial crossover ($A/cm^2\,sr$)	Initial beam diameter, d_0 (μm)	Energy spread, ΔE (eV)	Beam current stability (% hour)
Thermionic emitter:				
Tungsten hairpin	10^5	30 - 100	1 – 3*	1
LaB_6	10^6	5 - 50	1 - 2	1
Field emitter:				
Cold	10^8	<0.005	0.3	5
Thermal	10^8	<0.005	1	5
Schottky	10^8	0.015 - 0.030	0.3 - 1.0	~1

* E.g., a 15 keV electron beam actually has an energy of 15,000 ± 3 eV

Source: Goldstein et al. (2003) p. 35

Lens aberration

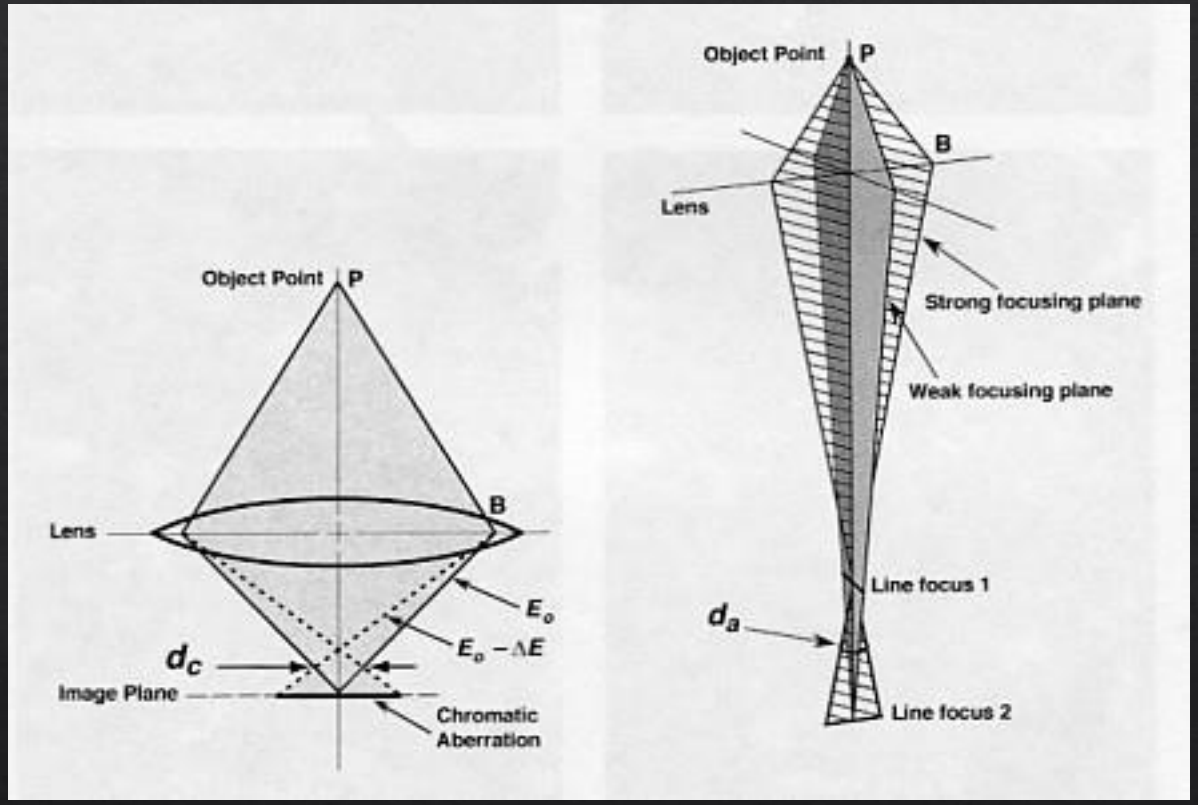

Electrons with different energies are focused at different distances

Chromatic aberration

more at low voltage

Astigmatism

corrected with stigmator controls

Electrons traveling on different planes are focused at different distances

Lens aberration

Electrons traveling through the center and edge of the lens are focused at different distances

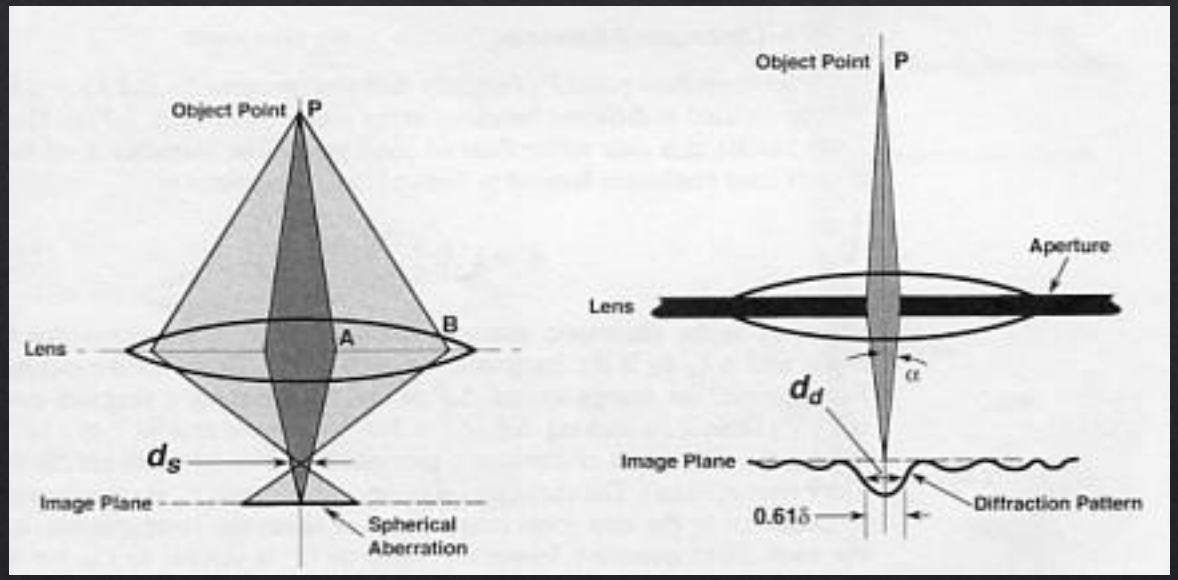

Very small apertures produce a concentric diffraction pattern instead of a spot

Spherical aberration

less with
smaller OL apertures

Aperture diffraction

very small OL apertures
have this artifact

Depth of focus

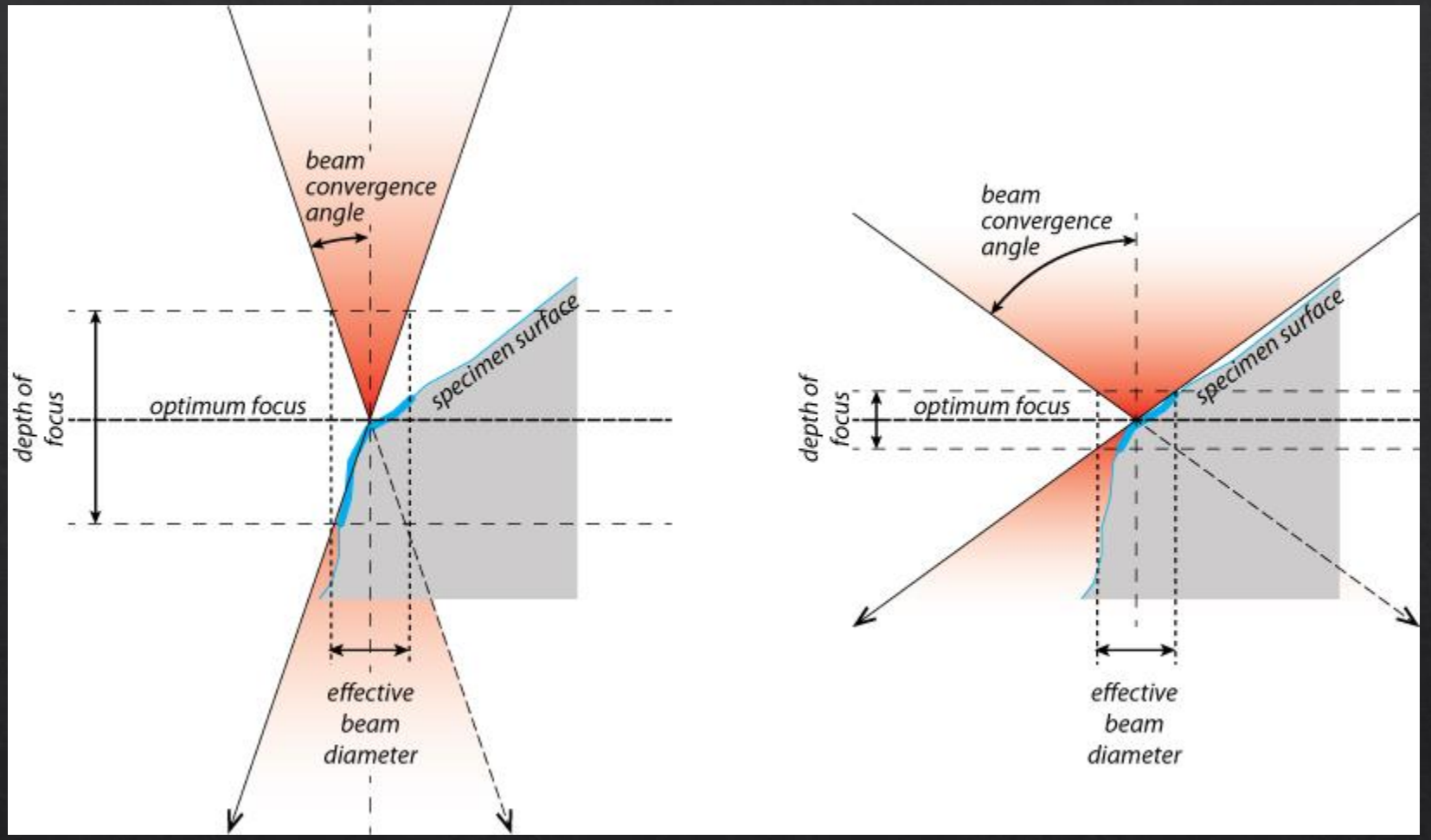

Large depth of focus

Small depth of focus

Column modes

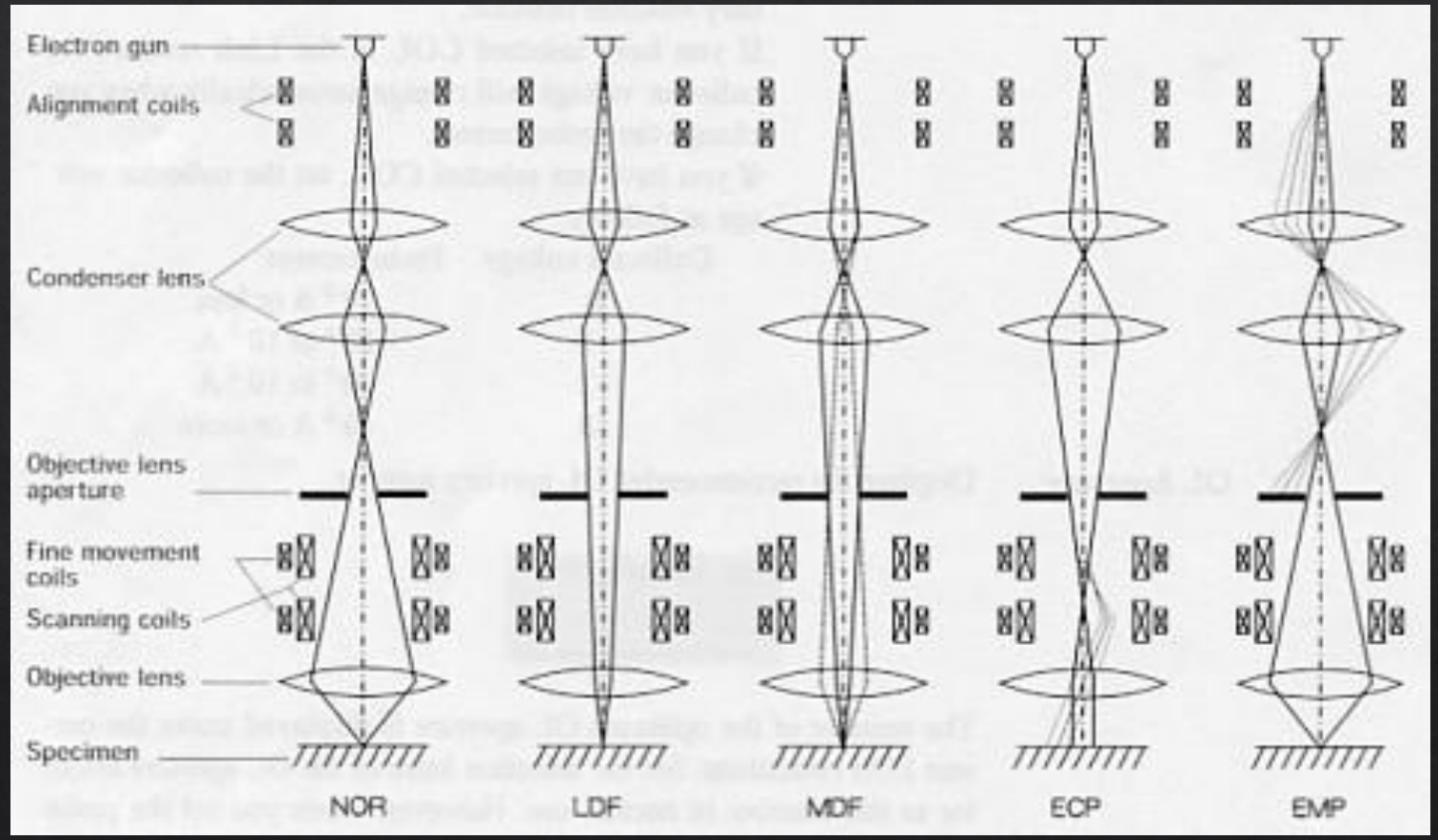

Normal	Large depth of focus	Maximum depth of focus	Electron channeling pattern	Emission pattern

Spatial resolution: electron interaction volume

Vertical electron beam, probe diameter = 0.1 μm

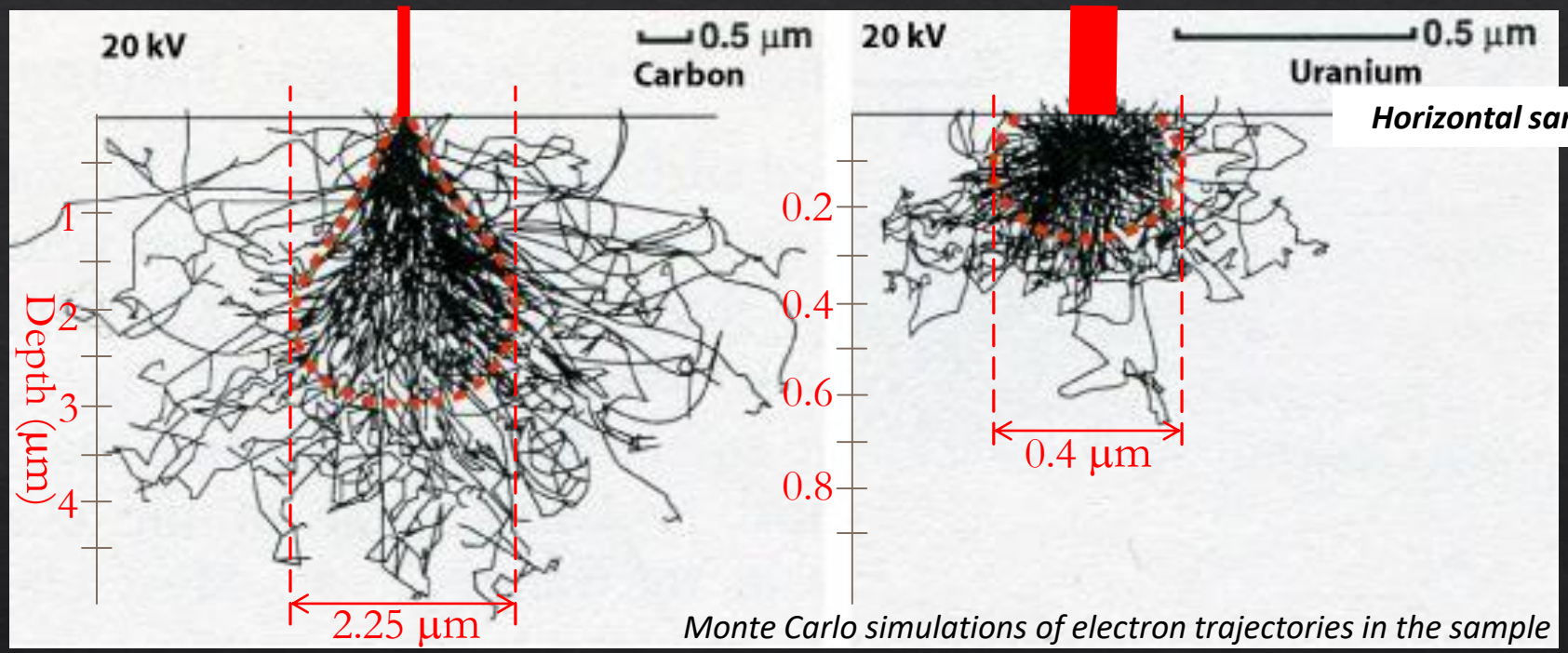

Monte Carlo simulations of electron trajectories in the sample

Low atomic number:
large tear-drop shape

High atomic number:
small hemisphere

Width of interaction volume >> probe diameter

(interaction volume can be reduced by reducing the probe diameter using a lower accelerating voltage)

Electron interaction depth (range)

$$R = 0.0276 \; E^{1.67} \frac{A}{\rho Z^{0.889}}$$

R : Kanaya-Okayama electron range

E : beam energy

A : atomic weight

ρ : density

Z : atomic number

Electron range increases as E increases, and decreases as ρ and ρZ increase

E.g., at 20 kV,

R = 4.29 μm in Carbon (Z = 6, A = 12.01, ρ = 2.26 g/cc)

R = 0.93 μm in Uranium (Z = 92, A = 238.03, ρ = 19.07 g/cc)

Electron interaction depth (range)

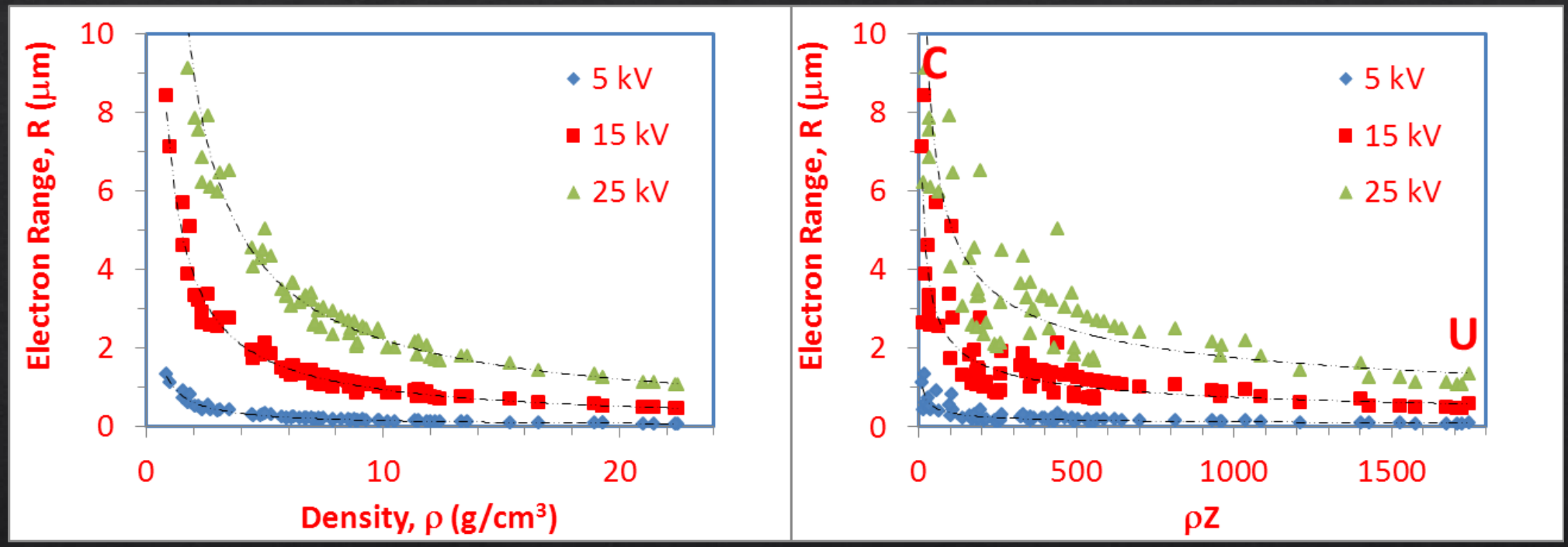

Electron range increases as E increases, and decreases as ρ and ρZ increase

Signal types

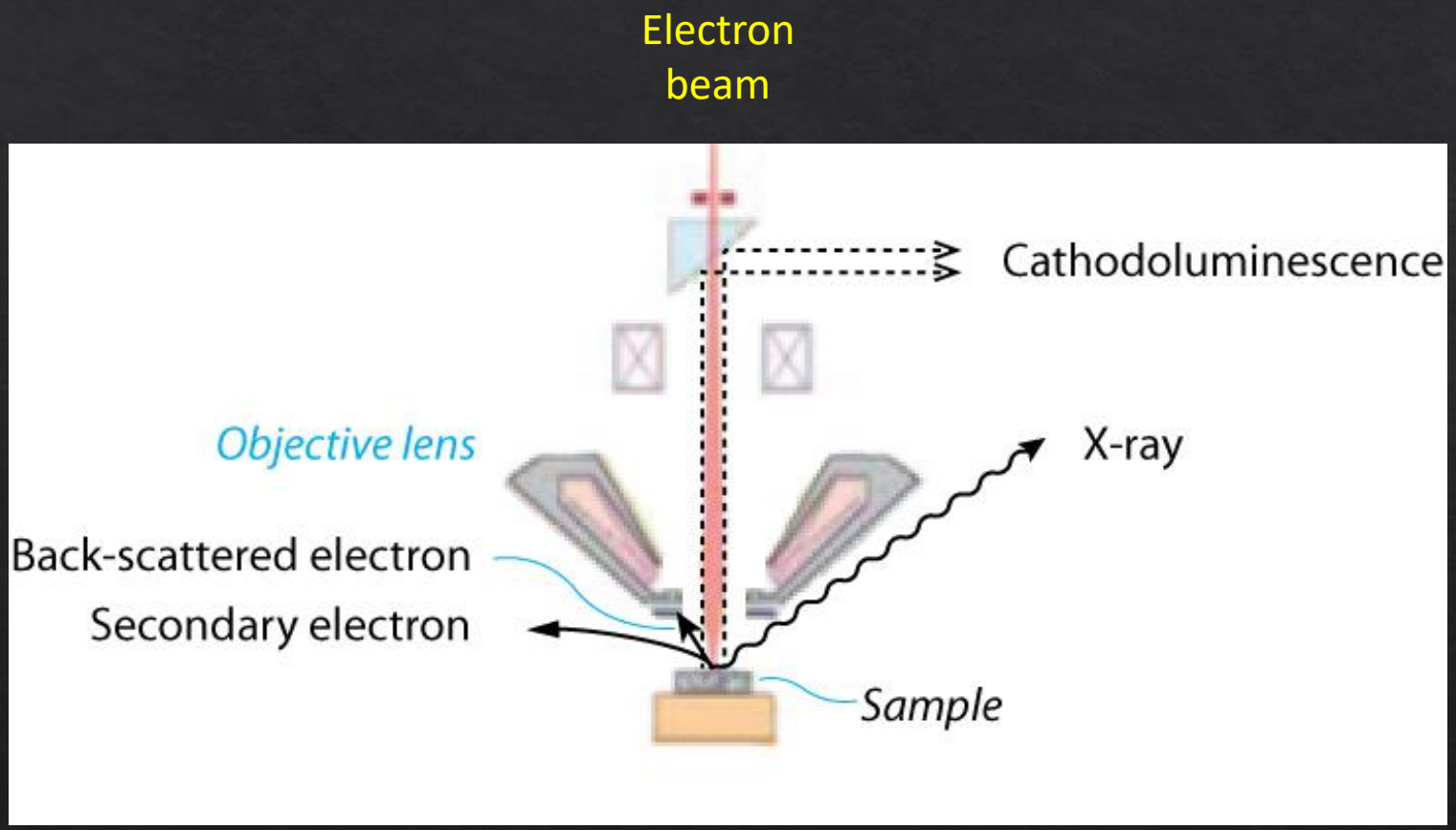

Spatial resolution for different signals (production volume)

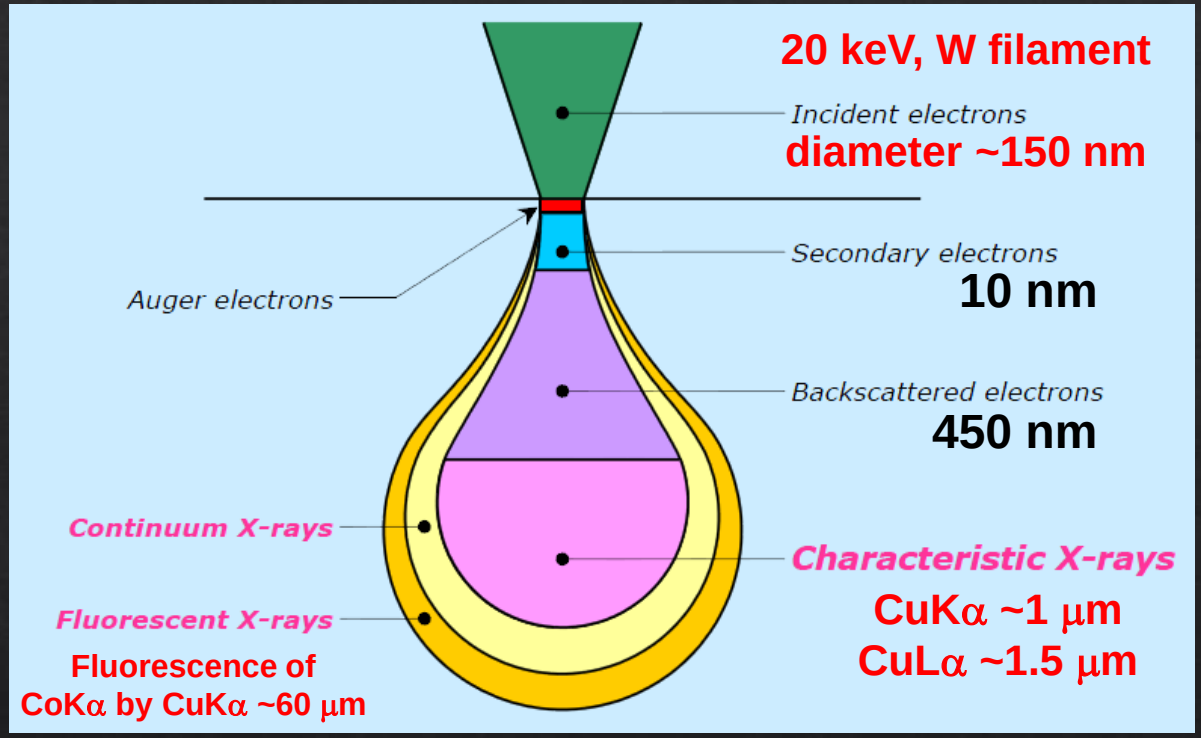

(not to scale)

Production volume for different signals is different

The "onion shell" model:
Cu-10%Co alloy

Spatial resolution for cathodoluminescence (production volume)

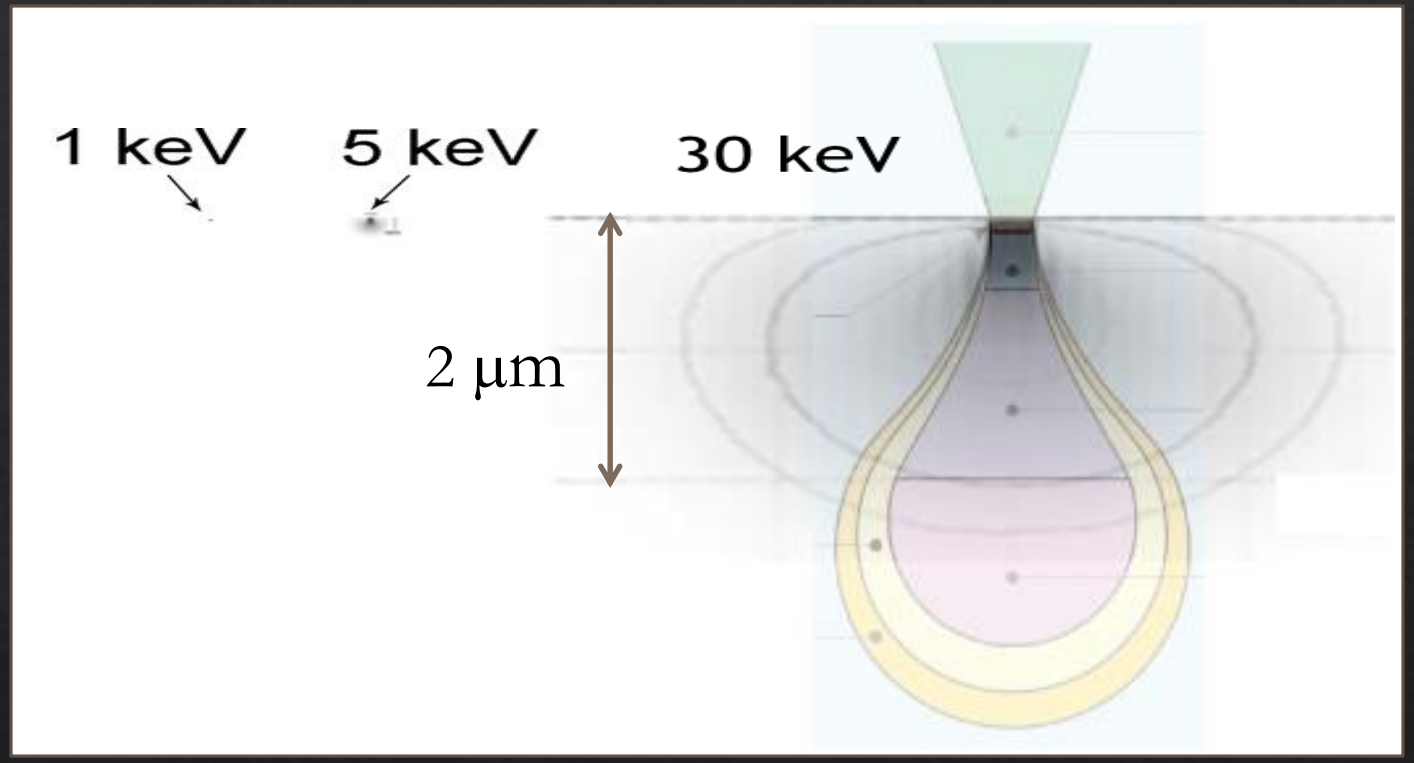

Gallium Nitride

Electron-specimen interactions: elastic scattering

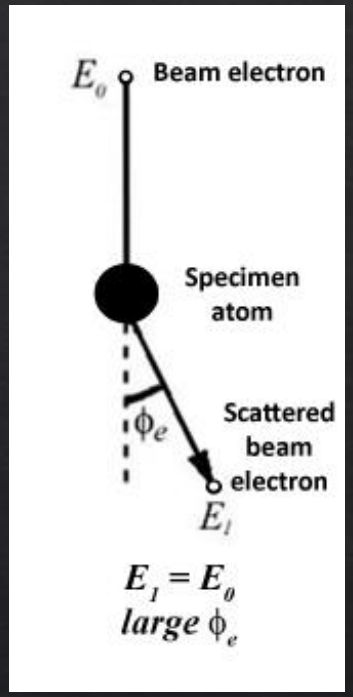

E.g., Back-scattered electron (BSE)

Electron-specimen interactions: inelastic scattering

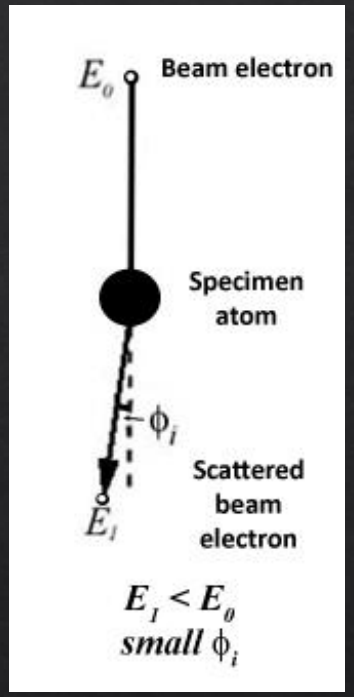

Inner shell interactions:

- Characteristic X-rays
- Secondary electron (SE)

Outer shell interactions:

- Continuum X-rays
- Secondary electron (SE)
- Cathodoluminescence (CL)

Back-scattered electron (BSE)

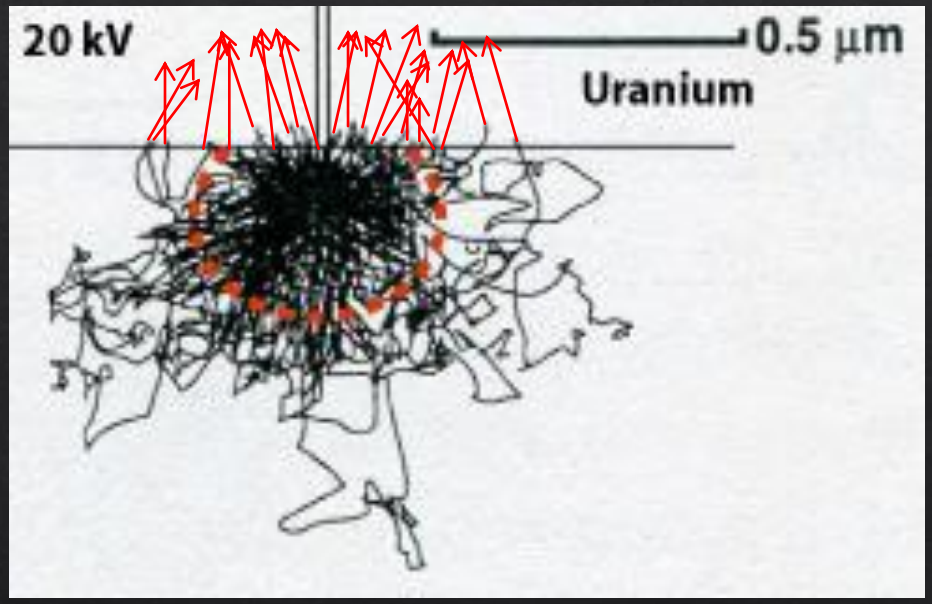

- *Beam electrons scattered elastically at high angles*
- *Commonly scattered multiple times, so energy of BSE ≤ beam energy*

Electron backscatter coefficient

Fraction of beam electrons scattered backward

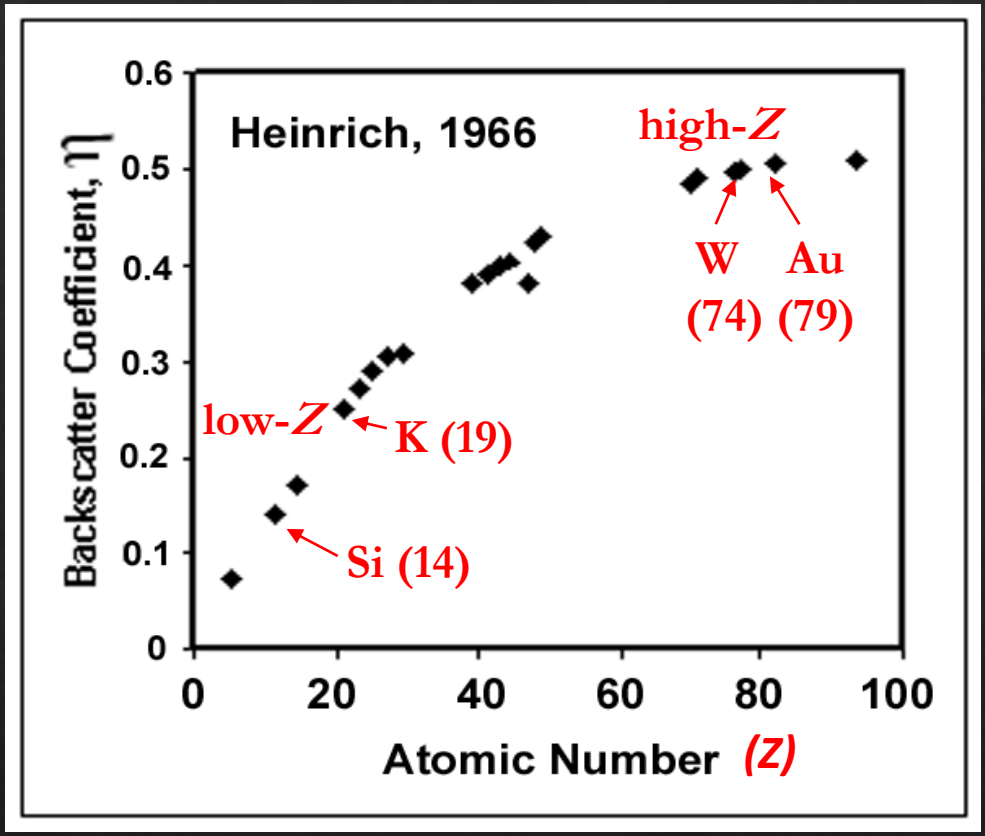

- *Large differences between high-Z and low-Z elements*
- *Larger differences among low-Z elements than among high-Z elements*

Back-scattered electron detector

Back-scattered electron detector

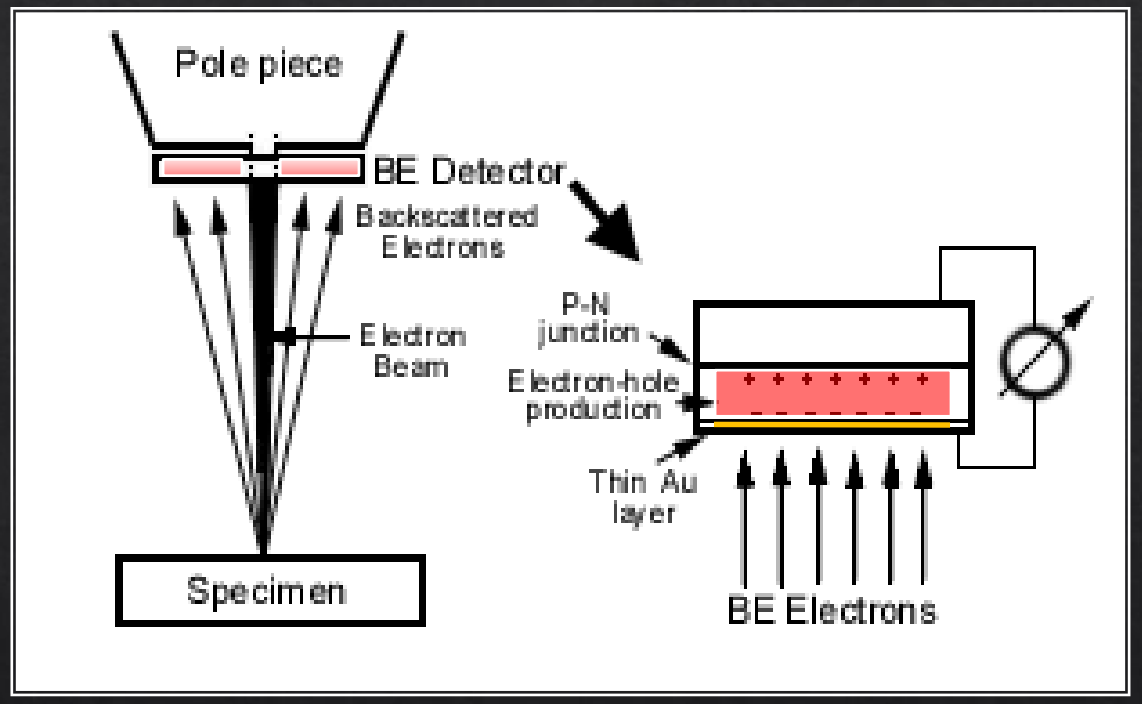

Solid-state diode

Compositional and topographic imaging with BSE

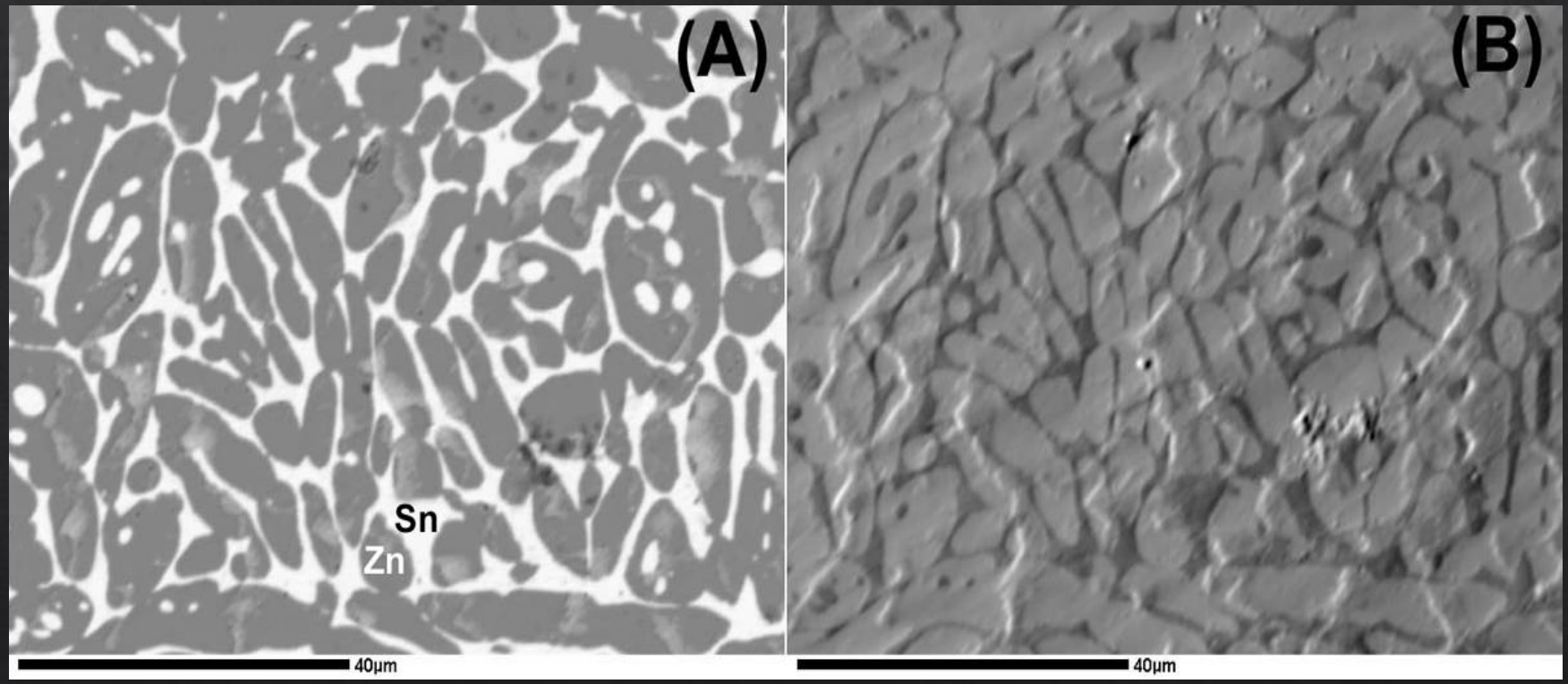

A+B

Compositional

mode

A-B

Topographic

mode

Secondary electron (SE)

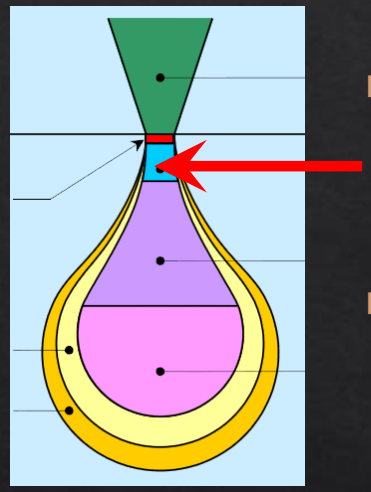

- *Specimen electrons mobilized by beam electrons through inelastic scattering (both outer and inner shell ionizations)*
- *Emitted at low energies (typical: <10 eV)*

  (recall BSE have high energies up to that of the electron beam)

Secondary electron detector

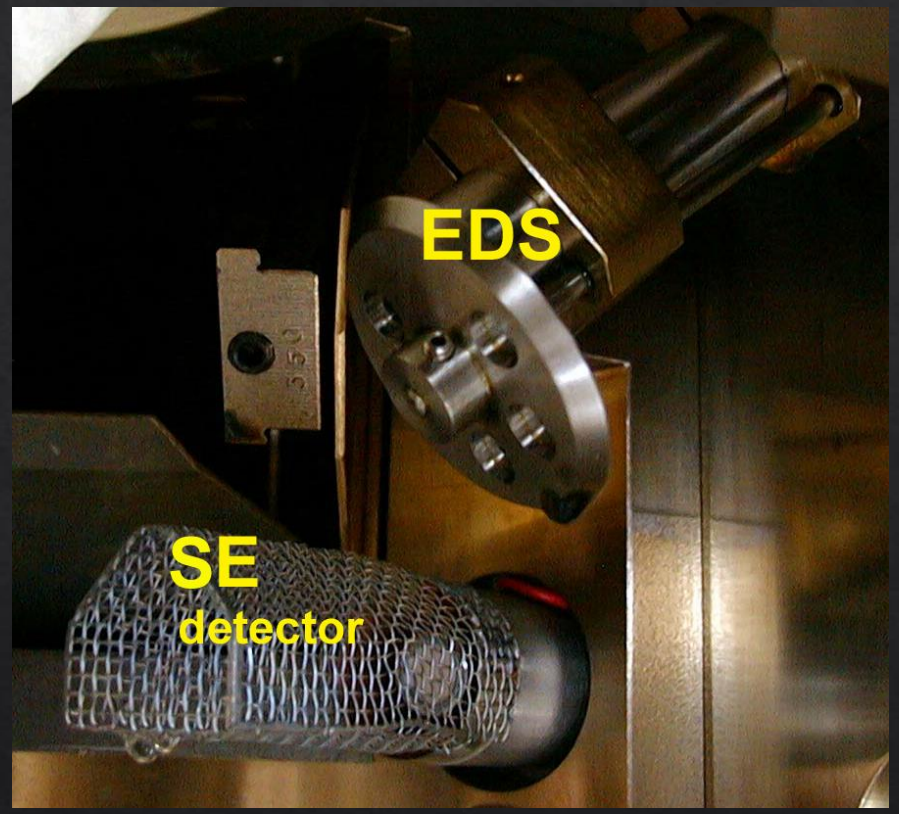

Located on the side wall of the sample chamber

Secondary electron detector

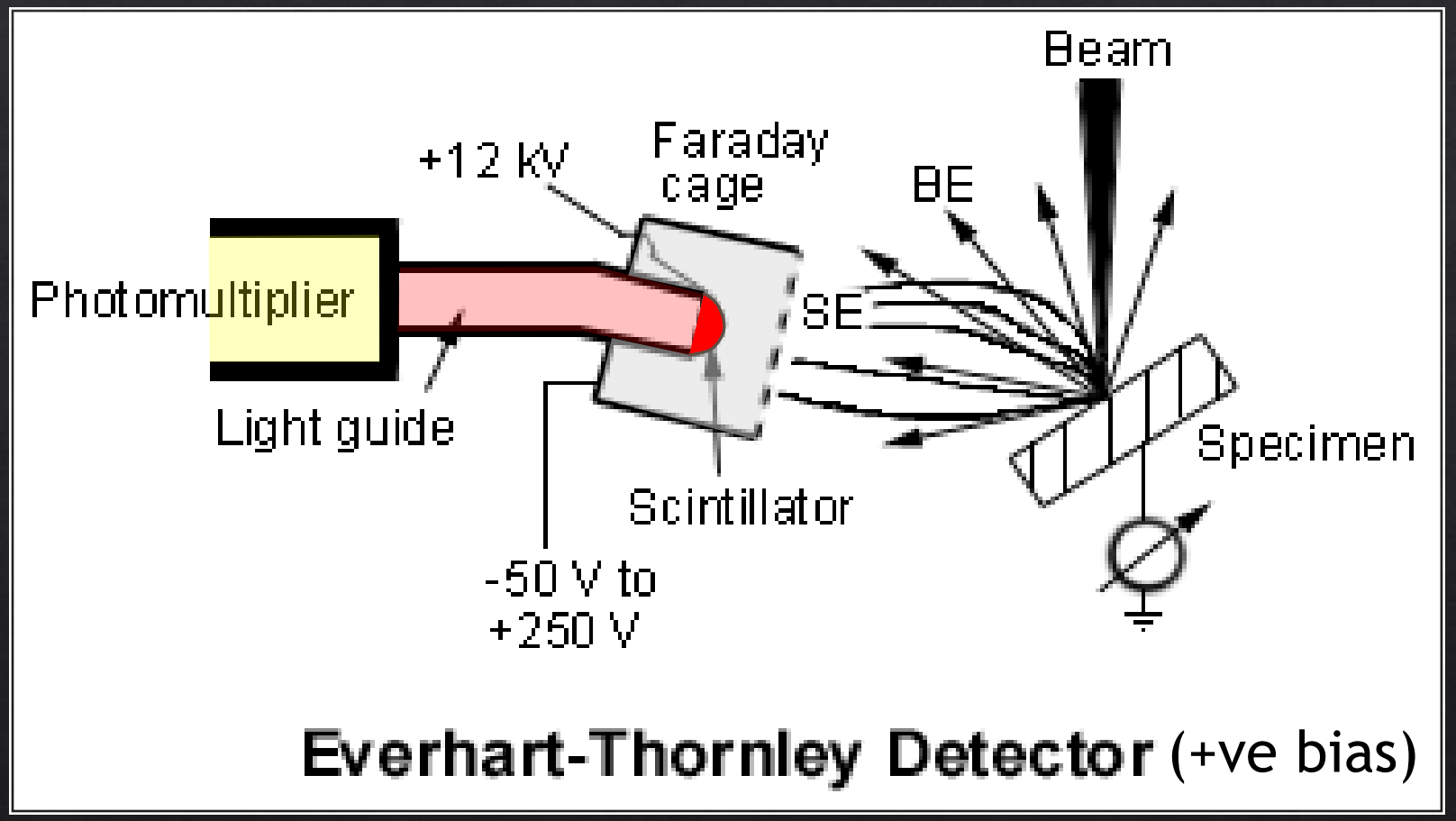

Everhart-Thornley Detector (+ve bias)

Imaging with the Everhart-Thornley detector

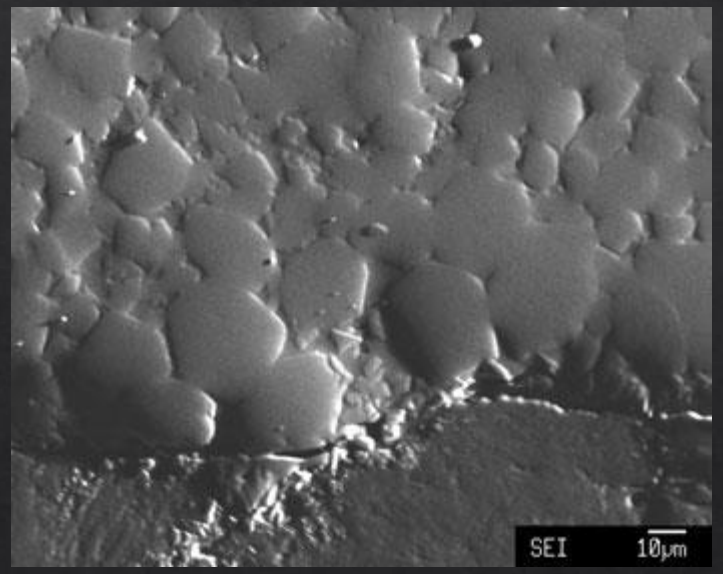

Negative Faraday cage bias

only BSE

Surfaces in direct line of sight are illuminated

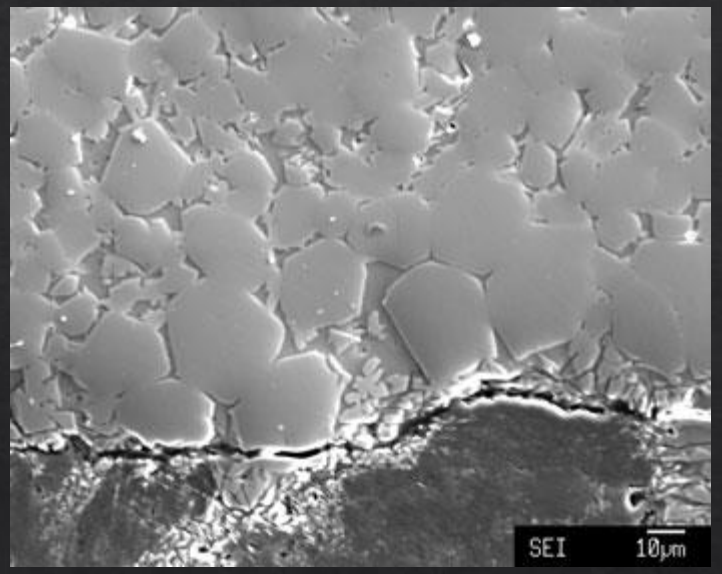

Positive Faraday cage bias

BSE + SE

All surfaces are illuminated

Cathodoluminescence (CL)

Caused by inelastic scattering of beam electrons in semiconductors

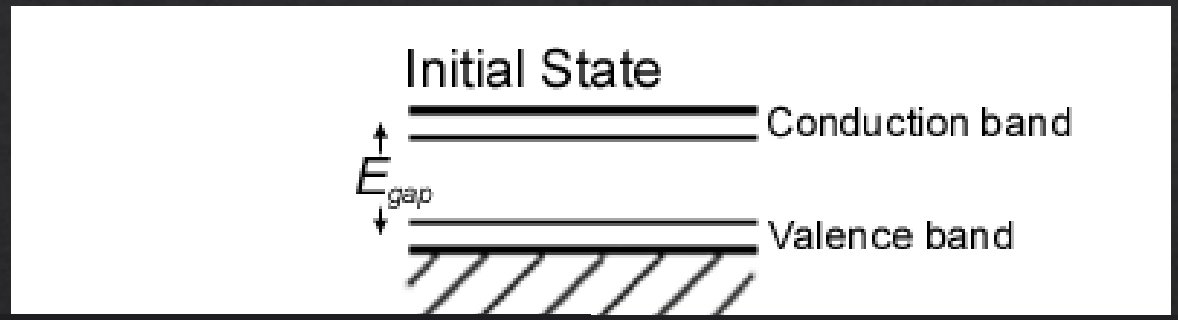

Filled valence band is separated from an empty conduction band by E_{gap}, characteristic of the compound

Electron recombines with the valence band to generate light with energy E_{gap}

Electron beam interacts:
Valence electron is promoted to the conduction band

Trace element impurities produce additional energy levels outside the conduction band and enable other electron transitions; emitted light has different colors with energies $E \neq E_{gap}$

Cathodoluminescence spectrometer

Optical microscope camera (not used)

Optical microscope light (turned off)

Optical spectrometer (CCD array detector)

Cathodoluminescence spectrum

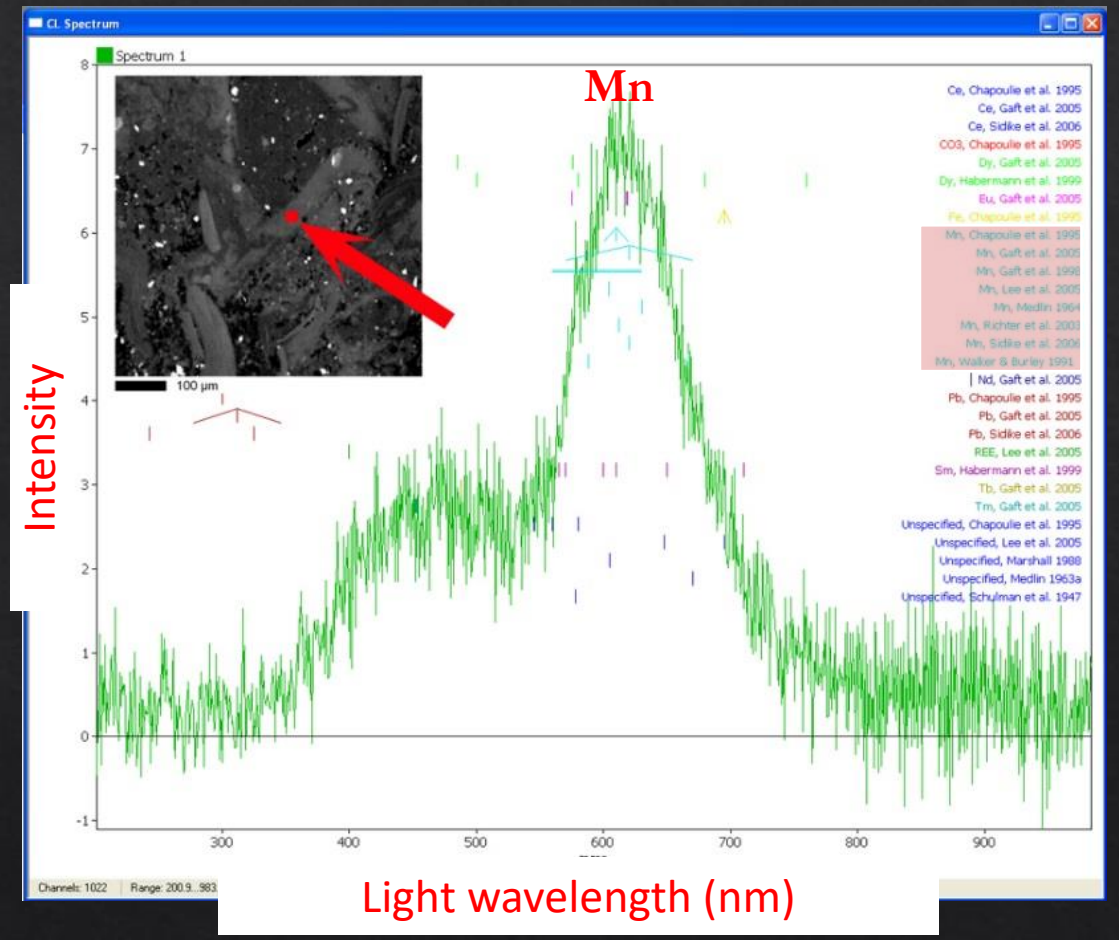

Dolomite with trace of Mn

Hyperspectral CL imaging

A continuous (λ = 200 to 950 nm) light spectrum is collected at each point of the image area

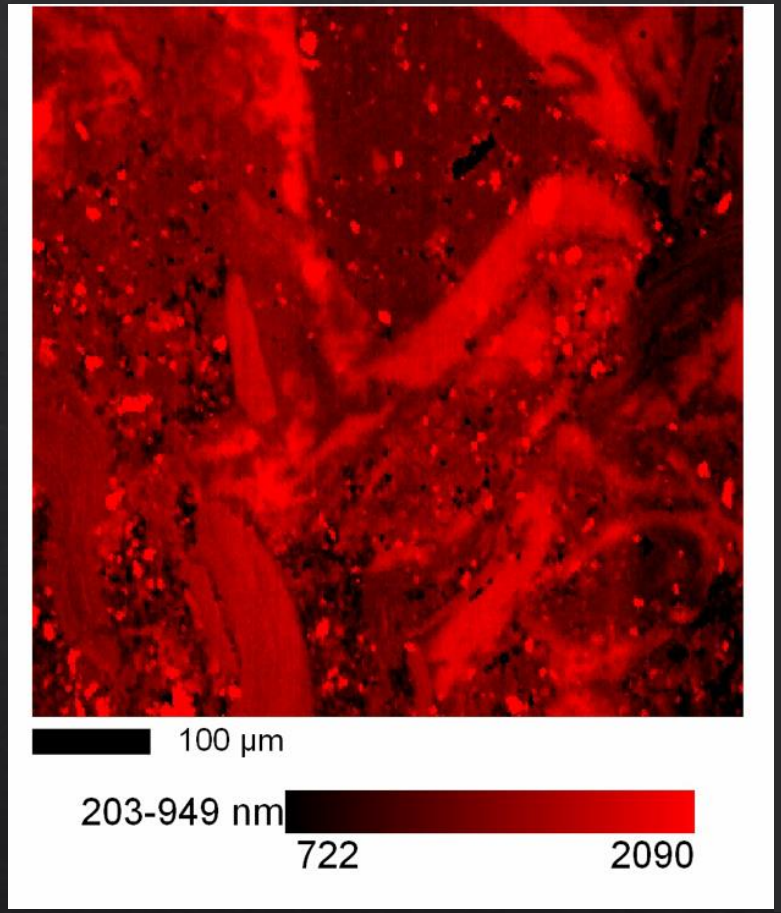

Intensity range of 203-949 nm light: 722-2090 counts (red shades)

Hyperspectral CL imaging

Intensity range of light (all wavelengths) in grey scale:

Black: no light
White: maximum intensity

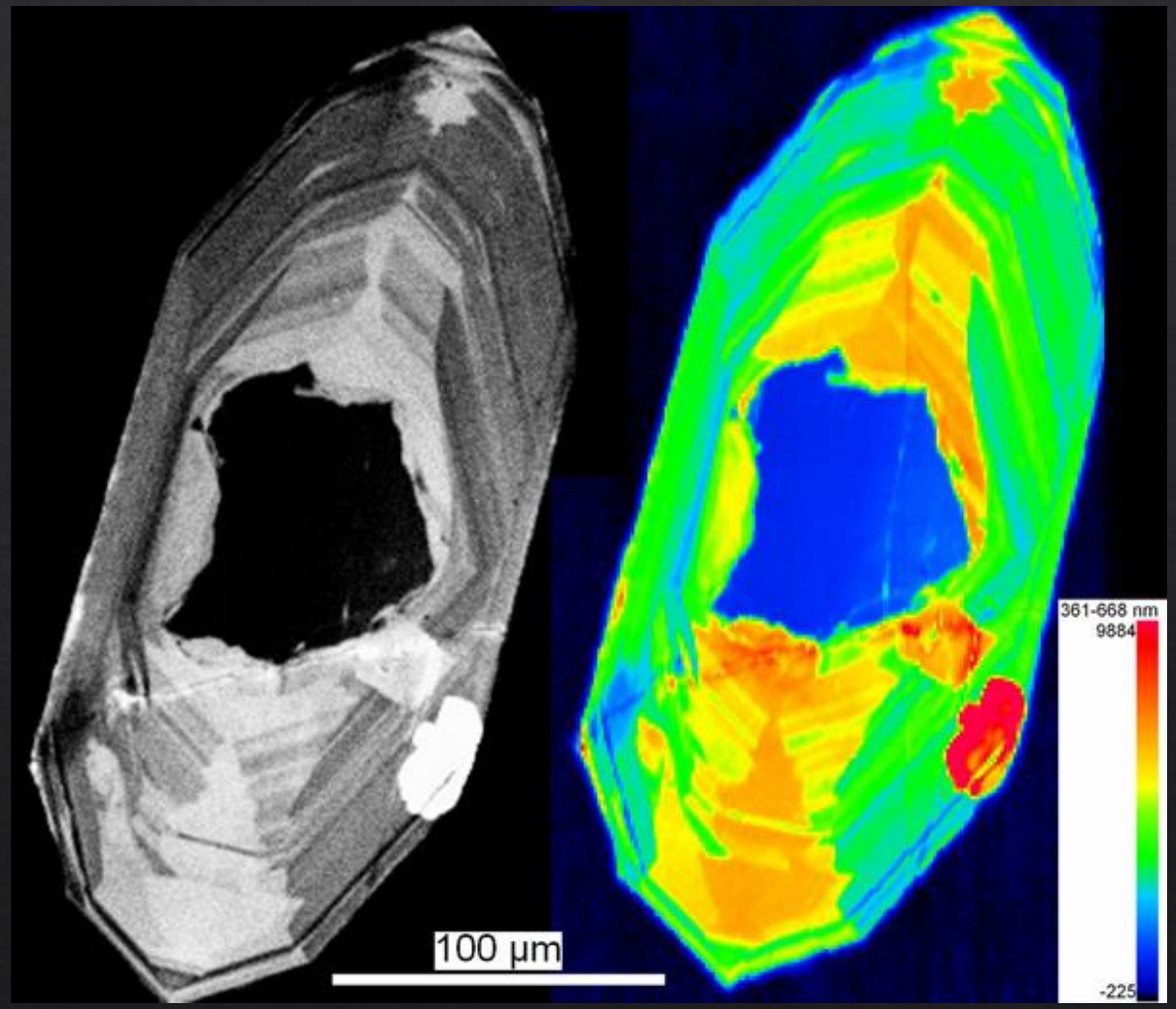

Intensity range of 361-668 nm light in multicolor scale:

Blue (≤ 0 counts): no light
Red (9884 counts): maximum intensity

Understanding X-rays: The electromagnetic spectrum

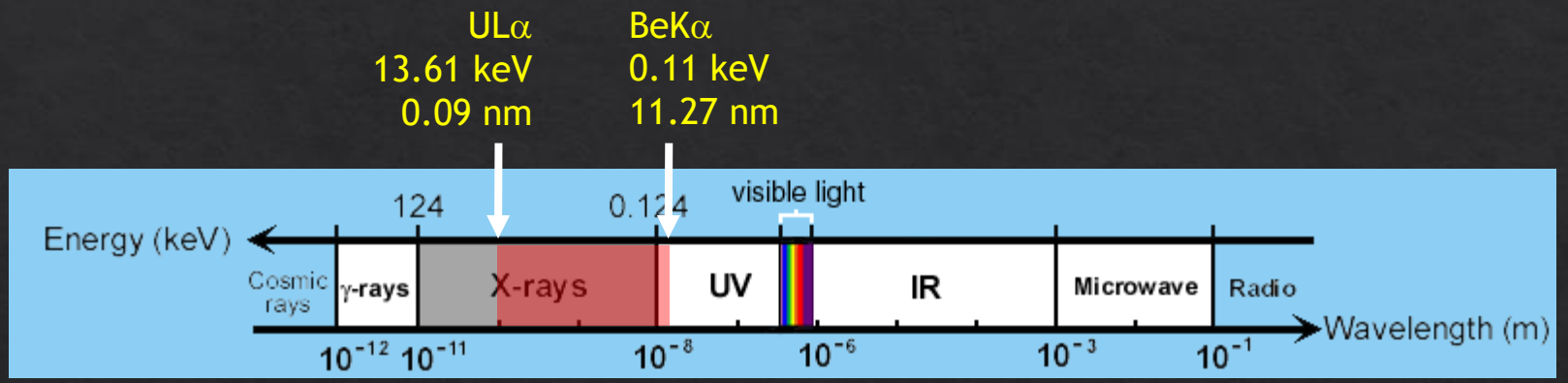

$E = h\nu = h\frac{c}{\lambda}$ where, E : energy, h : Planck's constant, ν : frequency, c : speed of light in vacuum, λ : wavelength

E (keV) $= h\frac{c}{\lambda} = 1.2398/\lambda$ (nm) or, λ (nm) $= h\frac{c}{E} = 1.2398/E$ (keV)

Examples:

$\lambda_{BeK\alpha}$ = 11.27 nm; Hence, $E_{BeK\alpha}$ = 1.2398/11.27 = 0.11 keV

E_{ULa} = 13.61 keV; Hence, λ_{ULa} = 1.2398/13.61 = 0.09 nm

Characteristic X-ray generation

Overvoltage, $U = E/E_c$, > 1

E : electron beam energy
E_c : critical excitation energy
(or, ionization energy)
of shell in target atom

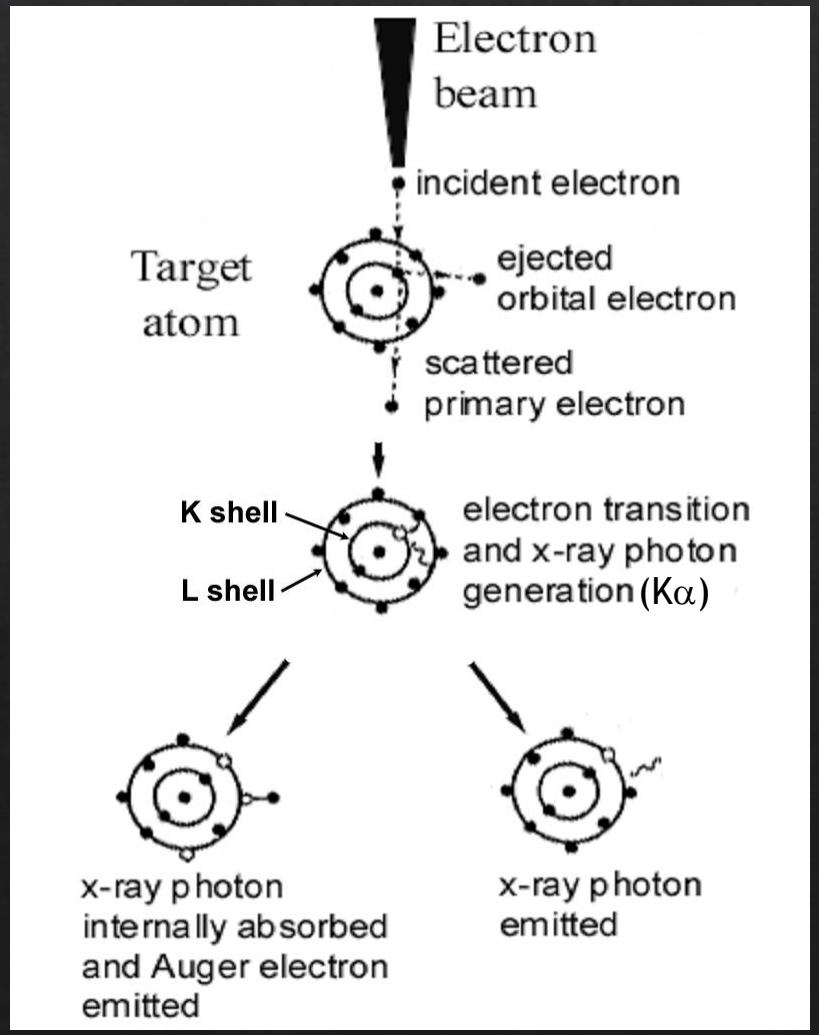

Inner shell ionization through inelastic scattering

Condition for ionization: Overvoltage

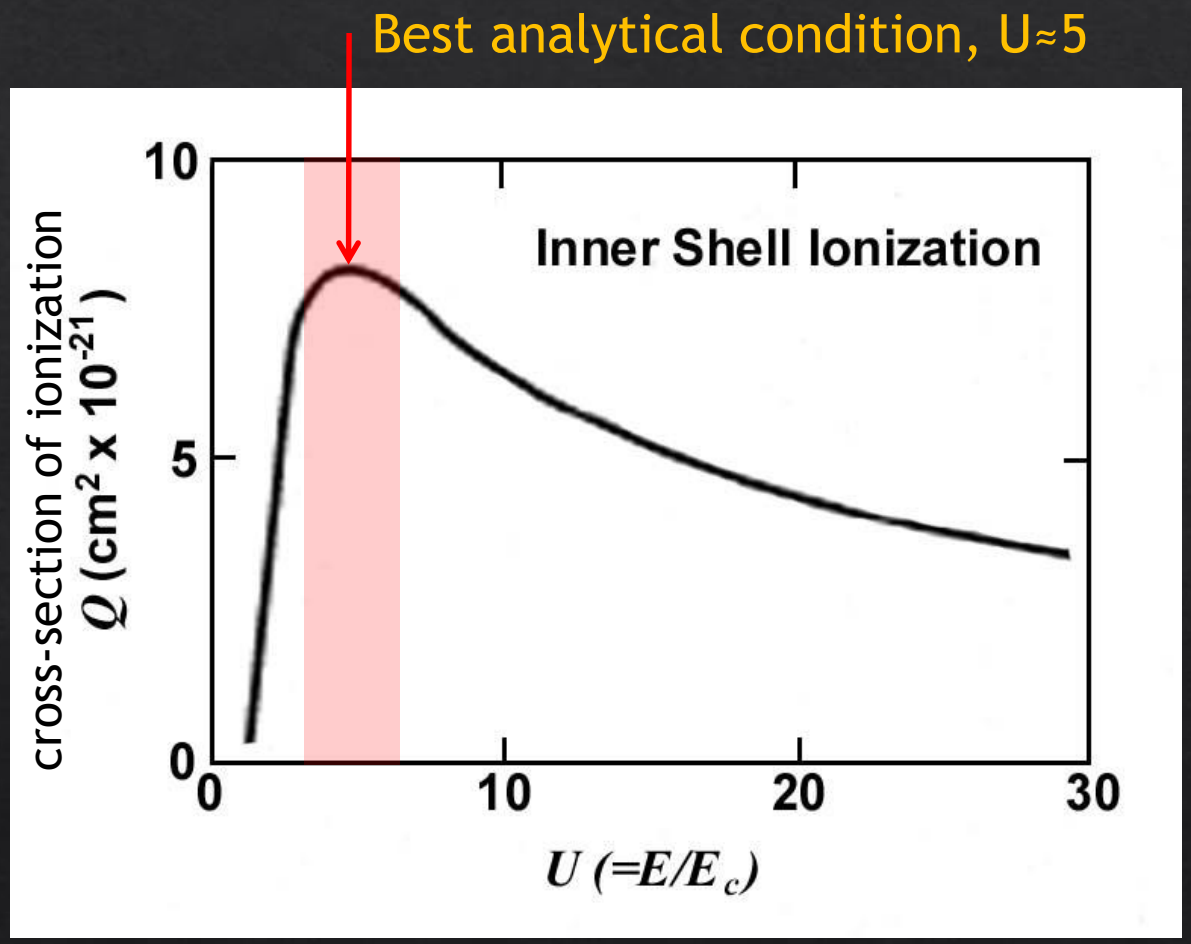

Characteristic X-ray energies

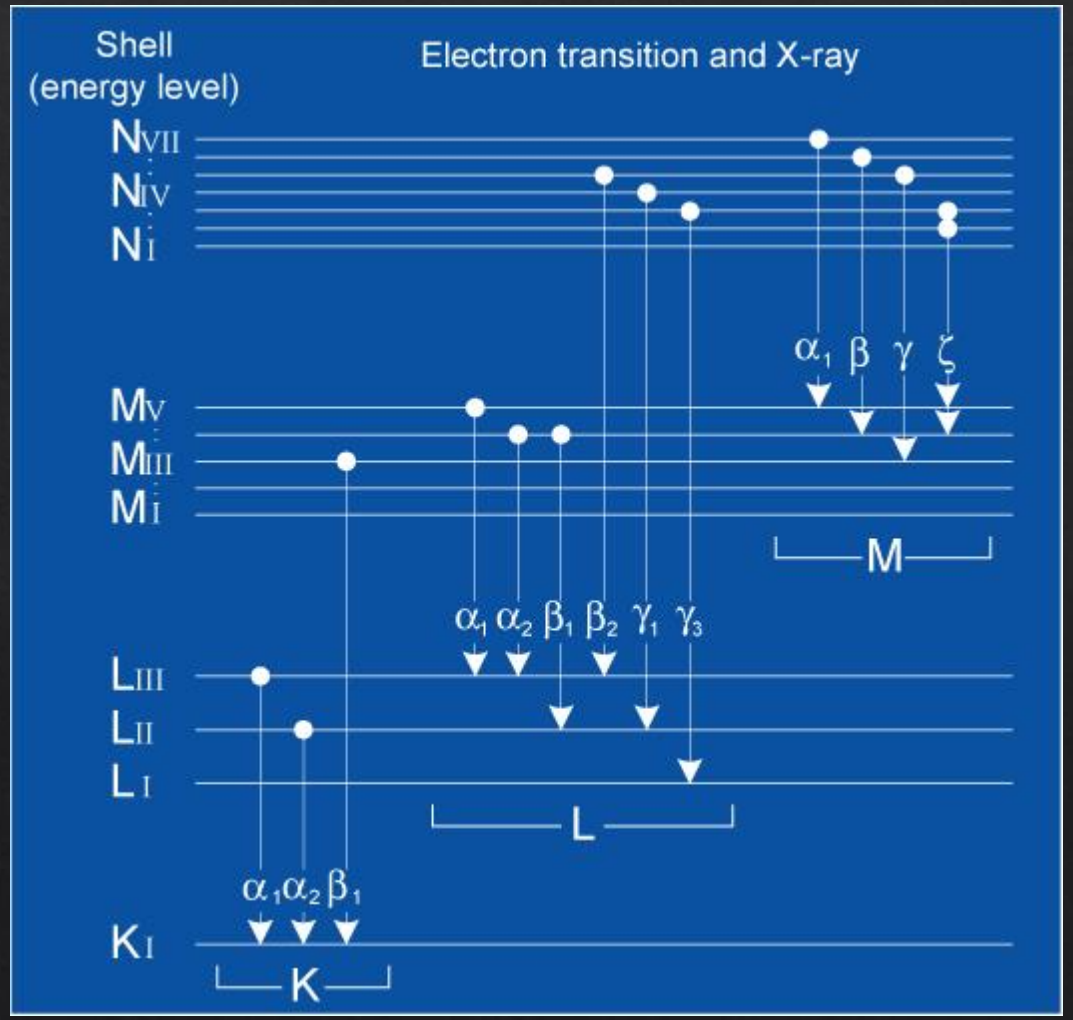

X-ray	Electron transition	Energy
Kα	L_{II+III} to K_I	$E_{K\alpha} = E_{c(K_I)} - E_{c(L_{II+III})}$
Kβ	M_{III} to K_I	$E_{K\beta} = E_{c(K_I)} - E_{c(M_{III})}$
Lα	M_{IV+V} to L_{III}	$E_{L\alpha} = E_{c(L_{III})} - E_{c(M_{IV+V})}$
Mα	N_{VII} to M_V	$E_{M\alpha} = E_{c(M_V)} - E_{c(N_{VII})}$

Characteristic X-ray energy and critical excitation energy

The energy required to generate UKα *must be higher than the critical excitation energy of the U K-shell,* $E_{c(K)}$*, i.e., overvoltage* $E/E_{c(K)} > 1$

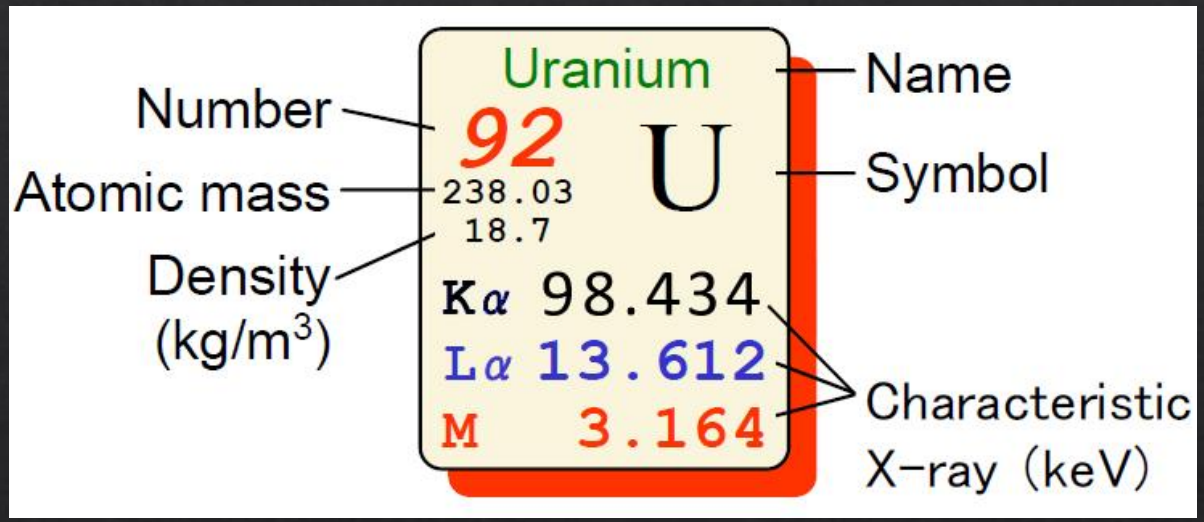

$E_{c(K)} \approx 98.4 + 13.6 + 3.2$

≈ 115.2 keV

Required energy > 115.2 keV

To calculate $E_{c(K)}$:

Start	$E_{K\alpha}$	$= E_{c(K)} - E_{c(L)}$
Rearrange	$E_{c(K)}$	$= E_{K\alpha} + E_{c(L)}$
Substitute $E_{c(L)} = E_{L\alpha} + E_{c(M)}$		$= E_{K\alpha} + (E_{L\alpha} + E_{c(M)})$
Substitute $E_{c(M)} = E_{M\alpha} + E_{c(N)}$		$= E_{K\alpha} + E_{L\alpha} + (E_{M\alpha} + E_{c(N)})$
Therefore,	$E_{c(K)}$	$\approx E_{K\alpha} + E_{L\alpha} + E_{M\alpha}$

Characteristic X-ray production depth (range)

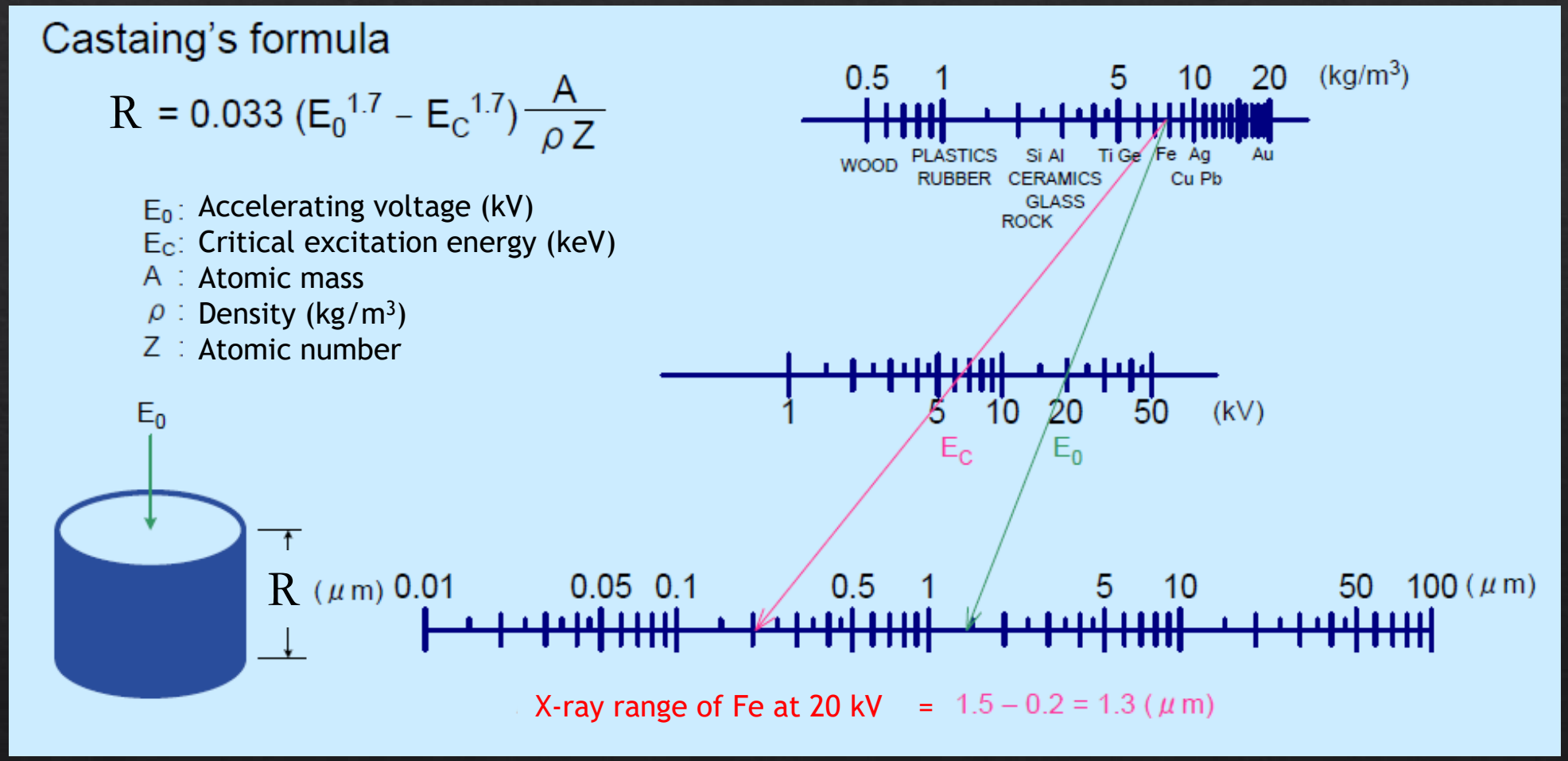

Characteristic X-ray production depth (range)

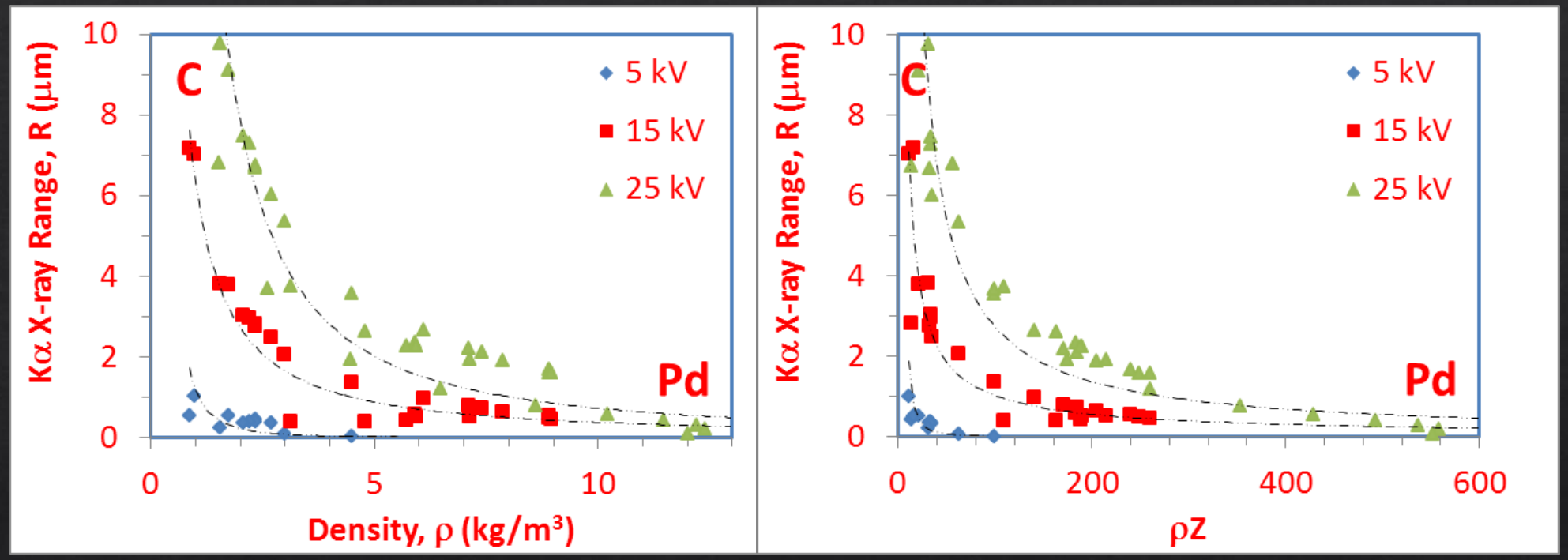

Characteristic X-ray range increases as E increases, and decreases as ρ and ρZ increase

Electron range versus Characteristic X-ray range

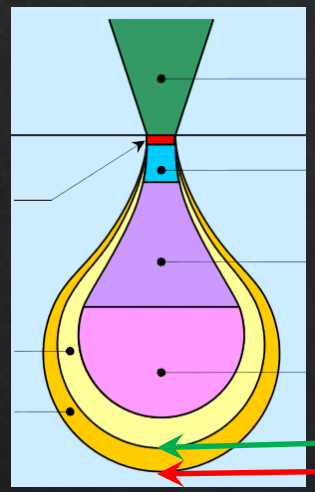

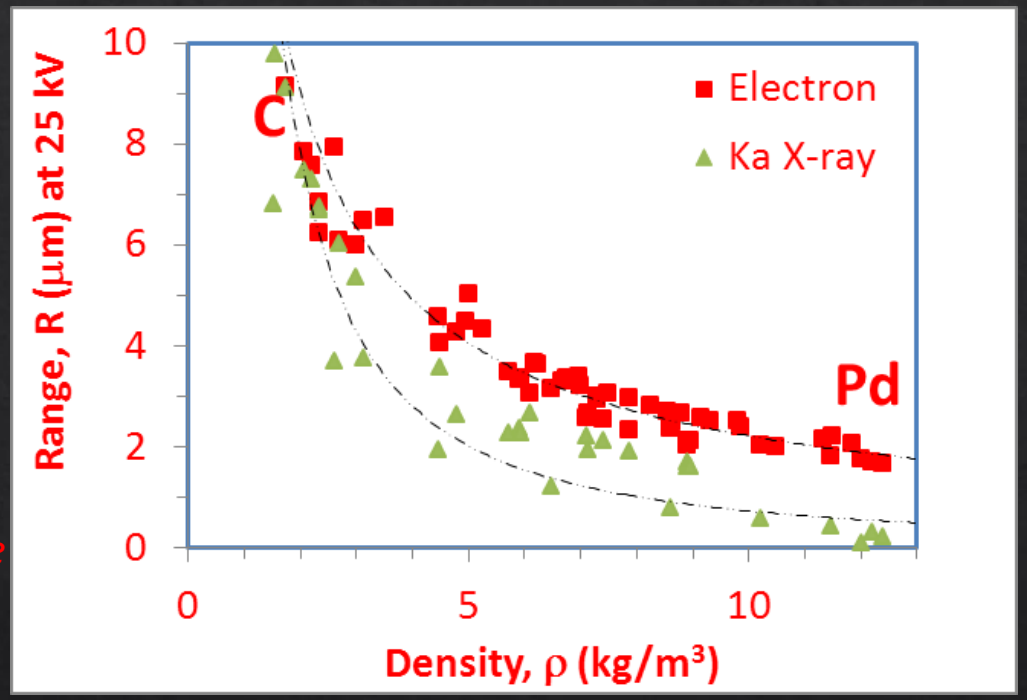

$$R_{electron} = 0.0276\ E^{1.67}\ \frac{A}{\rho Z^{0.889}}$$

$$R_{X\text{-}ray} = 0.033\ (E^{1.7} - E_c^{1.7})\ \frac{A}{\rho Z}$$

The characteristic X-ray range is always smaller than the electron range

- E = beam energy
- E_c = critical excitation energy of the sample atomic shell
- Z = atomic number
- A = atomic weight
- ρ = density

Continuum (Bremmstrahlung) X-ray generation

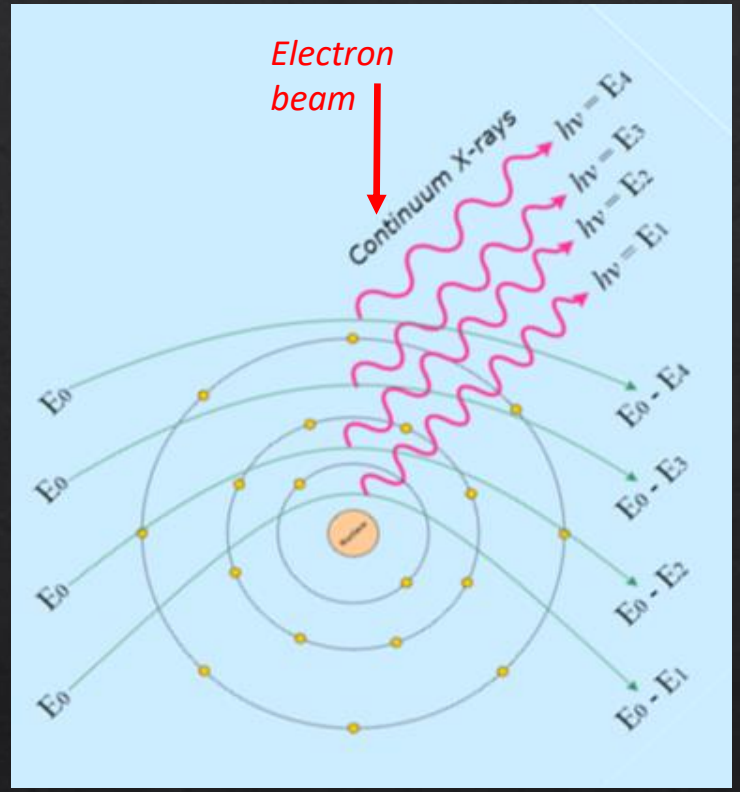

Produced by deceleration of beam electrons in the electrostatic field of target atoms

Energy lost by beam electrons is converted to x-ray

(Maximum energy of continuum X-rays = electron beam energy)

X-ray spectrum

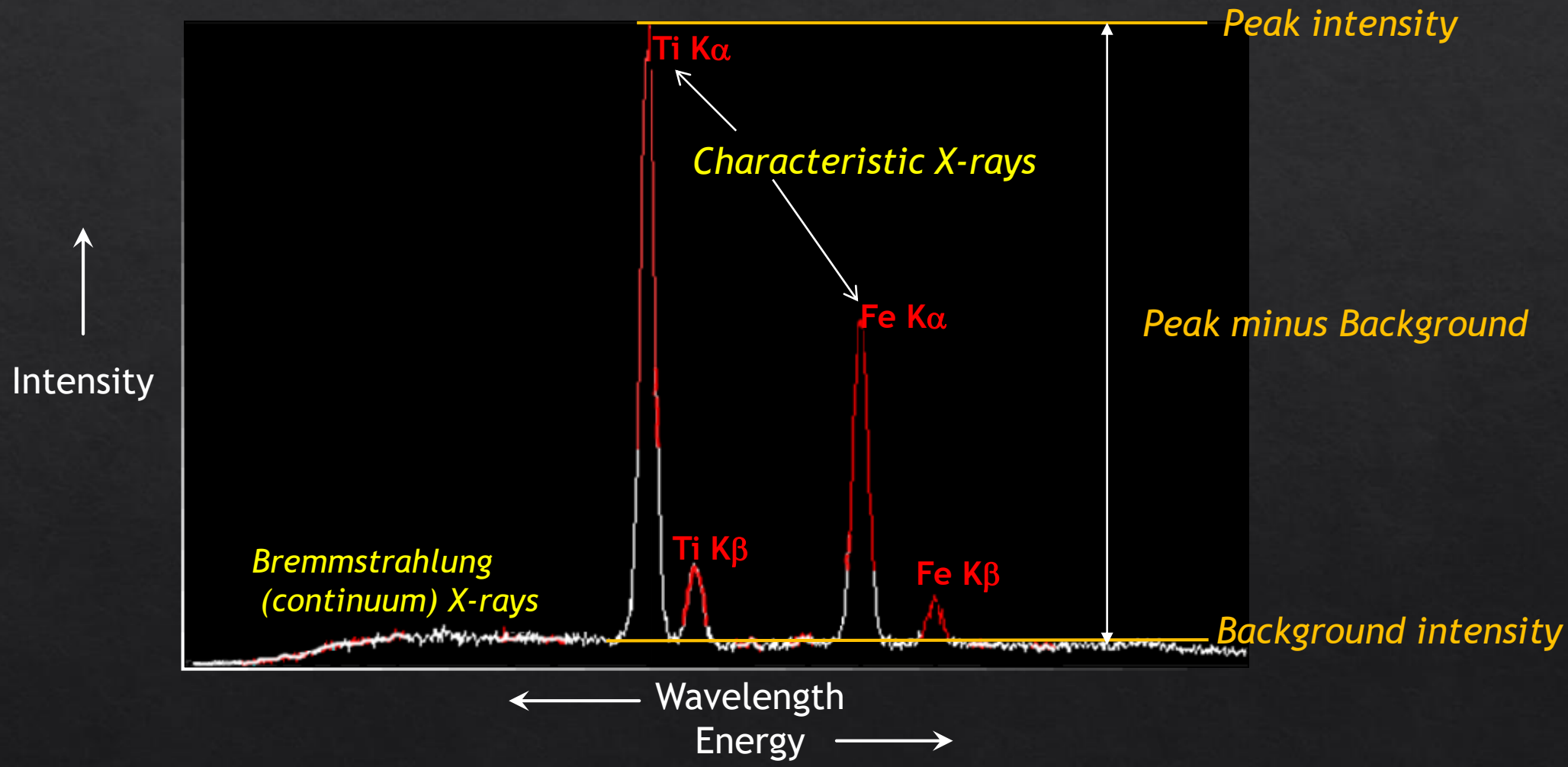

X-ray background intensity

Low-Z sample
(Ca-Fe poor)
Low background

High-Z sample
(Ca-Fe rich)
High background

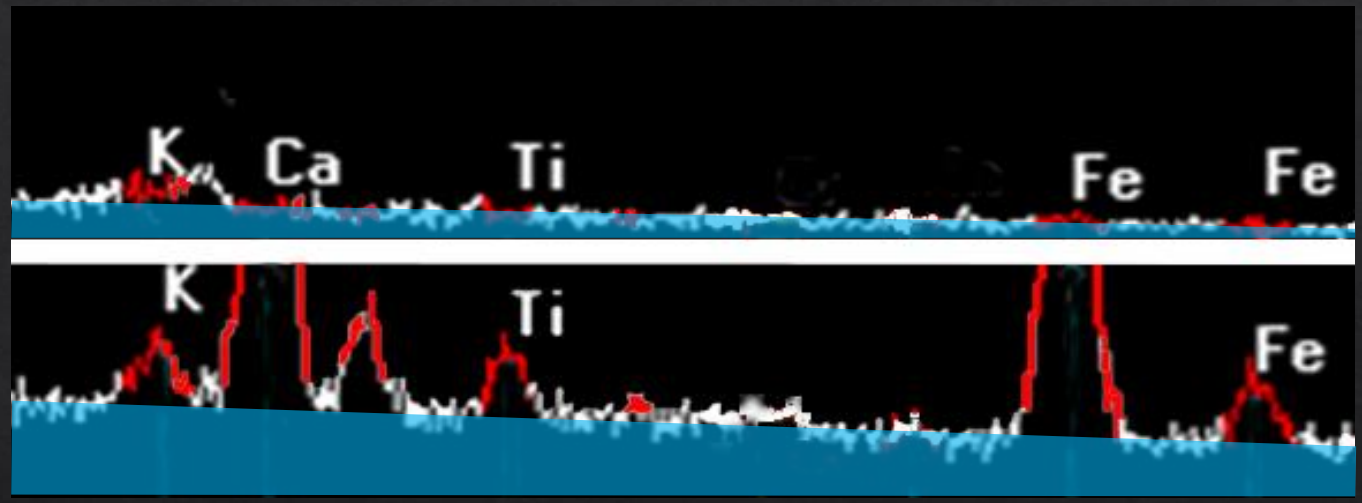

Increases with sample atomic number

Energy Dispersive Spectrometer (EDS)

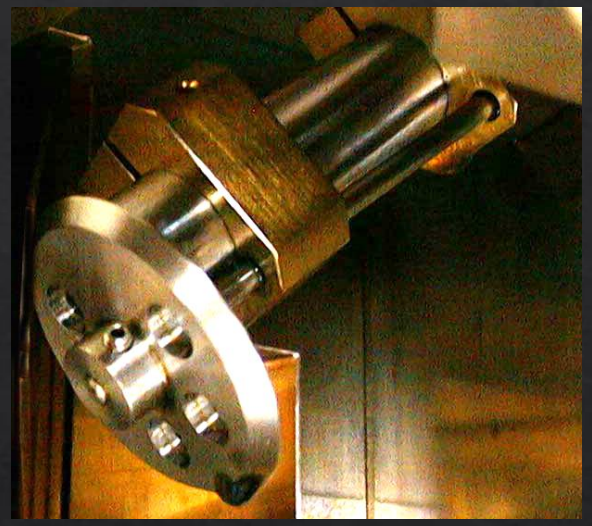

- *EDS detector: solid-state semiconductor, window and aperture*
- *Multichannel analyzer (MCA) to process x-ray signal*

Energy Dispersive Spectrometer (EDS)

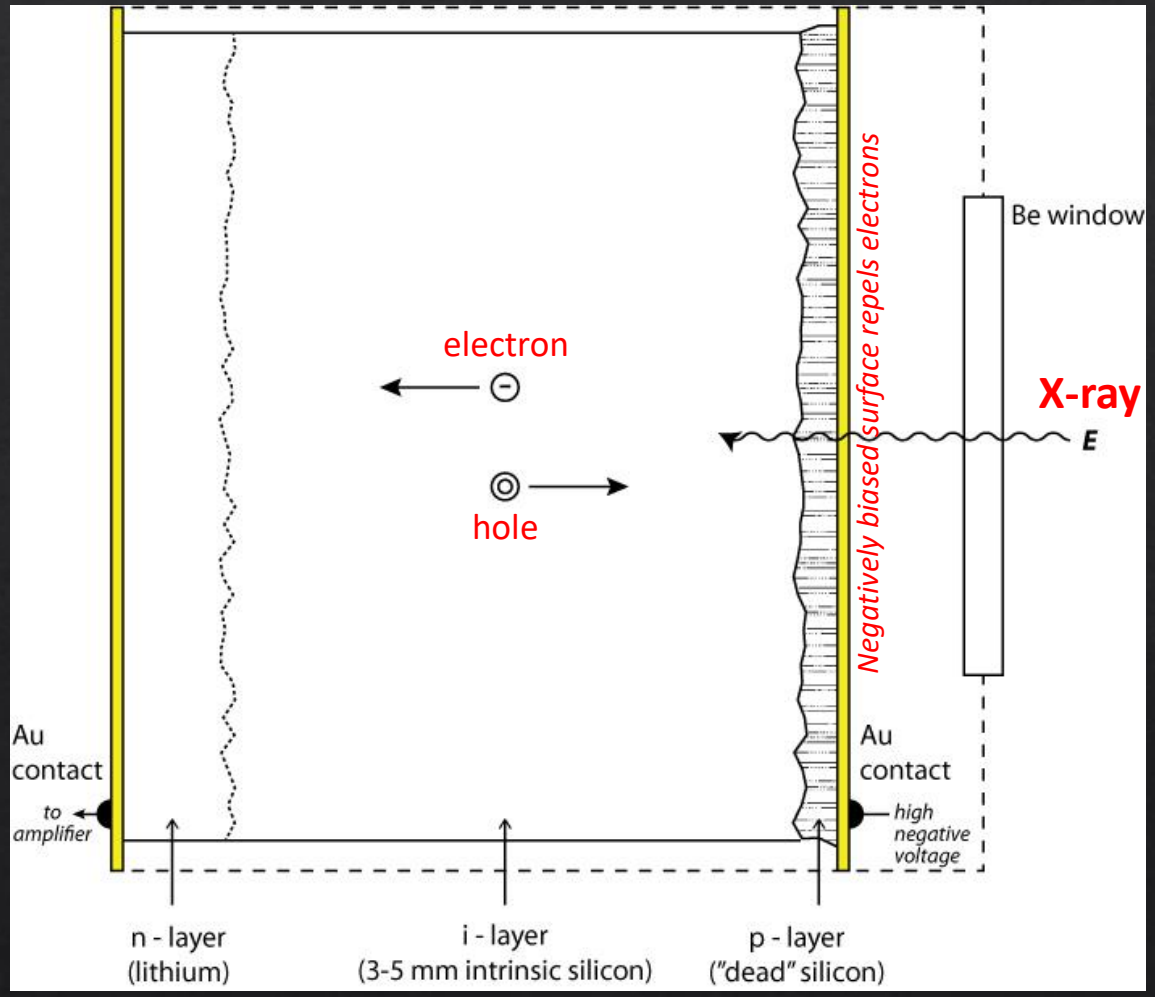

Lithium-drifted silicon, or Si(Li), "p-i-n" detector

- *A single crystal of silicon*
- *Pure Si is a semiconductor. But impurity of boron, a p-type dopant, makes it a conductor*
- *Lithium, an n-type dopant, counteracts the effect of boron and produces an intrinsic semiconductor*

Wavelength Dispersive Spectrometer (WDS)

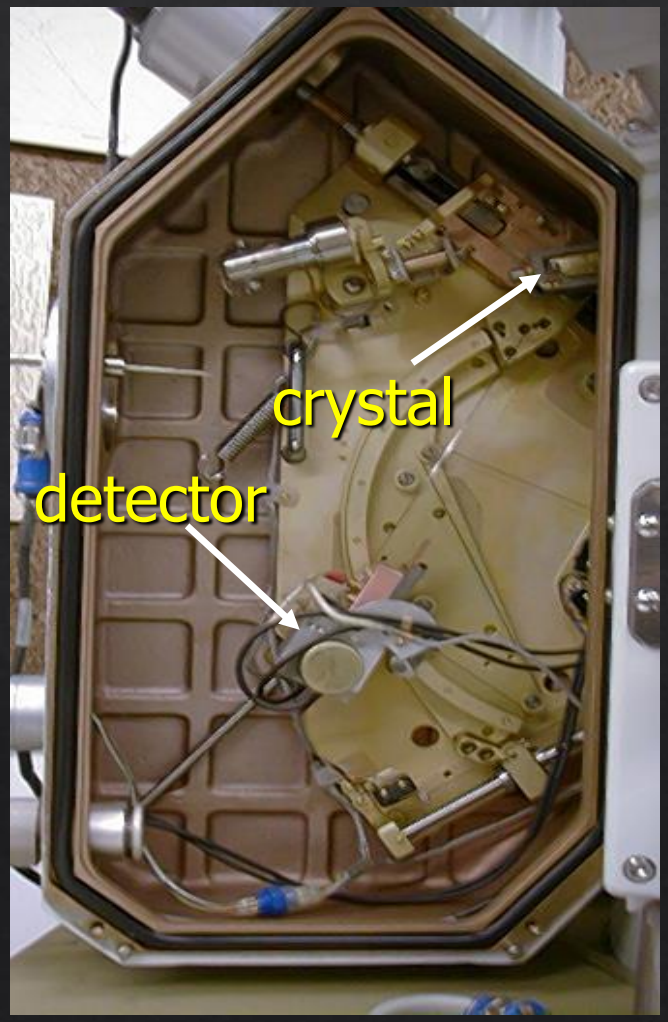

Wavelength Dispersive Spectrometer (WDS)

$$\sin\theta = \frac{L}{2R}$$

θ: angle of incidence or diffraction

L: distance between sample and crystal

R: radius of focusing (Rowland) circle

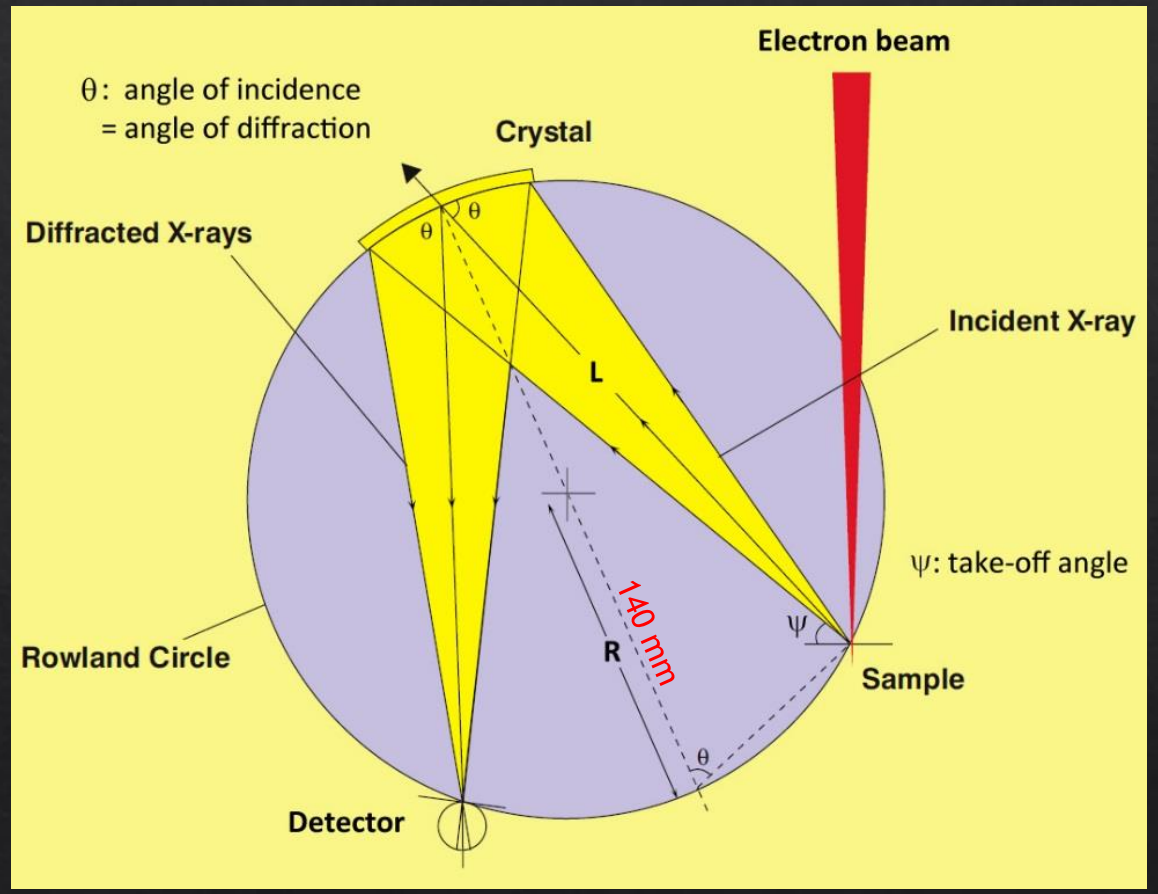

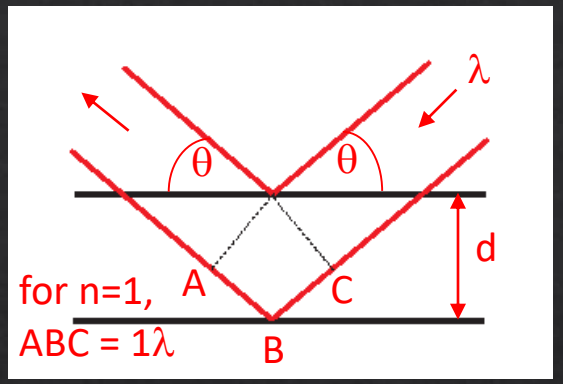

Bragg's Law:

$$n\lambda = 2d \sin\theta$$

n: order of diffraction

λ: wavelength of X-ray

d: lattice spacing in diffracting crystal

θ: angle of incidence or diffraction

"L-value": $L = n\lambda \frac{R}{d}$

L-value

Example 1.

Si Kα

Energy, E = 1.74 keV

$$\lambda\ (\text{nm}) = \frac{1.2398}{E\ (\text{keV})}$$

$$\text{Wavelength, } \lambda = \frac{1.2398}{1.74} = 0.7125 \text{ nm}$$

$$L\ (\text{mm}) = n\ \lambda\ (\text{nm})\ \frac{R\ (\text{mm})}{d\ (\text{nm})}$$

For n =1, R = 140, and d_{TAP} = 1.2879,

$$L_{TAP} = 1 \times 0.7125 \times \frac{140}{1.2879}$$

$$= \mathbf{77.45\ mm}$$

Example 2.

U Mα

Energy, E = 3.17 keV

$$\lambda\ (\text{nm}) = \frac{1.2398}{E\ (\text{keV})}$$

$$\text{Wavelength, } \lambda = \frac{1.2398}{3.17} = 0.3911 \text{ nm}$$

$$L\ (\text{mm}) = n\ \lambda\ (\text{nm})\ \frac{R\ (\text{mm})}{d\ (\text{nm})}$$

For n=1, R = 140, and d_{PET} = 0.4371,

$$L_{PET} = 1 \times 0.3911 \times \frac{140}{0.4371}$$

$$= \mathbf{125.27\ mm}$$

WDS operation: detecting a specific λ

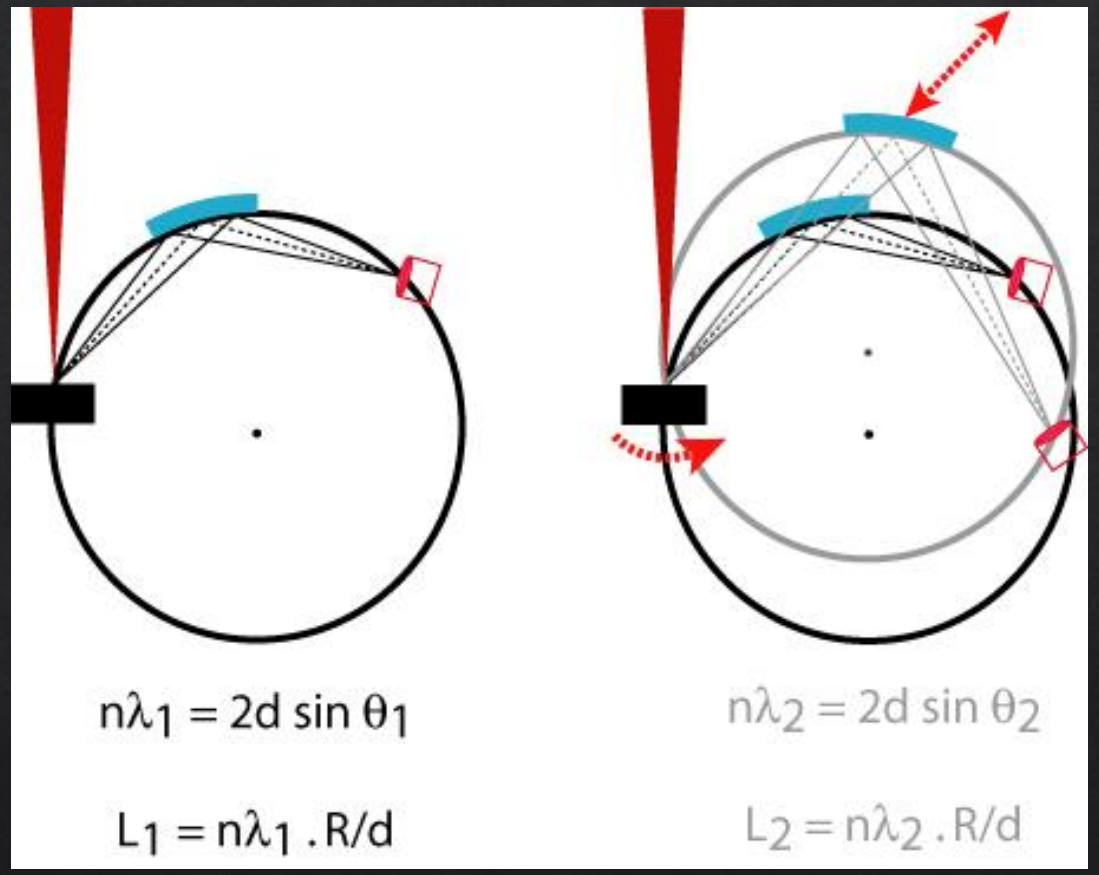

Radius of Rowland circle (R) *is fixed*

Different wavelengths (λ_1, λ_2) *can be diffracted using appropriate incidence angles* (θ_1, θ_2) *by changing the L-value* (L_1, L_2)

First and second order diffractions

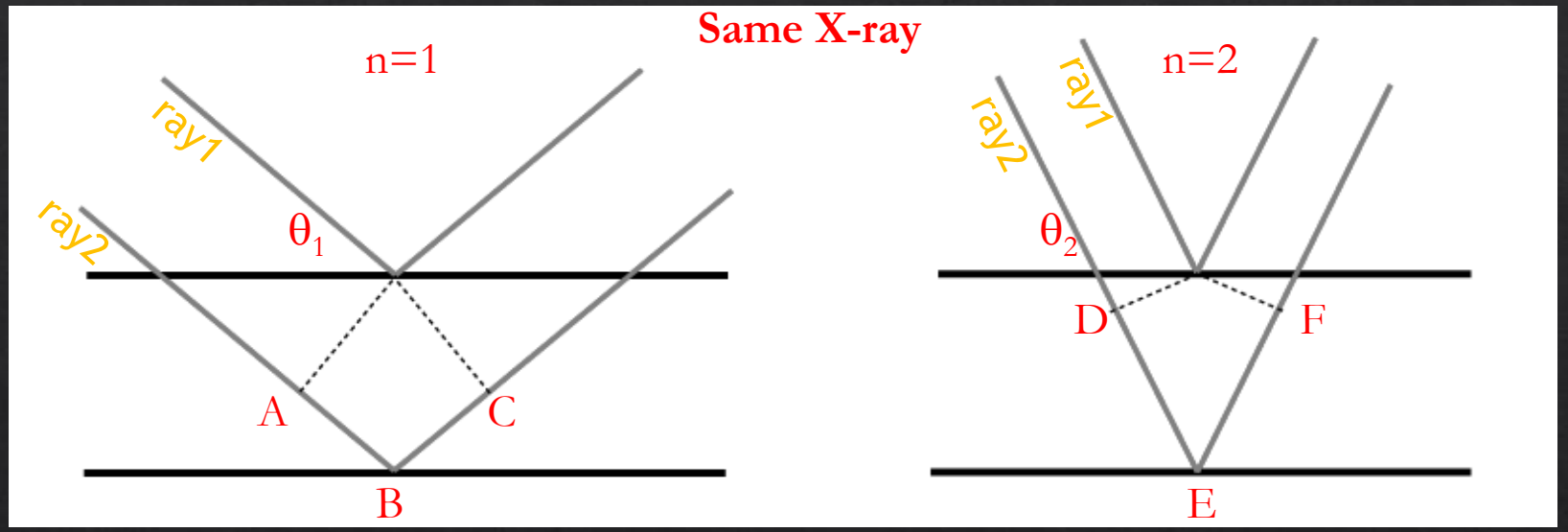

$1\lambda = 2d \sin\theta_1$
$= ABC$

$2\lambda = 2d \sin\theta_2$
$= DEF$

path DEF = 2 x path ABC

Same wavelength is diffracted at different diffraction angles; $\sin\theta_2 = 2\sin\theta_1$

Spectrometer movement

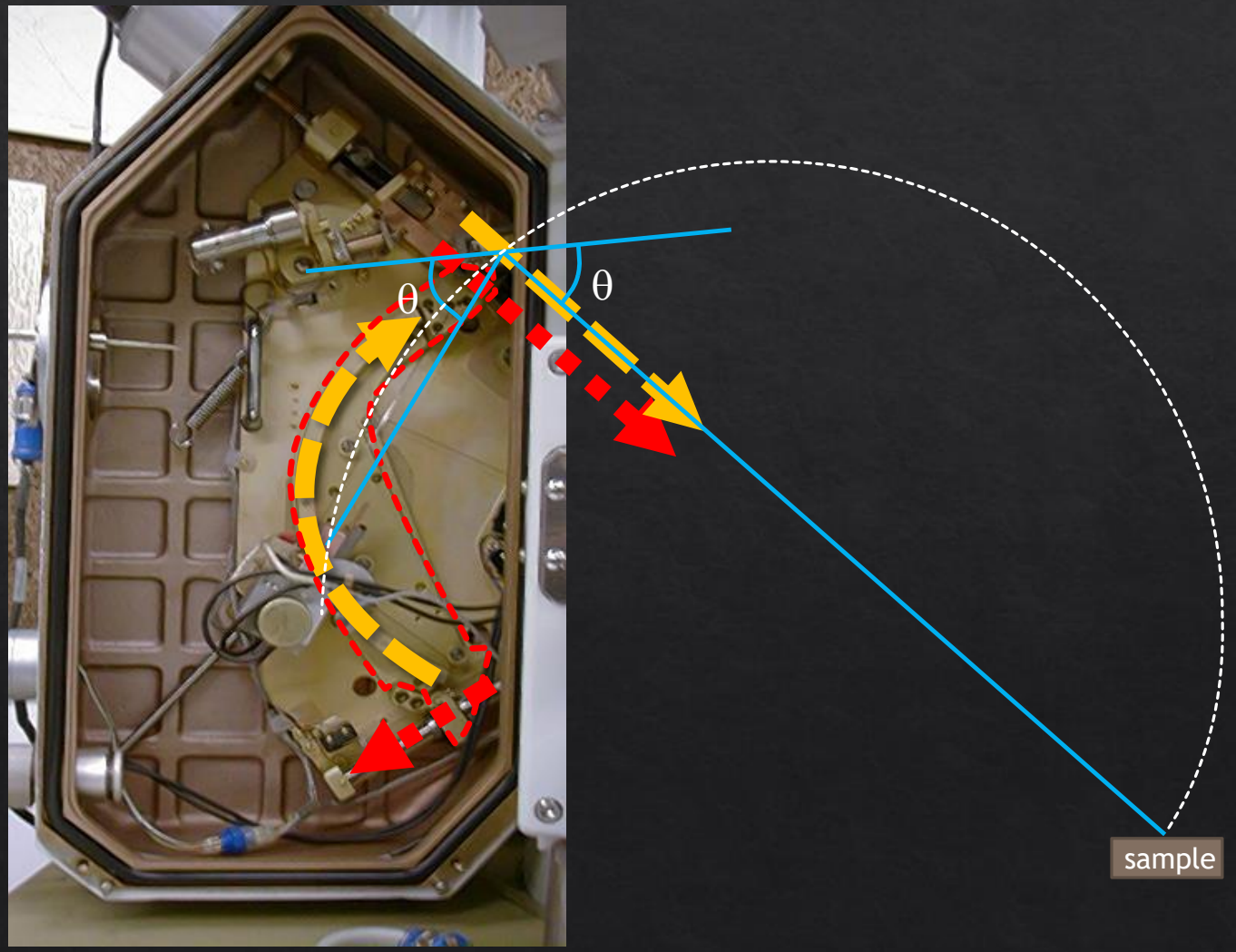

Theoretical limits of spectrometer movement

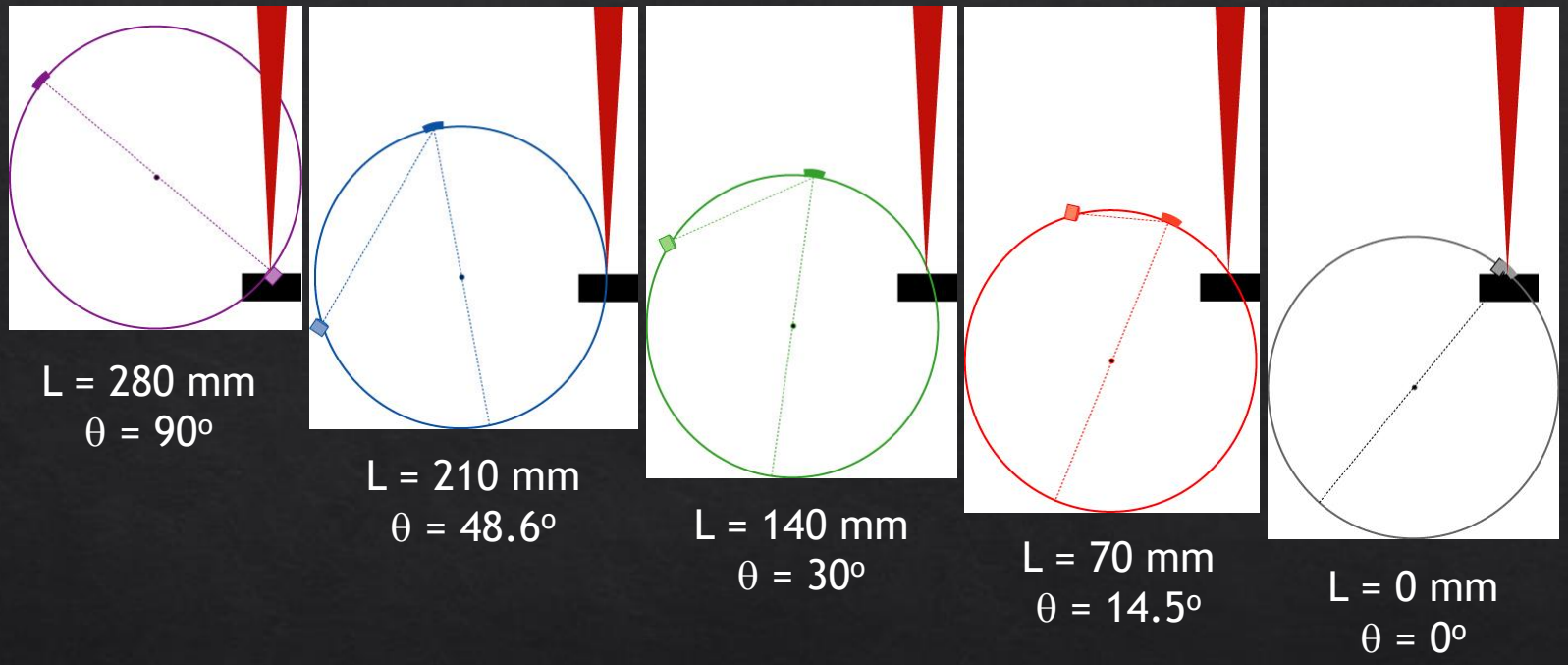

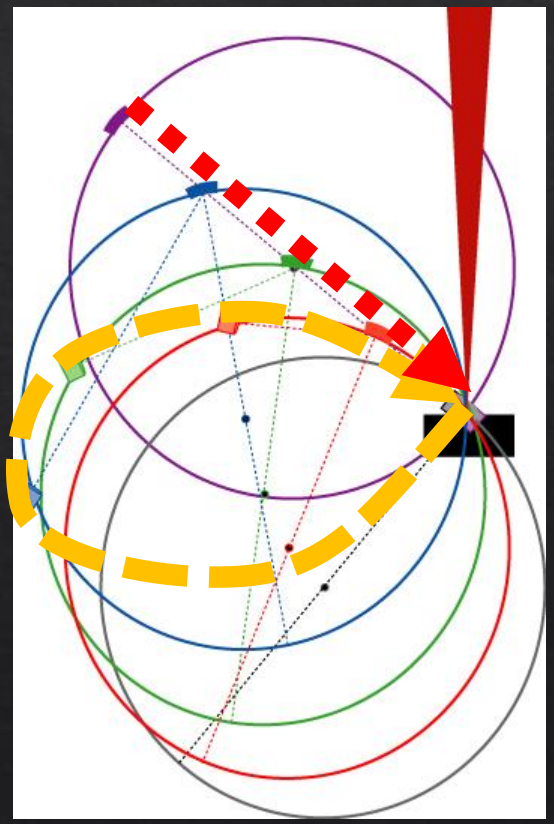

Theoretical limits:

$2R \geq L \geq 0$

$280\ mm \geq L \geq 0\ mm$

$90^{o} \geq \theta \geq 0^{o}$

Actual limits of spectrometer movement

Actual limits:
$60\ mm \leq L \leq 260\ mm$
$12.4^o \leq \theta \leq 68.2^o$

Typically,
$70\ mm \leq L \leq 230\ mm$
$14.5^o \leq \theta \leq 55.2^o$

Recall $\sin\theta = \frac{L}{2R}$, so $L = 2R\sin\theta$ and $\theta = \sin^{-1}\left(\frac{L}{2R}\right)$

Hence,

for $L = 60$ mm, $\theta = 12.4^o$ and $L = 260$ mm, $\theta = 68.2^o$

for $\theta = 15^o$, $L = 72.47$ mm and $\theta = 55^o$, $L = 229.36$ mm

Spectrometer with smaller focusing circle

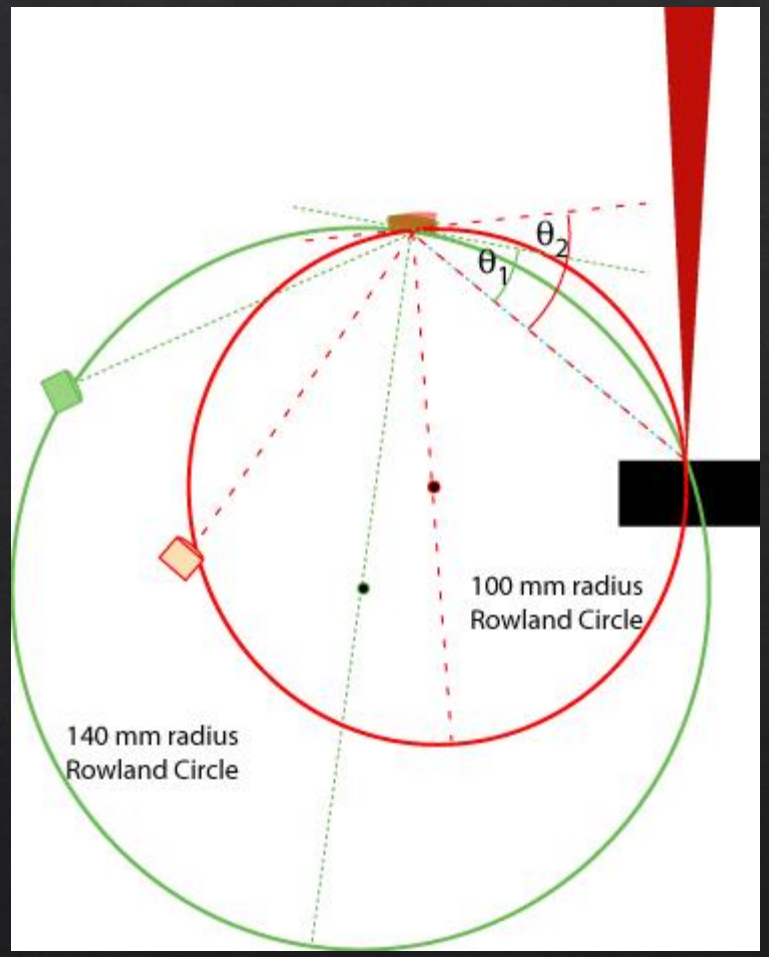

140 mm focusing circle:

$n\lambda_1 = 2d \sin \theta_1$

$L = n\lambda_1 \cdot 140/d$

100 mm focusing circle:

$n\lambda_2 = 2d \sin \theta_2$

$L = n\lambda_2 \cdot 100/d$

With the crystal at the same position (**same L**), *different X-rays* (λ_1, λ_2) *are diffracted by the two spectrometers*

Spectrometer with smaller focusing circle

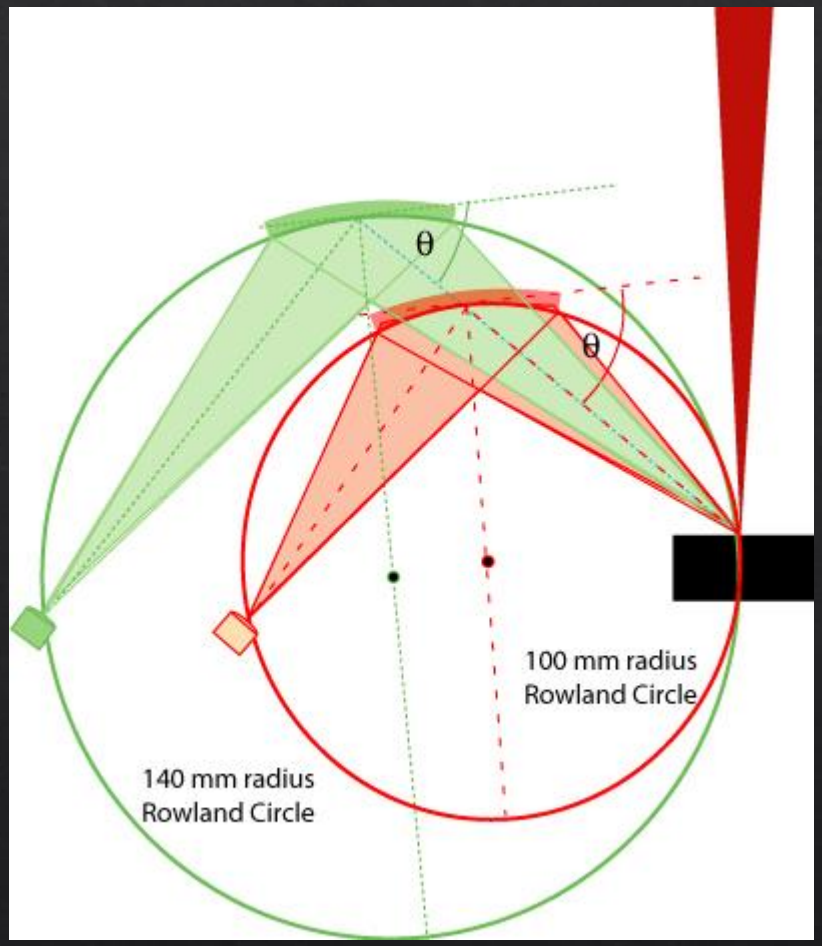

140 mm focusing circle:

$n\lambda = 2d \sin \theta$

$L_{140} = n\lambda \cdot 140/d$

100 mm focusing circle:

$n\lambda = 2d \sin \theta$

$L_{100} = n\lambda \cdot 100/d$

With the crystal at different positions (**L_{140}, L_{100}**), *the same X-ray* (**same λ**) *is diffracted by the two spectrometers*

L values for H-type WD spectrometer

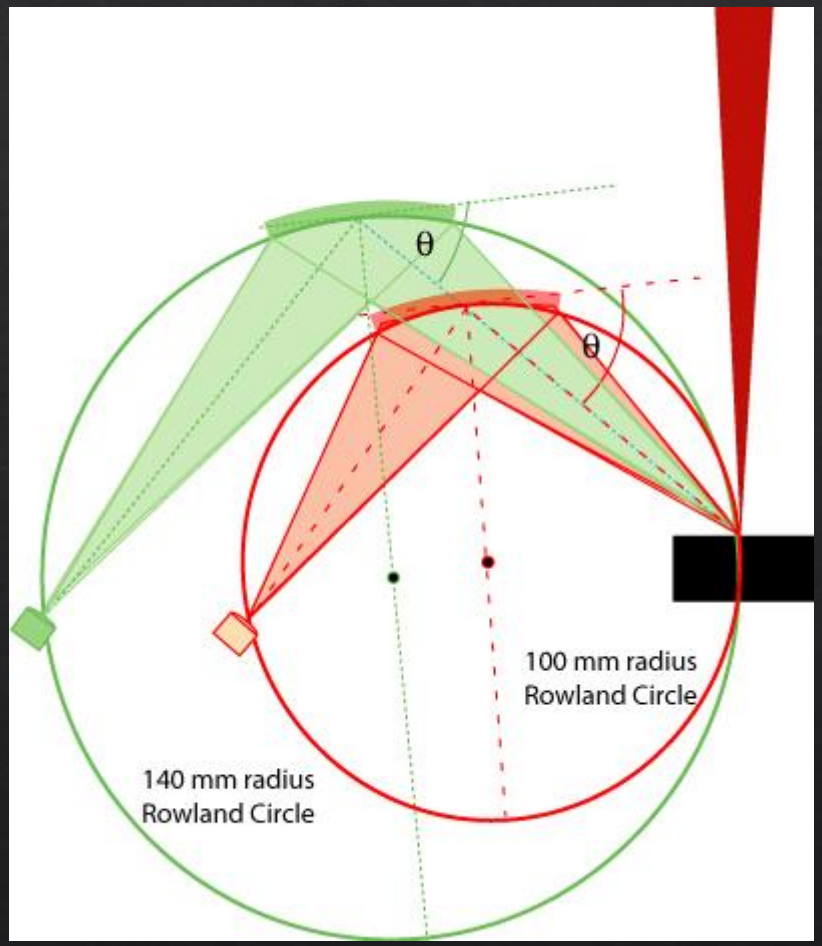

$L_{100} = n\lambda \,.\, 100/d$

L in "L-Value Chart" is L_{140}

L_{100} is converted to L as follows:

$L = GR \,.\, L_{100}$

$= GR \,.\, n\lambda \,.\, 100/d$

where

Gear Ratio, $GR = L_{140}/L_{100}$

Larger Johansson-type crystal closer to sample yields a higher count rate

2d of x-ray diffractors

Crystal lattices

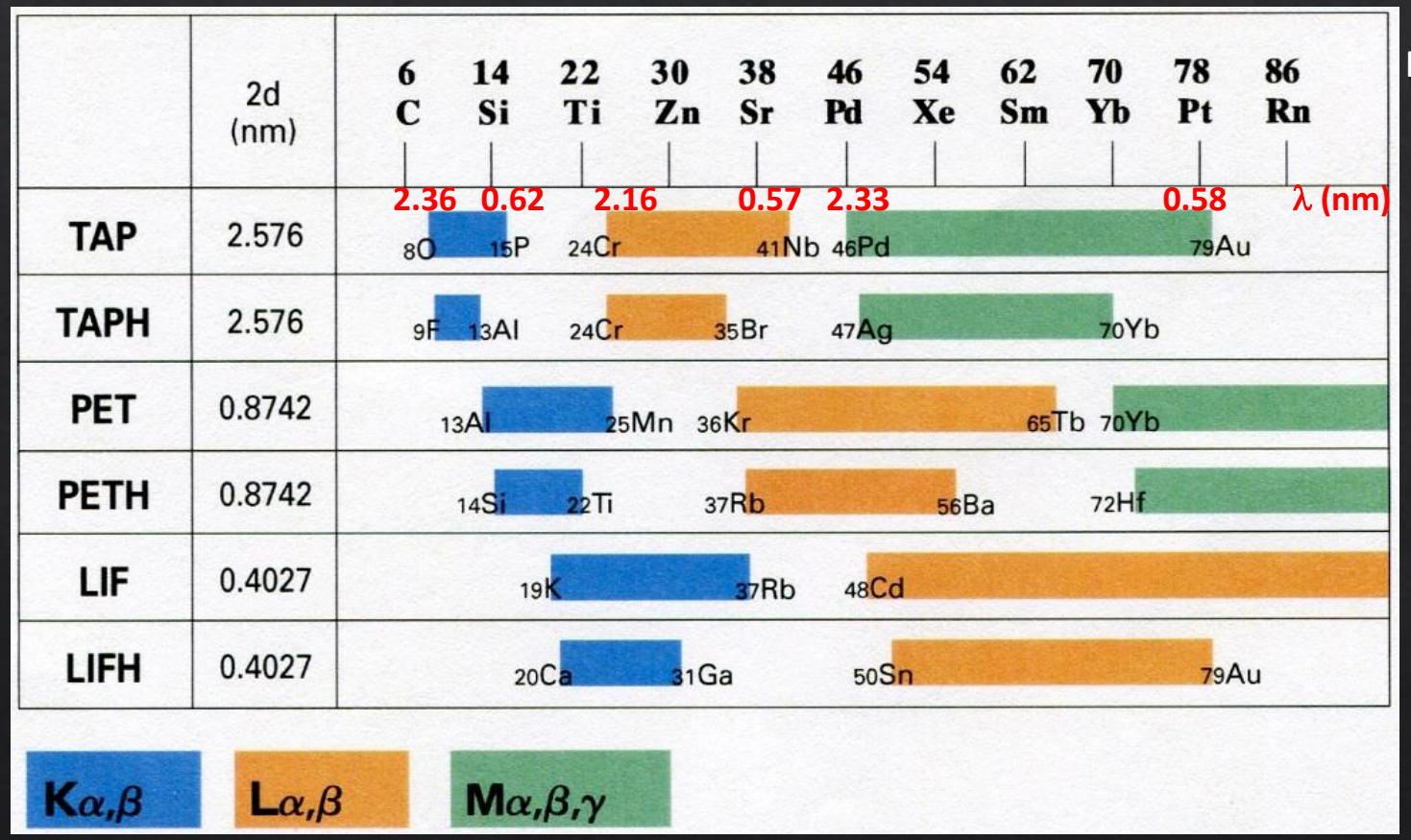

For n=1, ~ 0.5d < λ < 1.6d (L 73-230 mm or θ 15-55°)

Layered structures

	2d (nm)	Be	B	C	N	O	F
NSTE	Approx.10		○	○	○	○	
LDE1	Approx.6			△	◎	◎	◎
LDE2	Approx.10		◎	◎	◎	○	
LDEB	Approx.14.5	◉	○				
LDE1H	Approx.6			△	◎	◎	
LDE2H	Approx.10		◎	◎			
LDENH	Approx.8			○	◎		
LDE3H	Approx.20	◉	○				
LDE5H	Approx.8			◎	◎		
LDEBH	Approx.14.5	◉	◎				

λ *of* BeKα = 11.27 nm

BeKα *can be diffracted only by* 2d > 11.27 nm *diffractors,*

e.g., LDE3H with L= 157.8 mm, and LDEB or LDEBH with L=217.6 mm

X-ray diffractors

Analyzing crystals
and
layered structures

Table 4.6 Analyzing crystals and element analysis ranges for X-ray spectrometer

Analyzing crystals	2d (nm)	Type of spectrometer	Element analysis ranges
NEWSTE	10.04	TXE	B, O, S, V
TAPJ	2.5757	XCE	O, P, Cr, Nb, Pd, Au
		TXE	O, P, Cr, Nb, Pd, Hg
PETJ	0.8742	XCE	Al, Mn, Kr, Tb, Yb, U
		TXE	Al, Fe, Kr, Dy, Yb, U
LIF	0.40267	XCE, TXE	K, Rb, Cd, U
LDE1	About 6	XCE, TXE	C, Ne
LDE2	About 10	XCE, TXE	B, O
LDEB	About 14.5	XCE, TXE	Be, B
TAPH	2.5757	H	F, Al, Cr, Br, Ag, Yb
PETHS	0.8742	H	Si, Ti, Rb, Ba, Hf, U
LIFHS	0.40267	H	Ca, Ga, Sn, Au
LDE1H	About 6	H	C, O
LDE2H	About 10	H	B, C
LDE3H	About 20	H	Be, B
LDE4H	About 12	H	B, C
LDE5H	About 8	H	C, N
LDENH	About 8	H	C, N
LDEBH	About 14.5	H	Be, B

K line (Kα or Kβ) L line (Lα or Lβ) M line (Mα, Mβ or Mγ)

XCE: XCE type X-ray spectrometer (XM-86010)
TXE: TXE type X-ray spectrometer (XM-86020)
H: H type X-ray spectrometer (XM-86030)

Curved diffracting crystals

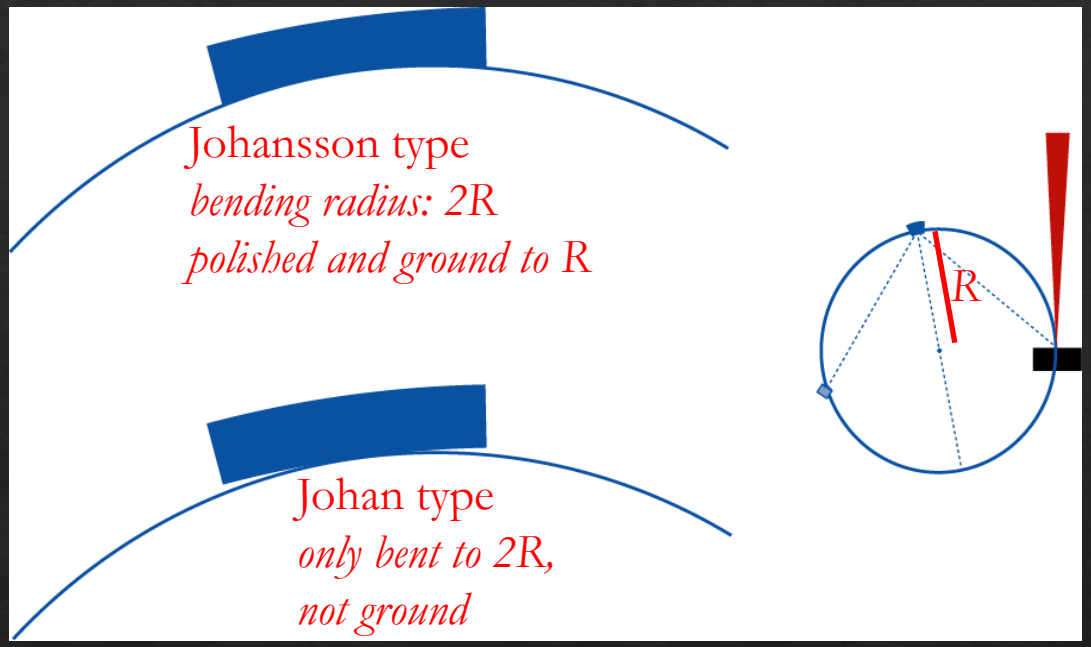

Peak resolution with fully focusing Johansson-type crystal: FWHM ~10 eV

Some defocusing in Johan-type, but resolution is not compromised

X-ray focusing ellipsoid

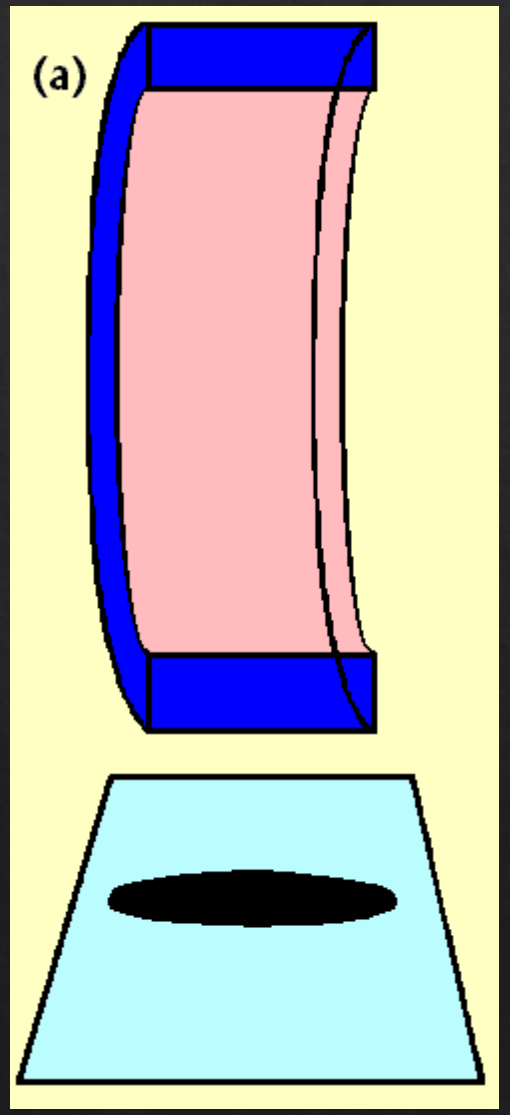

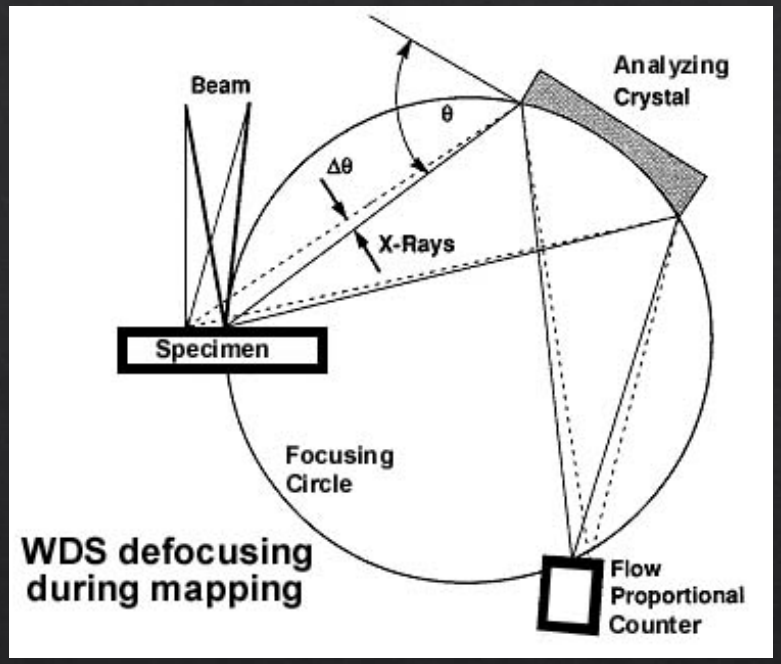

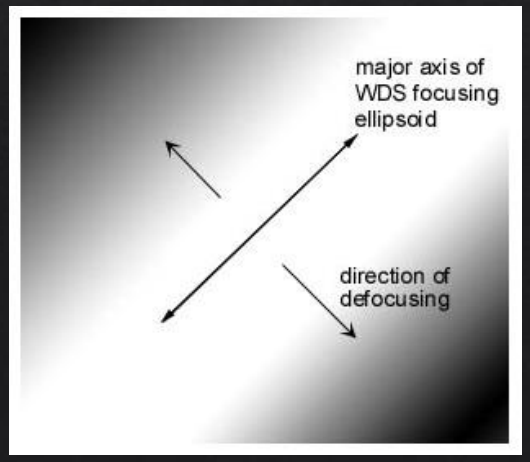

Spectral resolution: Full-Width Half-Maximum (FWHM)

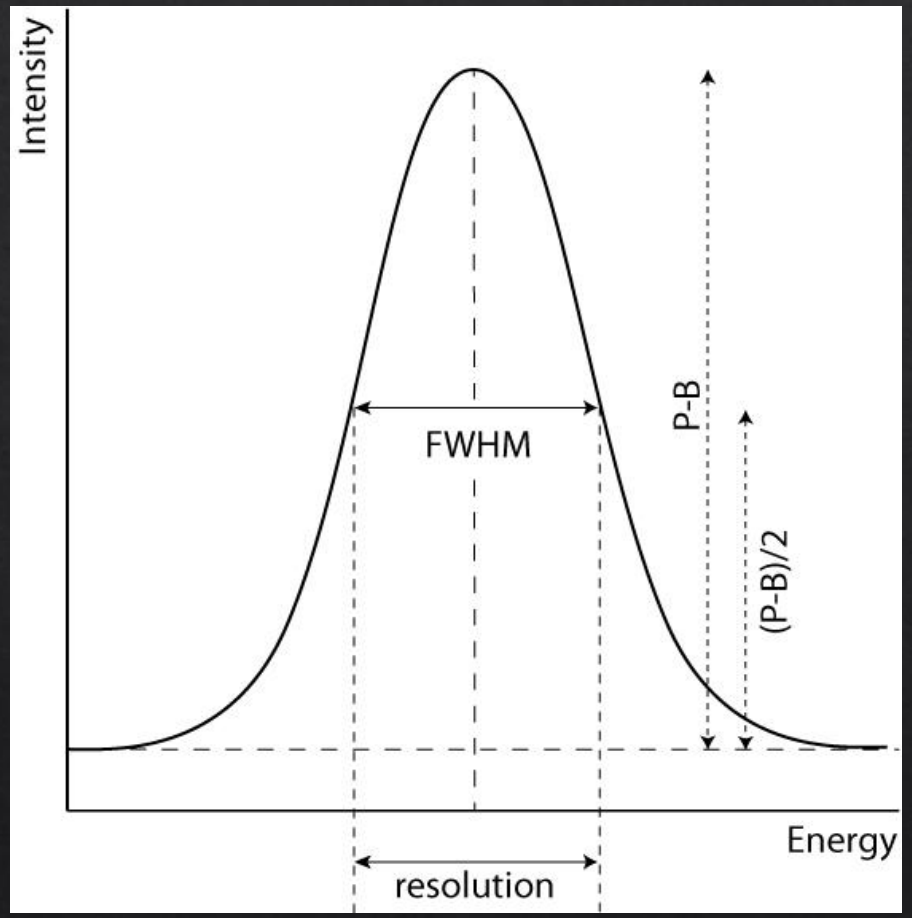

WDS vs. EDS spectral resolution

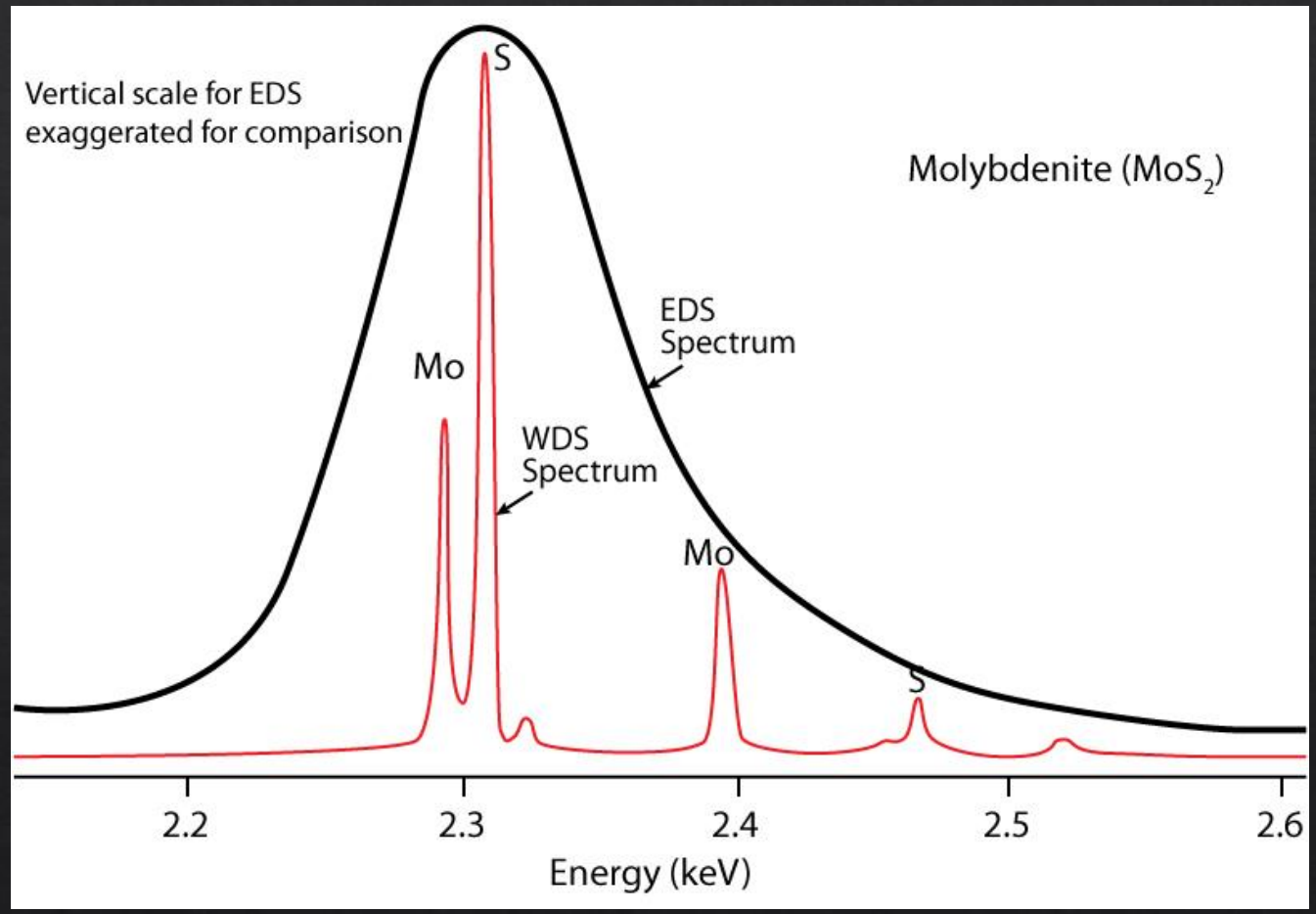

Peak overlaps in EDS spectrum

*Peak resolution of WDS spectrum (FWHM **~10 eV**)*
*EDS spectrum (FWHM **~150 eV**)*

WDS detector: Proportional counter

Tungsten collection wire at 1-3 kV voltage

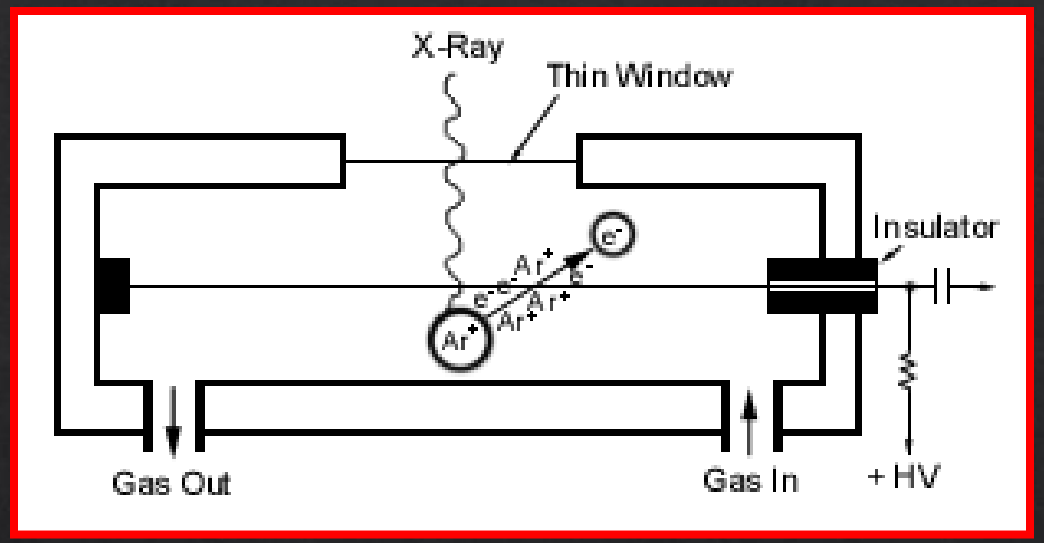

- *Pulse voltage generated is proportional to the voltage in the collection wire*
- *Signal is amplified through a chain of outer-shell ionizations in the gas by the incoming X-ray*

- *Flow counter:*
  - *P-10 gas (90% Argon + 10% methane quenching agent)*
  - *Polypropylene window*
- *Sealed counter:*
  - *Xenon gas*
  - *Beryllium window*

Signal amplification

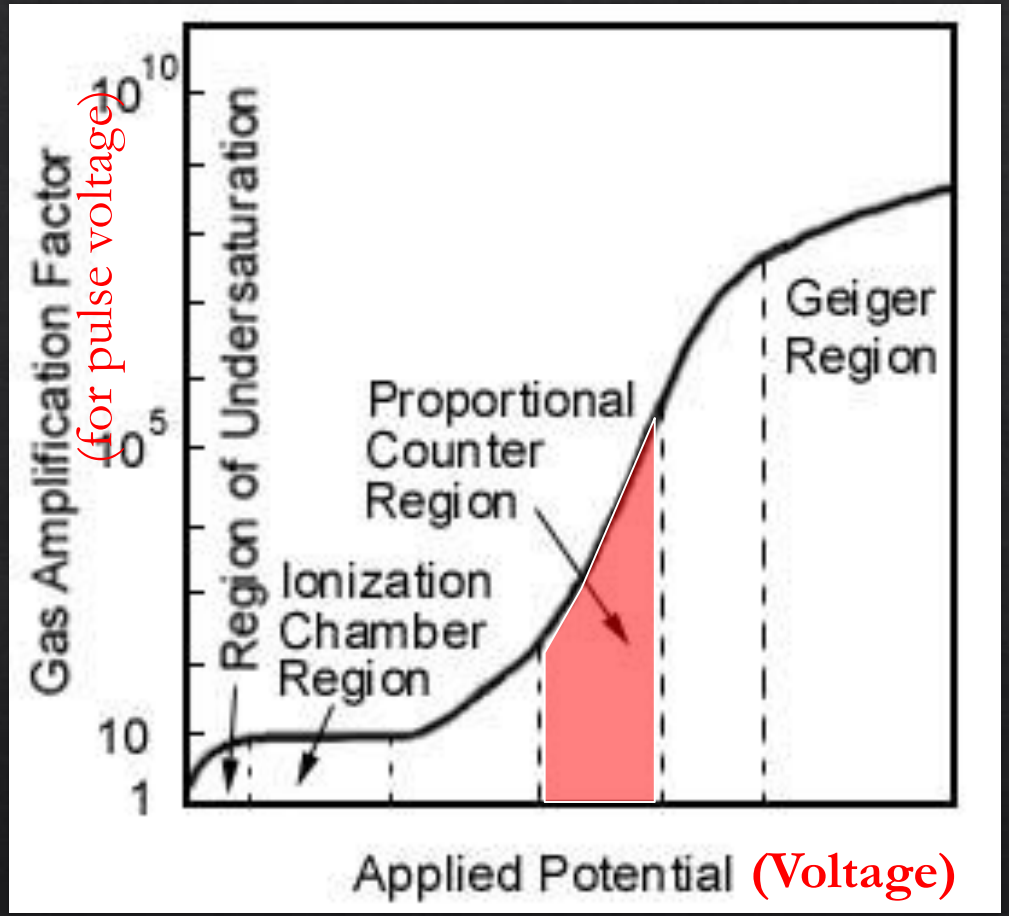

Typical voltage range in the proportional counter region for a W wire: 1600-1850 V

The amplification factor is proportional to the voltage in the collection wire in the proportional counter region

Quantum efficiency of counter gas

Highest when the incoming X-ray is least absorbed by the gas

Decreases when the X-ray is absorbed by ionizing an inner shell of the gas atom, generating ArKα or XeLα

Lowest when $E_{X\text{-}ray}$ is slightly higher than the $E_{c(Ar\ K\text{-}shell)}$ or $E_{c(Xe\ L\text{-}shell)}$ absorption edges

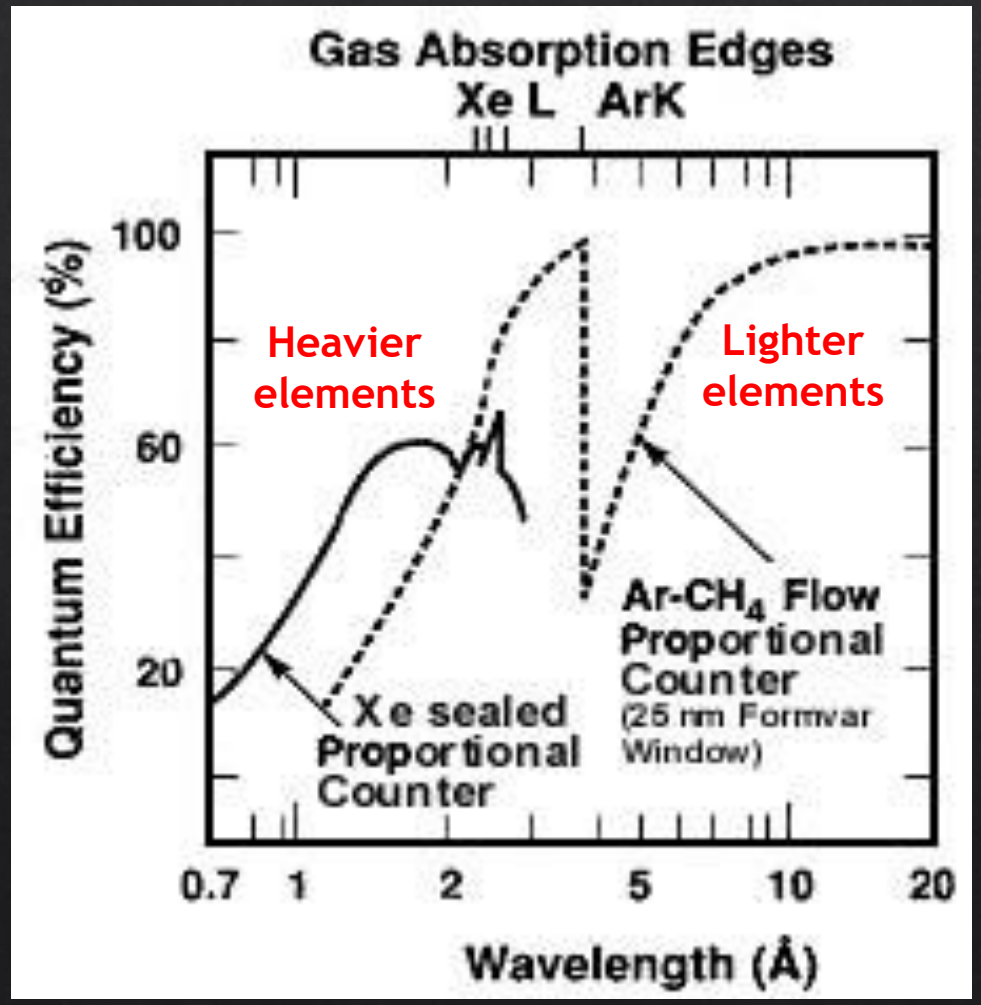

- *Argon: long wavelength (low energy) detection*
- *Xenon: short wavelength (high energy) detection*

Proportional counter setup

Proportional counter output:

Voltage pulses including noise and X-ray signal

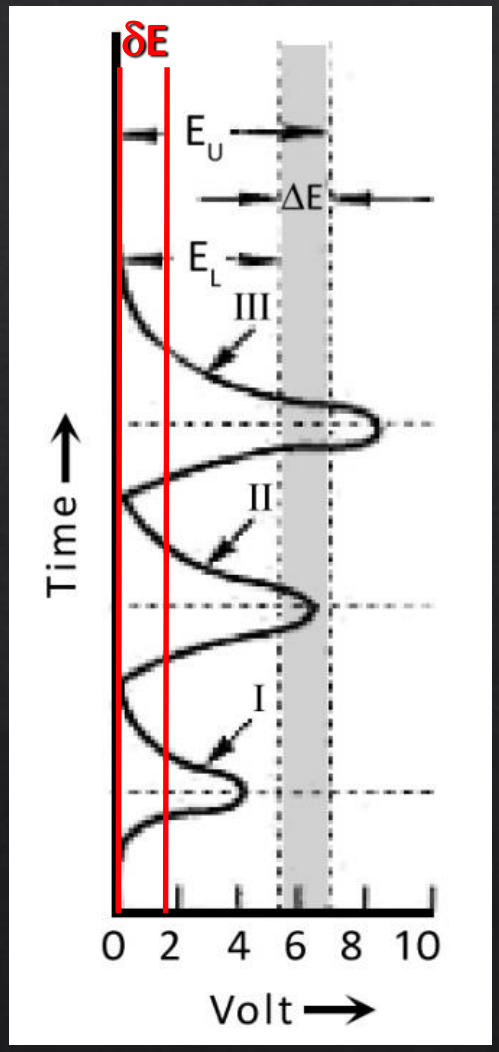

baseline

window

A Single Channel Analyzer (SCA) allows only X-ray pulses to pass through **ΔE** *and enter the detector*

*An SCA scan shows the variation in count rate as a small voltage window (*δ**E**) *is moved across the voltage range*

*Baseline and window voltages (*Δ**E**) are set to filter out noise*

ΔE *is determined through Pulse Height Analysis (PHA) using an SCA scan*

Pulse voltage in SCA scan

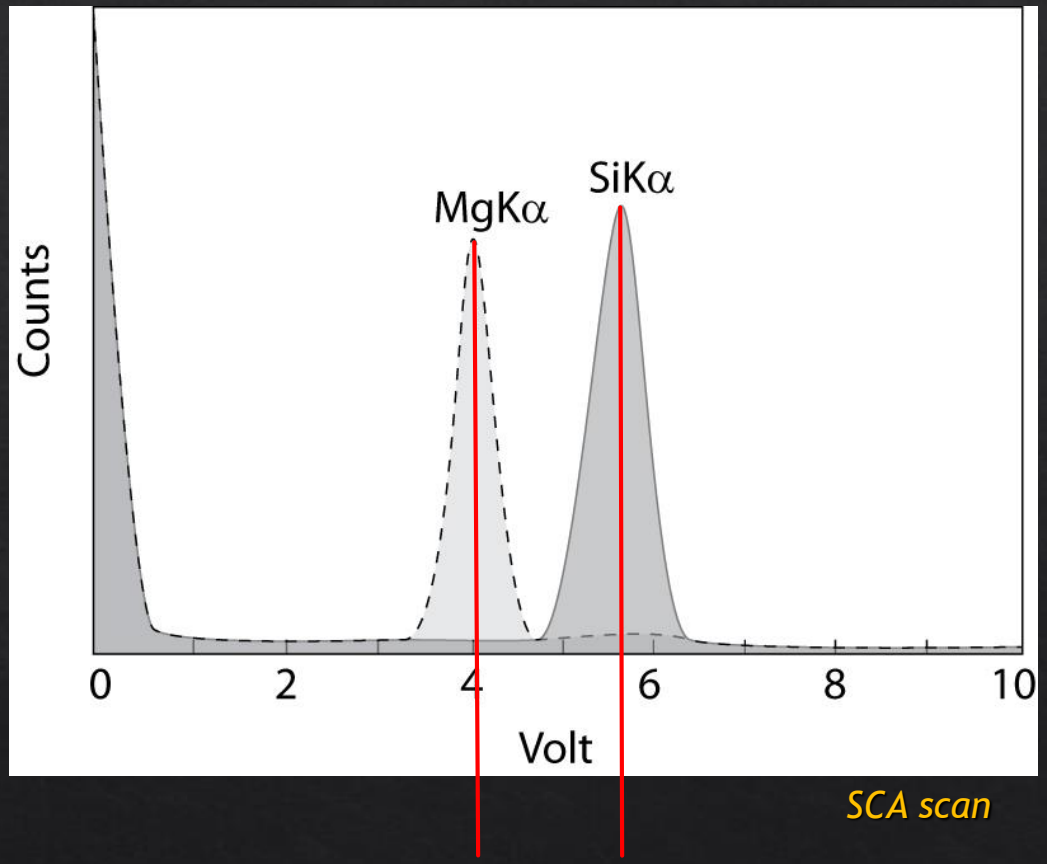

Pulse voltage is proportional to energy of the X-ray being detected

Energy of SiKα (1.739 keV) is ~1.39 times the energy of MgKα (1.253 keV)

If the pulse for MgKα is at 4 V, the pulse for SiKα will be at 4 x 1.39 = 5.56 V

Escape peak in SCA scan

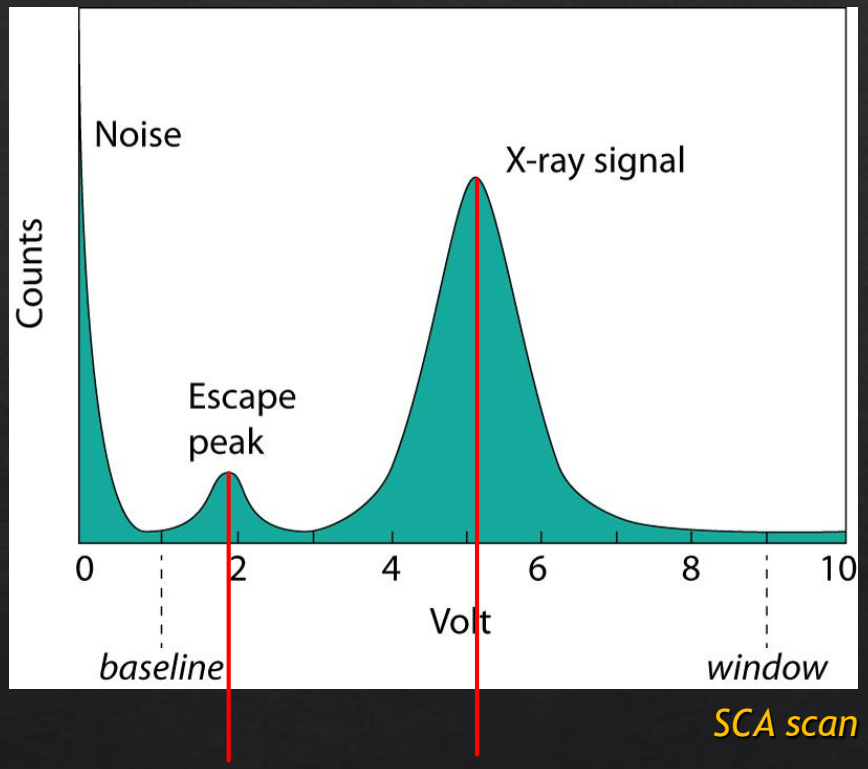

Energy difference between incoming X-ray and ArKα or XeLα

Escape peaks fluoresced by incoming X-ray:

- P-10 counter: ArKα
- Xenon counter: XeLα

If the pulse for NiKα (7.47 keV) is at 5.20 V, the XeLα (4.11 keV) escape peak will be at 5.2 - (7.47-4.11) = 1.84 V

Proportional counter window

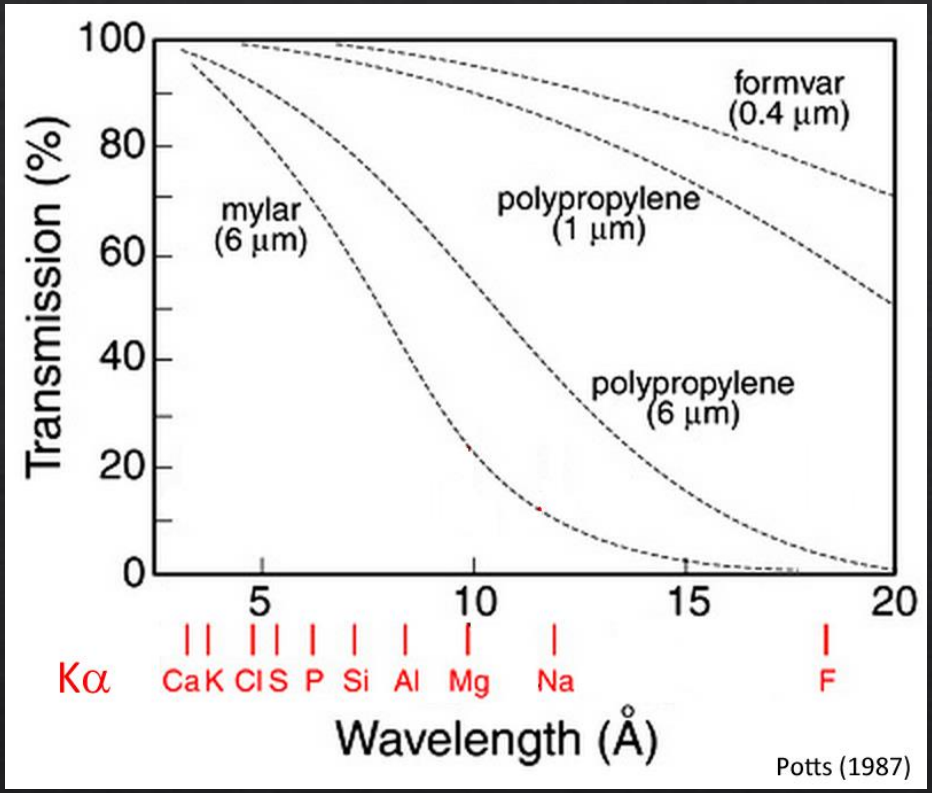

- *Mylar has lower transmittance than polypropylene, especially for light element X-rays*
- *Thin windows are better for light elements*
  - *1 µm thick polypropylene window transmits ~60% of the F Kα*
  - *6 µm thick polypropylene window transmits only ~5% of the F Kα*

SCA configurations

Analyzing crystal	X-ray detector	Standard pulse height of a specified X-ray		SCA Configuration setting				
		X-ray	Pulse height (V)	Mode	Base (V)	Window (V)	Gain	HV (V)
NEWSTE, STE, LDE2	GPC	CKα	2.5	Diff	0.7	9.3	64	Set the HV so that the specifie d X-ray has the standard pulse height.
TAPJ, TAPH	GPC/GPCH	MgKα	4.1	Diff	0.7	9.3	32	
PETJ, PETHS	XPC/XPCH	TiKα	5.8	Int	0.7	9.3	64	
LIF, LIFHS	XPC/XPCH	CuKα	5.0	Int	0.7	9.3	32	
PETJ, LIF, PETHS, LIFHS	GPC/GPCH	TiKα	7.0	Int	0.7	9.3	16	
LDE1	GPC	OKα	3.0	Diff	0.7	9.3	64	
LDEB, LDEBH	GPC/GPCH	BKα	3.5	Diff	0.7	9.3	128	
LDE1H	GPCH	CKα	2.0	Diff	0.7	9.3	64	
LDE2H, LDE4H	GPCH	CKα	3.0	Diff	0.7	9.3	64	
LDE3H	GPCH	BKα	3.5	Diff	0.7	9.3	128	
LDENH, LDE5H	GPCH	CKα	2.5	Diff	1.0	8.0	64	

Detector slit

Table 4.5 Relationship of analyzing crystals' lattice planes and spacings to standard detector slit settings

Analyzing crystals	STE NEWSTE	TAPJ TAPH	PETJ PETHS	LIF LIFHS	LDE1 LDE1H	LDE2 LDE2H	LDEB LDEBH	LDE3H	LDE5H LDENH	LDE4H
Lattice planes	STE Film	TAP (100)	PET (002)	LIF (200)	Super-lattice	Super-lattice	Super-lattice	Super-lattice	Super-lattice	Super-lattice
2d (nm)*	10.04	2.5757	0.8742	0.40267	About 5.8 – 6.2	About 9.5 – 10.5	About 14.5 – 15	About 19 – 21	About 7.6 – 8.4	About 11.5 – 12.5
Standard slit settings	Open	300 – 550 μm			Open					

* LDE series of analyzing elements having artificial superlattice structures differ from 2d, lattice spacing, each other, even if they are the same kind.

Table 4.8 X-ray spectrometer detector slit settings

X-ray spectrometers	Position that allows slit exchange (mm)	Slit settings		
		Pushed-in position	Midway position	Pulled-out position
XCE	L ≒ 110	300 μm	Open	550 μm
TXE				
H	L ≒ 140			500 μm
FCS	L ≒ 110	300 μm with Mylar film		300 μm

Positioned at convergence point of diffracted X-rays (on the Rowland circle)
Cuts off stray X-rays and electrons

Crystal, counter and slit combinations

Table 4.4 Standard combination of analyzing crystals, detector slits and detectors

X-ray spectrometers	TXE type X-ray spectrometer		XCE type X-ray spectrometer		H type X-ray spectrometer		FCS type four-crystal X-ray spectrometer			
Radius of Rowland circle (mm)	140		140		100		140			
Spectrometer installation ports	2nd or 1st*4		All		Other than 3rd		1st or 2nd			
Analyzing crystals	NEWSTE	TAPJ	PETJ	LIF	LIFHS*1	PETHS*1	STE	TAPJ	PETJ	LIF
Detector slits	Open	300 μm or 550 μm	300 μm or 550 μm		500 μm*2		Open	300 μm	300 μm with Mylar film	
Detectors	Gas flow proportional counter		Xe-filled proportional counter		Xe-filled proportional counter*3		Gas flow proportional counter			
Remarks	The 733-NEW STE, a new large stearate crystal, is provided for analysis of light elements.		Analyzing crystals can be exchanged at any desired analysis position.		A stronger X-ray intensity is available than with another X-ray spectrometer. The dedicated analyzing crystals and detector are used. The analyzing crystals can be exchanged at any desired position within 90% of the analysis range.		Four crystals (STE, TAPJ, PETJ, LIF) are provided, allowing a wide range of analysis (a combination of these crystals allows analysis from B to U). The analyzing crystals can be exchanged at any desired position within 90% of the analysis range.			

*1: An LDE1H/LDE2H combination is available for analyzing light elements.
*2: Select "Open" for the light element analysis combination.
*3: Use a gas flow proportional counter (GPCH) for the light element analysis combination.
*4: When the front-type EDS detector is installed, the TXE X-ray spectrometer cannot be installed to the 1st port.

Mylar is used when light elements are not being analyzed

Electron Probe Microanalysis

Wavelength Dispersive Spectrometry (WDS)

Goals:

- High resolution elemental mapping
- Measurement of concentration of all elements in a microscopic volume

EPMA: Analytical procedure

- Sample preparation (mounting, polishing, carbon coating)

Carbon coating is essential for electrically insulating material

- Setting up the Electron Microprobe

Voltage, beam conditions, spectrometers, etc.

- Qualitative analysis with EDS and WDS

Important if nothing is known about the chemical composition

- Measurement of X-ray intensities in standards (calibration)

A different standard can be used for each element

- Measurement of X-ray intensities in the specimen and matrix corrections

Different components of matrix corrections

Sample preparation

- Sample cut and mounted in epoxy, if necessary
- Coarse polished with 240-600 SiC paper (53-16 μm)
- Fine polished with alumina slurry or diamond paste on cloth (grit size 1.00-0.25 μm)
- Washed with water in ultrasonic cleaner after each polishing step, dried after final step, wiped with ethanol
- Carbon coated (25 nm thick) in vacuum

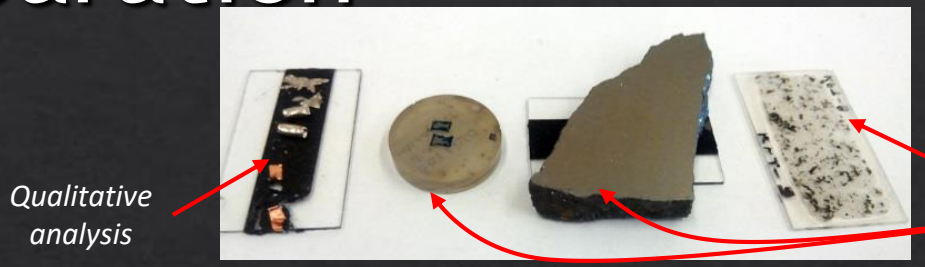

brass monitor

Setting up the Electron Microprobe

Voltage, filament saturation and beam alignment

- Accelerating voltage
  - *Depends on overvoltage requirement,*

    e.g., FeKα is not emitted with a 5 keV beam because $E_{c(K\text{-}shell)}$=7.111 keV, and U < 1.
  - *For a particular accelerating voltage, overvoltage will be different for different elements. U should be about 2-10.*

- Filament saturation and beam alignment
  - *Saturation: filament current is adjusted to ensure saturation*
  - *Gun bias should be properly set to ensure optimum emission*
  - *Shift and tilt alignment: beam current is maximized*
  - *Wobble adjustment: image defocusing should be symmetrical above and below the optimum beam focusing plane. If not, position of the objective lens aperture is adjusted*
  - *Astigmatism correction: image is distorted if the spot is elliptical. Stigmator controls are used to remove distortion*

Setting up the Electron Microprobe

Spectrometer choice

- Crystal/diffractor

  E.g., FeKα ($\lambda_{K\alpha}$ = 0.1937 nm, $E_{FeK\alpha}$ = 6.4 keV) can be diffracted by TAP (2d = 2.5757 nm), PET (2d = 0.8742 nm) and LIF (2d = 0.4027 nm).

  For n = 1, equation $\lambda = 2d\sin\theta$, i.e., $\theta = \sin^{-1}\left(\frac{\lambda}{2d}\right)$, and for R = 140 mm, equation $L = n\lambda\frac{140}{d}$ indicate:

  θ = 4.3° and L = 191.2 mm for TAP

  θ = 12.8° and L = 62.0 mm for PET

  θ = 28.8° and L = 134.6 mm for LIF

  Acceptable ranges for θ and L are 15-55° and 70-230 mm. Therefore, LIF is the correct choice.

- Counter and window

  Xe has a better quantum efficiency for FeKα. So, a Xe counter with a Be window is the right choice.

- SCA settings

  Using LIF/Xe counter and an appropriate collection wire voltage, the CuKα ($E_{CuK\alpha}$ = 8.04 keV) pulse should be set at 5 V by performing PHA. Since $E_{FeK\alpha} = 0.8 \times E_{CuK\alpha}$, the FeK$\alpha$ pulse should be at 0.8 x 5 = 4 V.

- Detector slit

  For higher energy X-rays, smaller slits are recommended. The 300-550 μm slit should be selected.

Setting up the Electron Microprobe

Beam current, counting time and probe diameter

- Beam current and counting time depend on concentration of the element of interest

Higher beam current increases count rate and longer counting time increases total counts (improves precision)

For N counts, the counting uncertainty is $\frac{1}{\sqrt{N}}$ *X 100 %. Counting is more precise as N increases. E.g.,*

For 25 counts, the uncertainty is 20 %

For 100 counts, the uncertainty is 10 %

For 10,000 counts, the uncertainty is 1 %

- Probe diameter

Sometimes necessary to use a defocused beam (large spot size). E.g.,

Average composition of fine-grained material (spot size > grain size)

Hydrous, and Na or F containing glass: Na migrates away, F migrates toward the spot (spot size ~ 10 μm)

Qualitative analysis with BSE and EDS

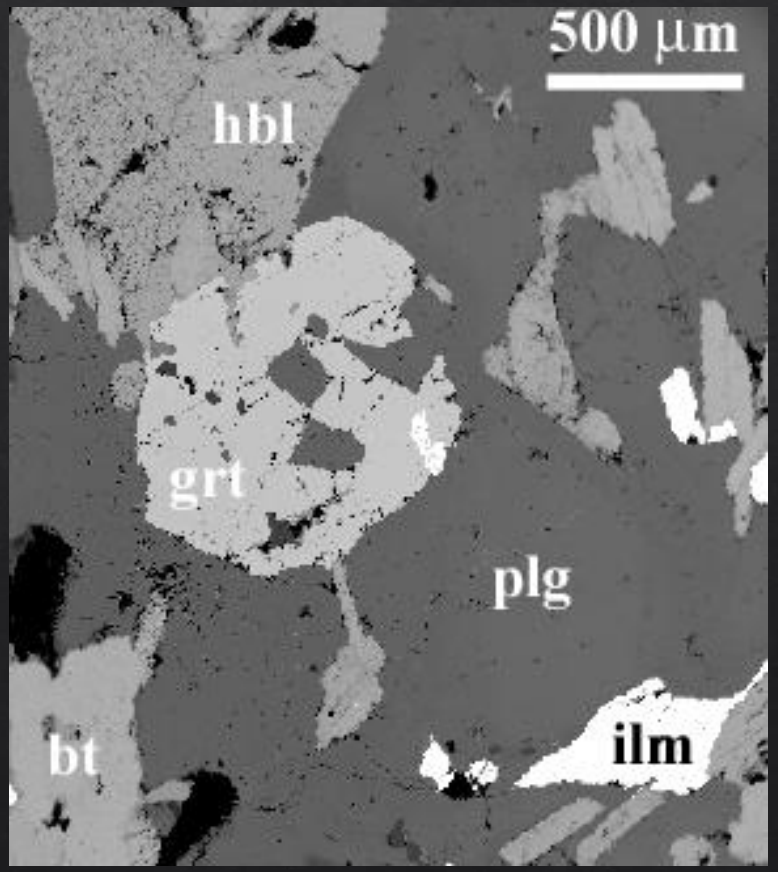

Mean atomic number: plg < hbl < bt < grt < ilm

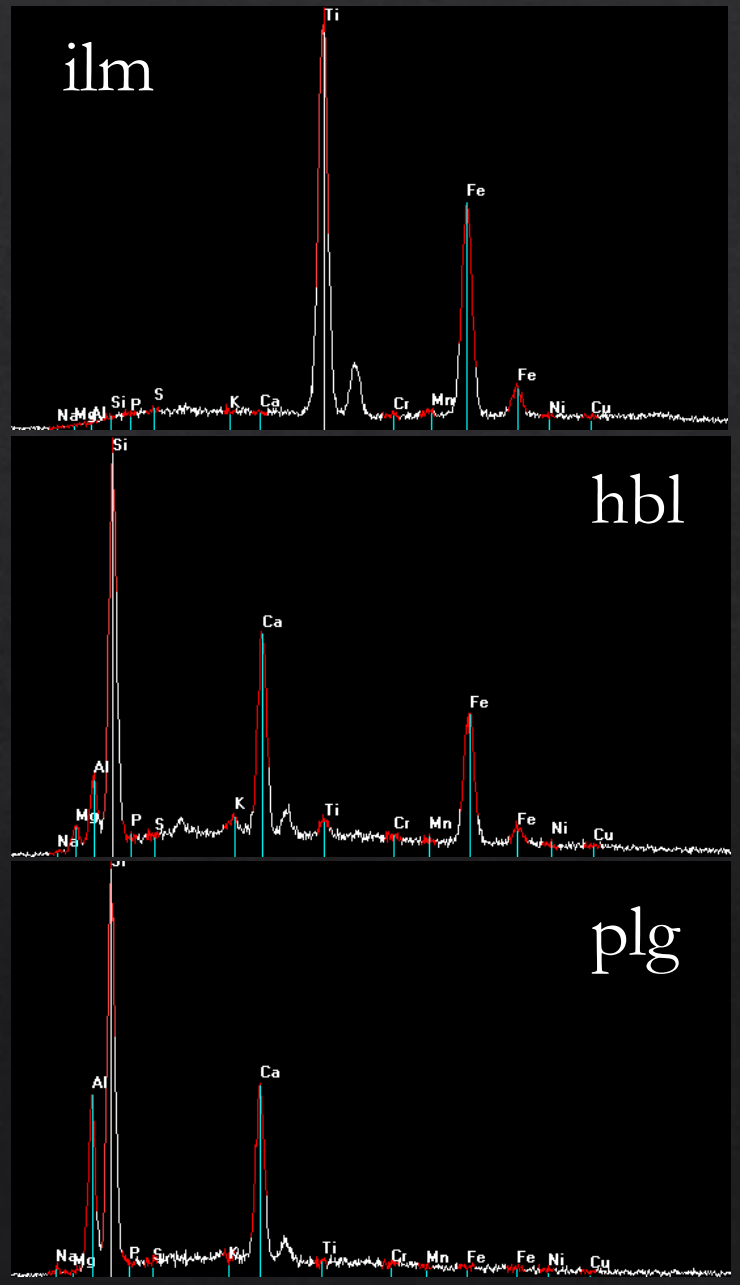

EDS spectra

Qualitative and semi-quantitative analysis with WDS

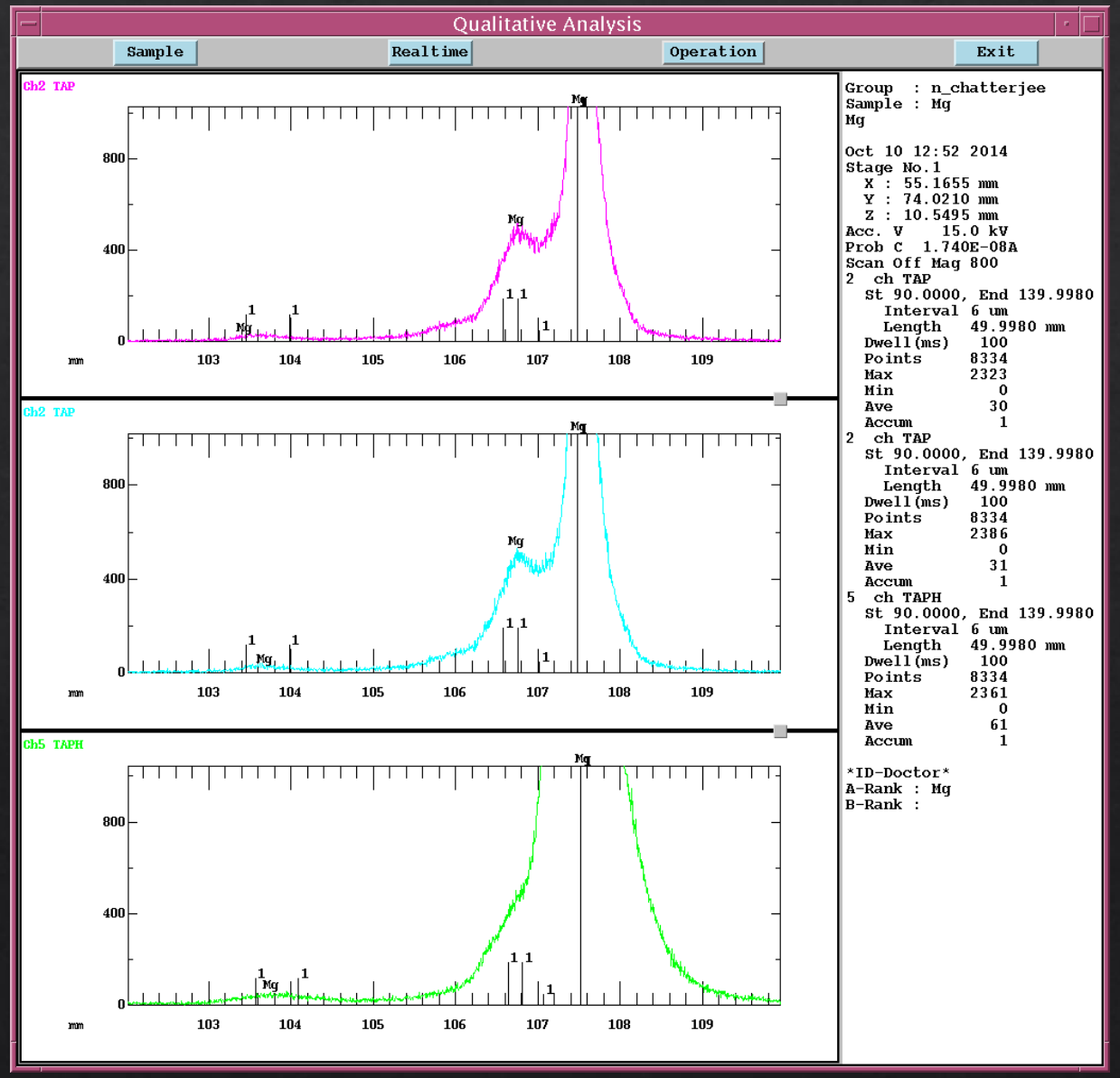

Standard X-ray intensity measurement (calibration)

- Calibration is performed on standards, a set of homogenous, natural or synthetic compounds with well known composition

- A good calibration is essential for accurate analysis.
  It eliminates systematic errors (fixed but unknown offsets from the actual values in all measurements)

- After primary calibration, secondary standards (working standards) are analyzed to make sure the results are as expected

X-ray intensity measurement: peak minus background

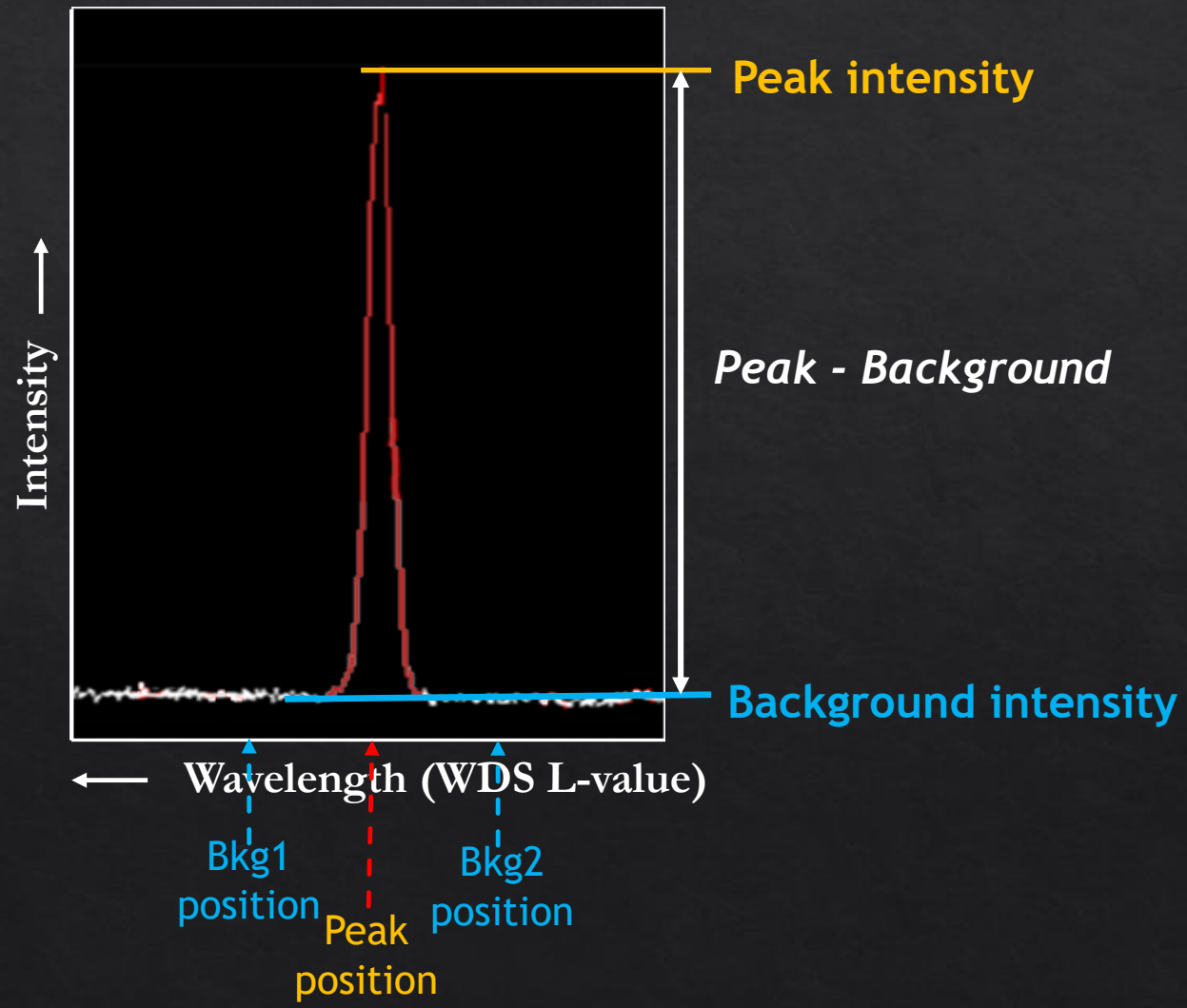

Long counting times are used to achieve statistical precision

X-ray background measurement: special case

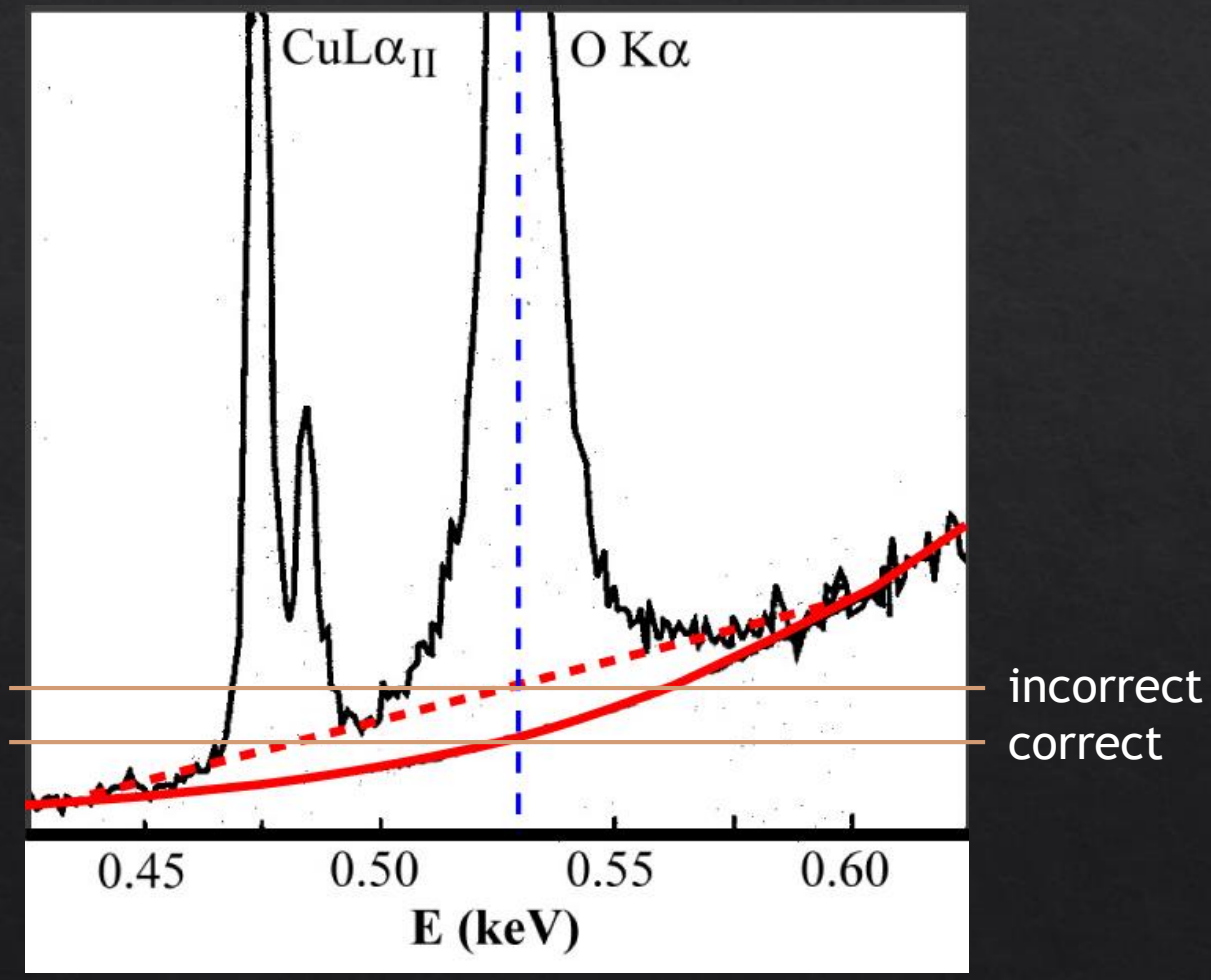

Peak overlap in X-ray spectra

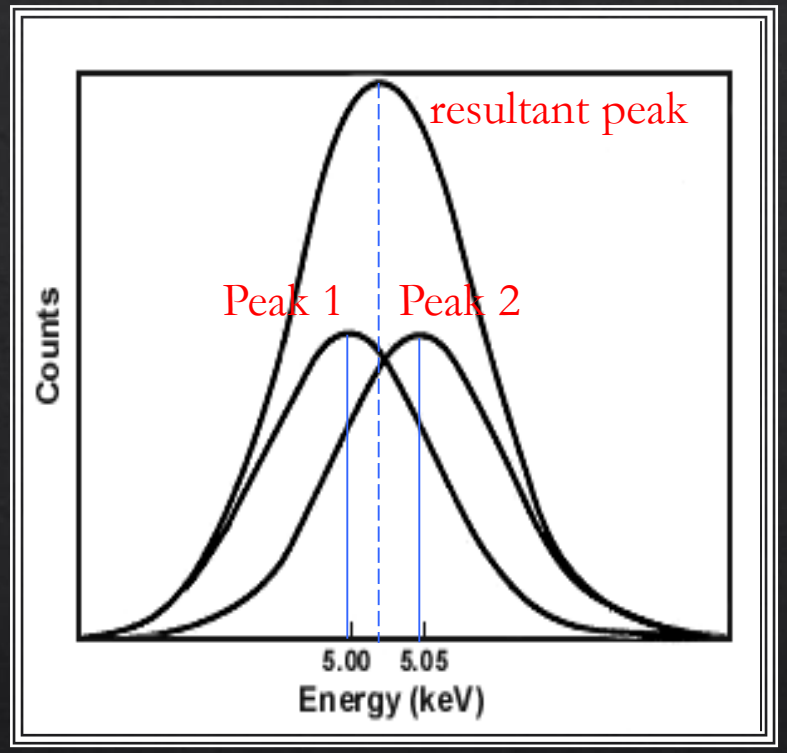

Overlap between Peak 1 and Peak 2 results in a broad single peak

PHA reduces peak and background overlaps

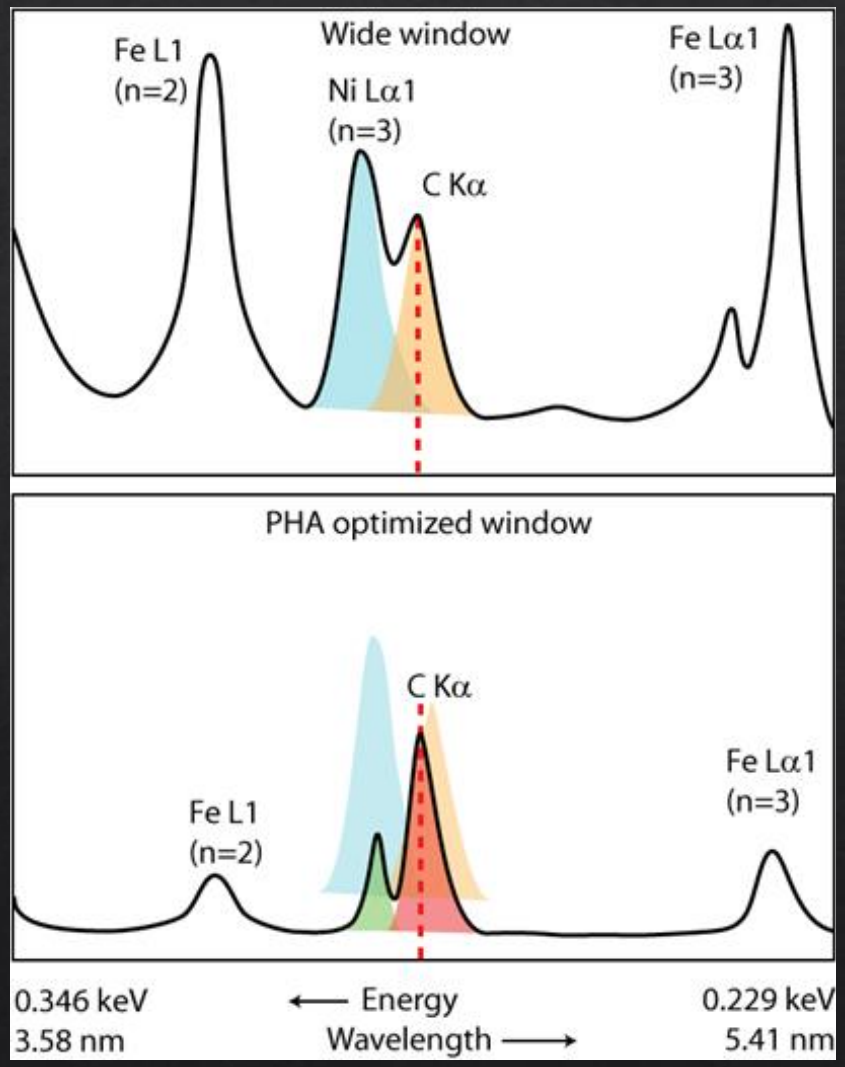

Wide open SCA voltage window

PHA optimized SCA voltage window

Spectrum of carbon steel

Peak overlap corrections for Ti-V-Cr

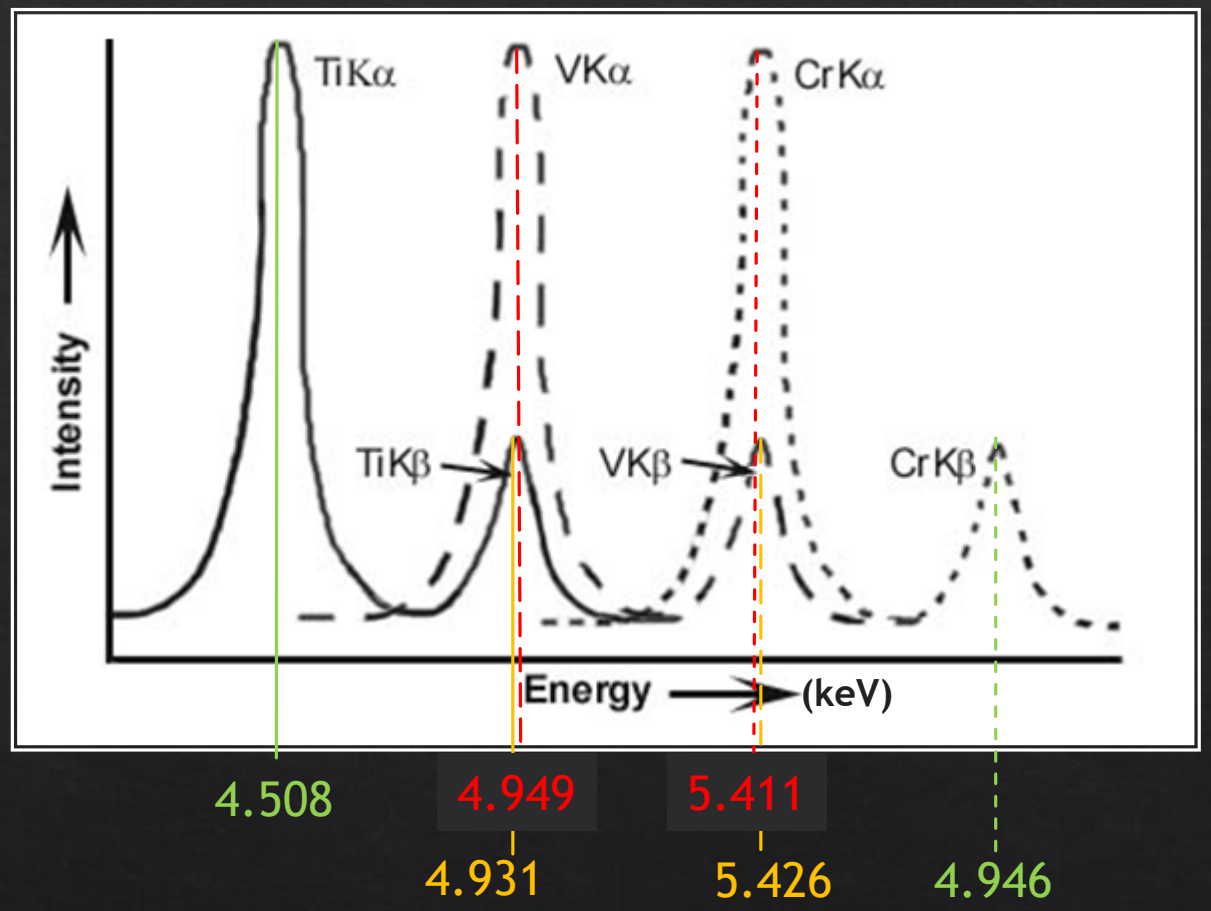

$$I^{\text{corr}}_{\text{VK}\alpha} = I^{\text{meas}}_{\text{VK}\alpha} - \frac{I^{\text{meas}}_{\text{TiK}\alpha}}{I^{\text{Ti - std}}_{\text{TiK}\alpha}} I^{\text{Ti - std}}_{\text{VK}\alpha}$$

$$I^{\text{corr}}_{\text{CrK}\alpha} = I^{\text{meas}}_{\text{CrK}\alpha} - \frac{I^{\text{corr}}_{\text{VK}\alpha}}{I^{\text{V - std}}_{\text{VK}\alpha}} I^{\text{V - std}}_{\text{CrK}\alpha}$$

Peak resolution with LIF

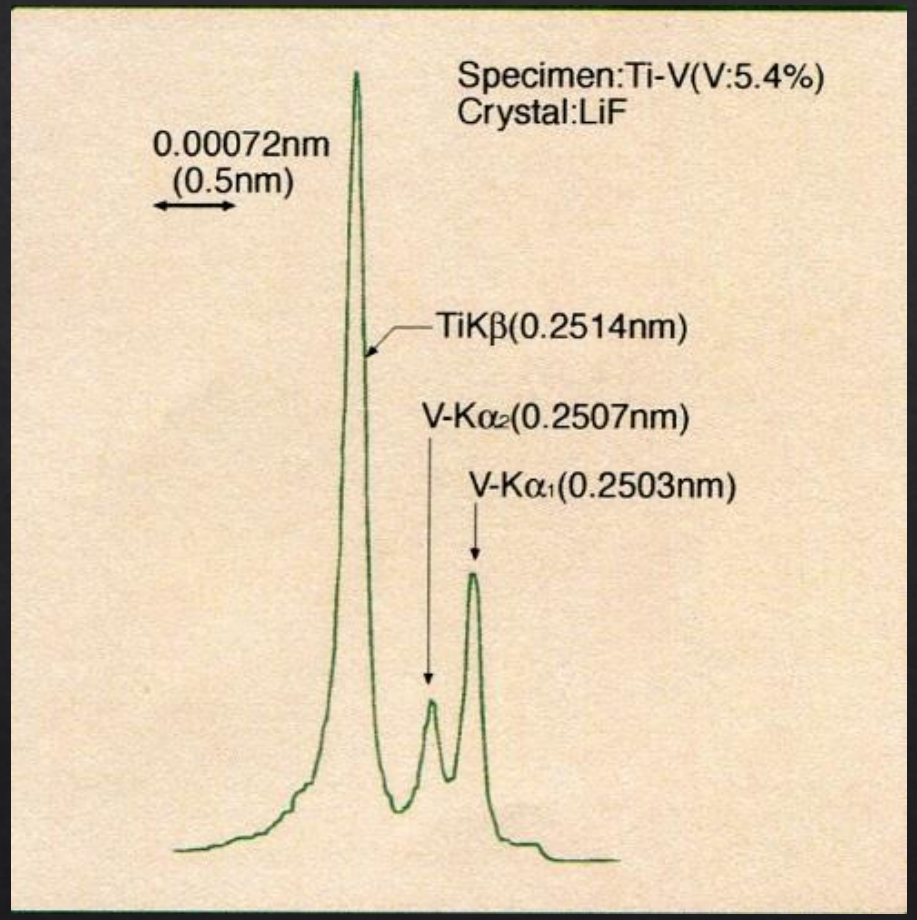

XCE type spectrometer with Xe counter

LIF is able to resolve the TiKβ, VKα_1 and VKα_2 peaks

EPMA Quantitative analysis

X-ray intensity is proportional to the concentration, $C \propto I$

$$\frac{C_i}{C_{(i)}} \propto \frac{I_i}{I_{(i)}}$$

C_i , I_i : concentration and intensity in sample

$C_{(i)}$, $I_{(i)}$: concentration and intensity in standard

$$\frac{I_i}{I_{(i)}} = k_i \,(\text{k-ratio})$$

$$\frac{C_i}{C_{(i)}} = k_i \cdot [\text{ZAF}]_i$$

Matrix (ZAF) corrections

Z : atomic number correction

electron back-scattering difference between standard and sample

A : absorption correction

absorption of x-ray inside the sample

F : fluorescence correction

fluorescence of x-ray due to absorption of a higher energy x-ray inside the sample

X-ray absorption

$$I = I_0 \exp^{-\left(\mu/\rho\right)(\rho x)}$$

$$= I_0 \exp^{-\left(\mu/\rho\right)(\rho z \, cosec \, \psi)}$$

$$I = I_0 \exp^{-\left(\mu/\rho\right)(\rho x)}$$

$$= I_0 \exp^{-\left(\mu/\rho\right)(\rho z \, cosec \, \psi)}$$

I : Intensity emitted

I_0 : Intensity generated

μ/ρ : mass absorption coefficient

ρ : density

z : depth

ψ : take-off angle

Mass absorption coefficient, $(\mu/\rho)_{absorber}^{x-ray}$

Variation of $(\mu/\rho)_{Ni}^{x-ray}$ as a function of incident X-ray energies

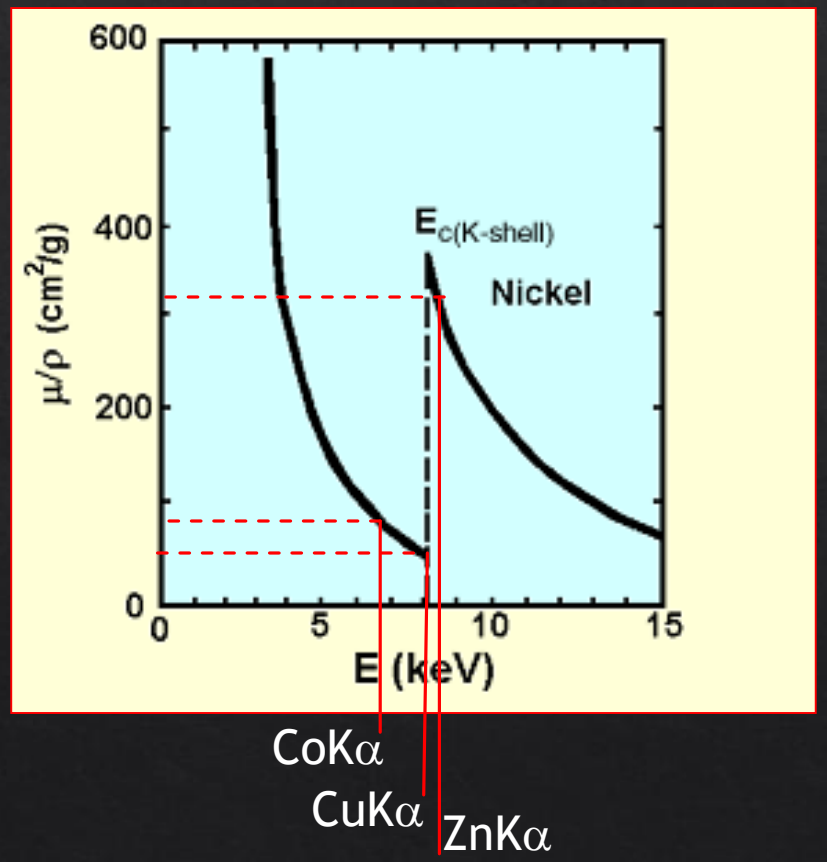

Sharply increases at the critical excitation energy of Ni K-shell, $E_{c(Ni\ K\text{-}shell)}$

Any X-ray with a slightly higher energy than $E_{c(Ni\ K\text{-}shell)}$ (e.g., ZnKα) is efficiently absorbed as it ionizes the Ni K-shell and generates (fluoresces) NiKα

Depth-distribution of x-rays: $\phi(\rho z)$ function

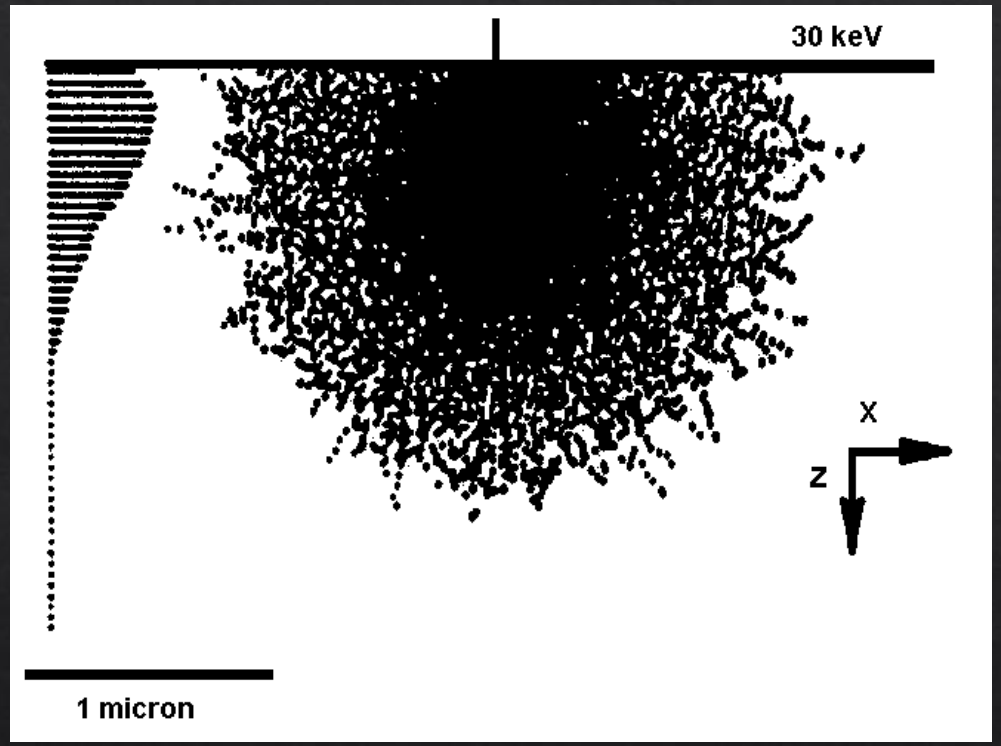

Intensity from each layer normalized by intensity from a free-standing layer of the same material

$\phi(\rho z)$ correction

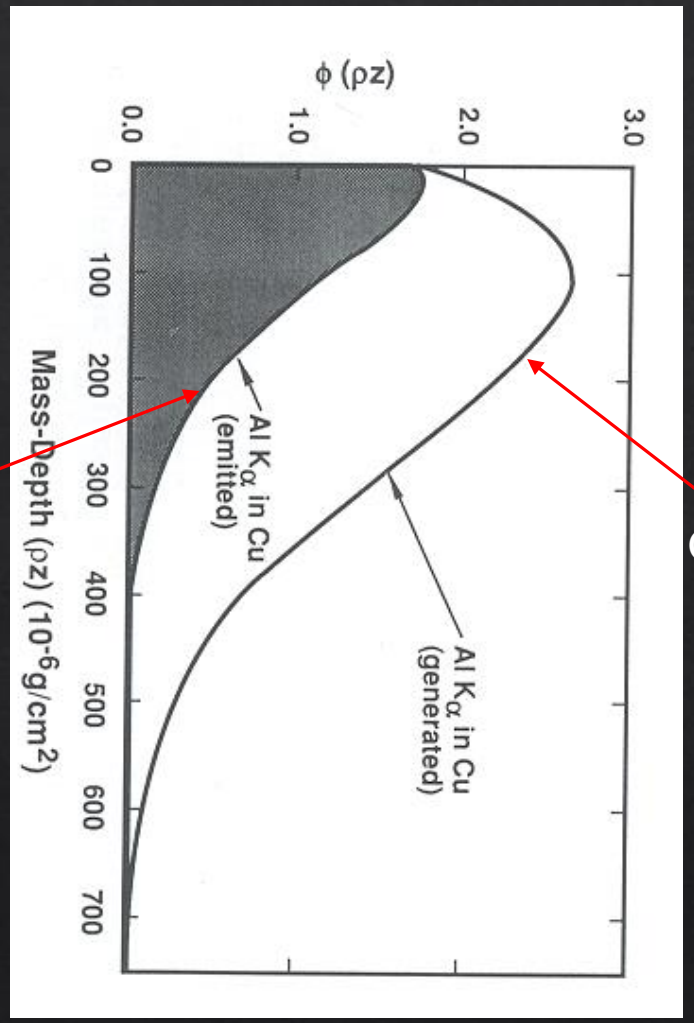

Emitted (after absorption) Intensity curve

Generated Intensity curve

AlKα is efficiently absorbed by Cu in Al-Cu alloy

X-ray fluorescence

A consequence of X-ray absorption when

$$E_{incident\ X\text{-}ray} > E_{c(absorber\ shell)}$$

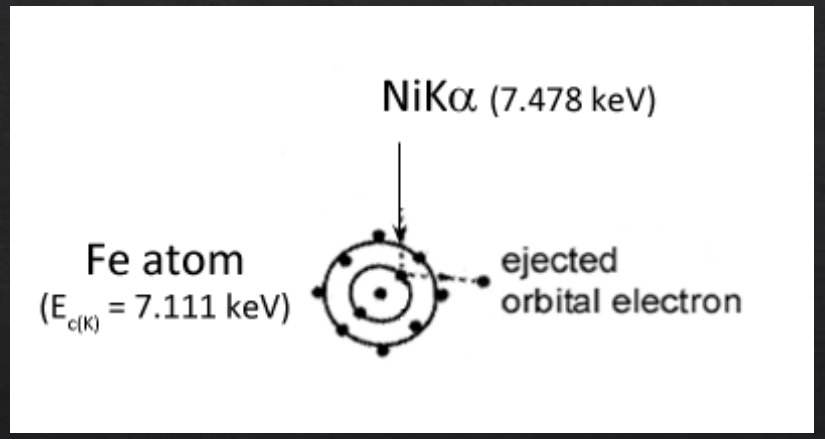

- NiKα is absorbed by Fe atom
- FeKα is fluoresced

X-ray absorption and fluorescence

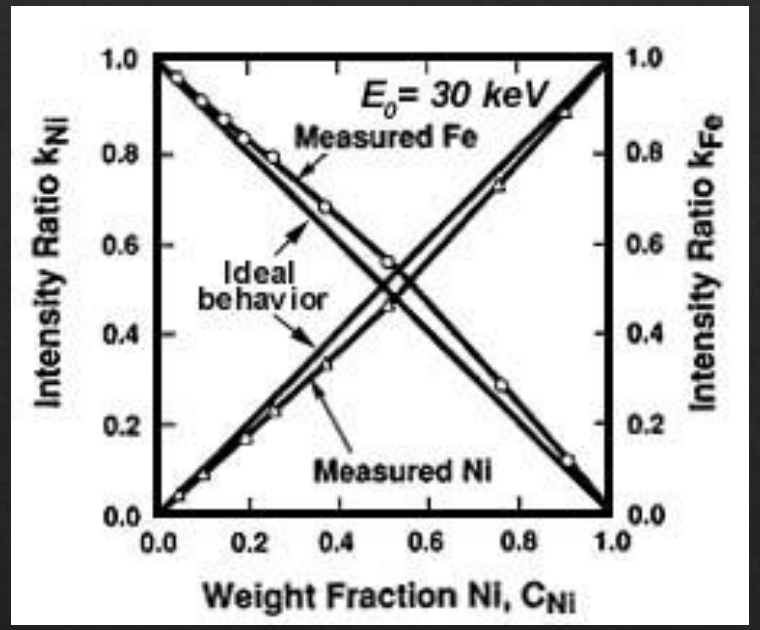

- NiKα is absorbed by Fe atom
- FeKα is fluoresced

Matrix correction flowchart

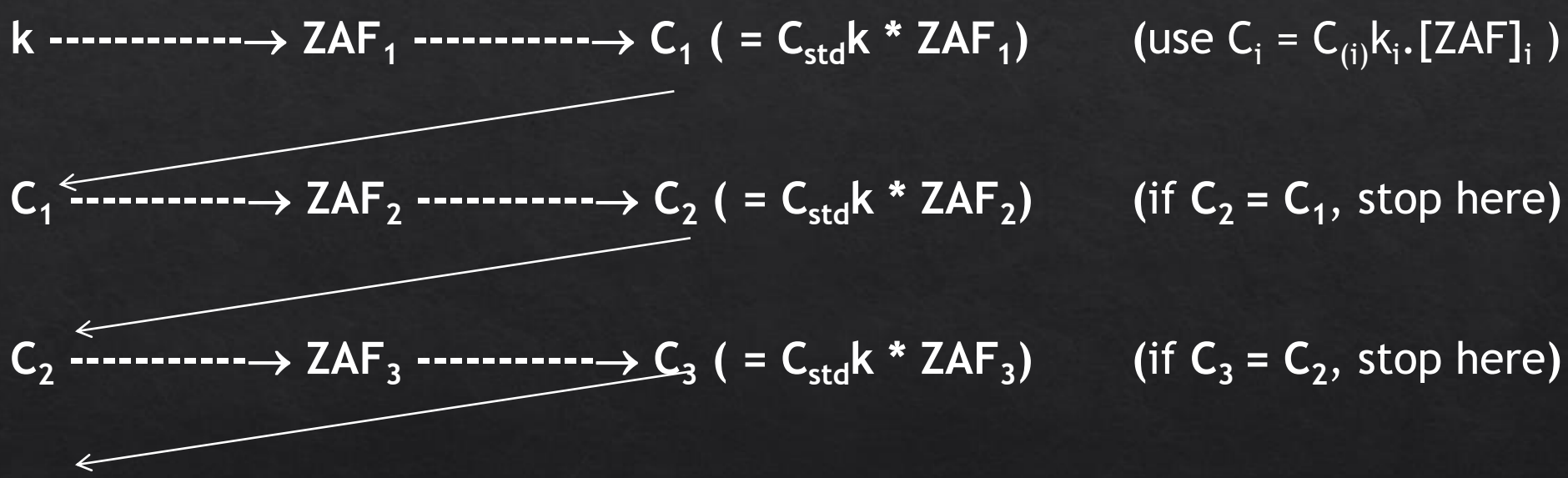

Compositional imaging with X-rays: elemental mapping

- **Beam-rastered image:**

  electron beam rasters over the area to be imaged

- **Stage-rastered image:**

  electron beam is stationary, stage moves

Background in x-ray image

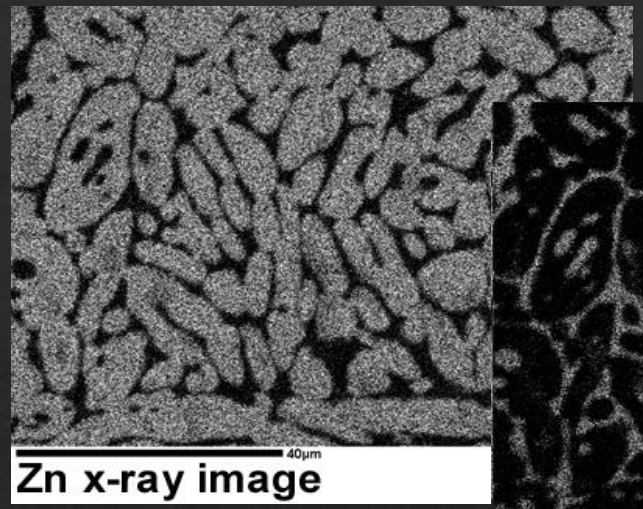

Zn-Sn composite

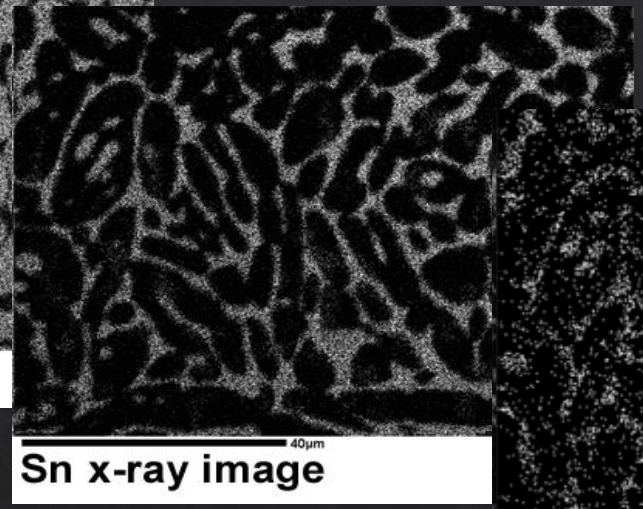

Background image

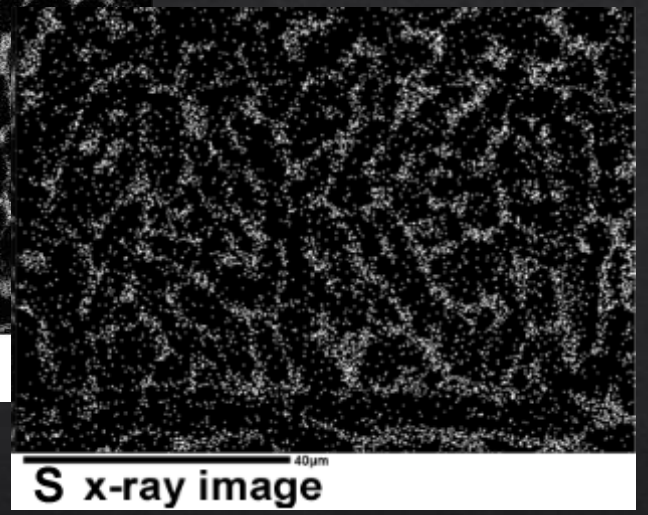

Zn-rich phase (low Z)

Sn-rich phase (low Z)

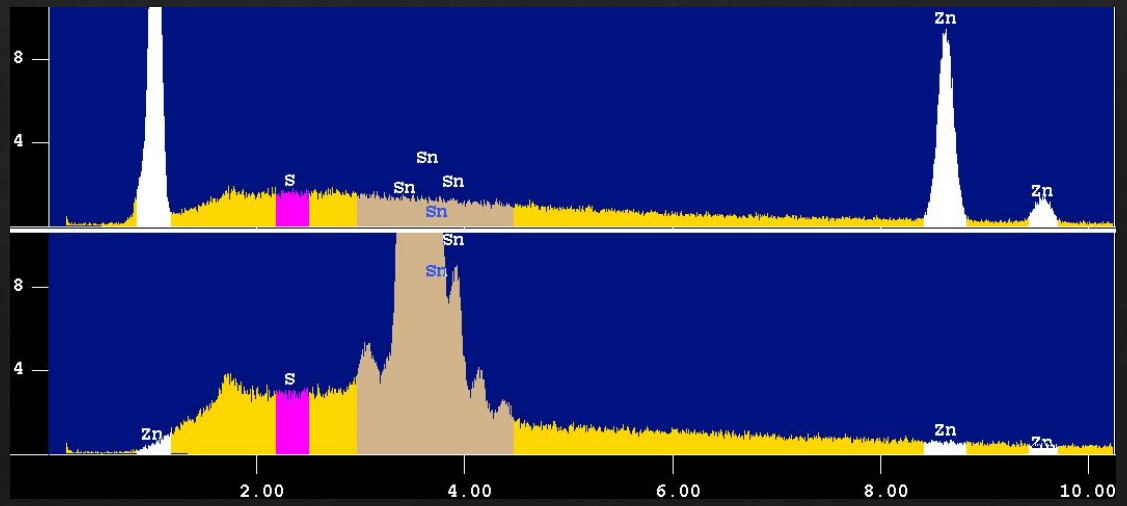

X-ray defocusing in beam-rastered image

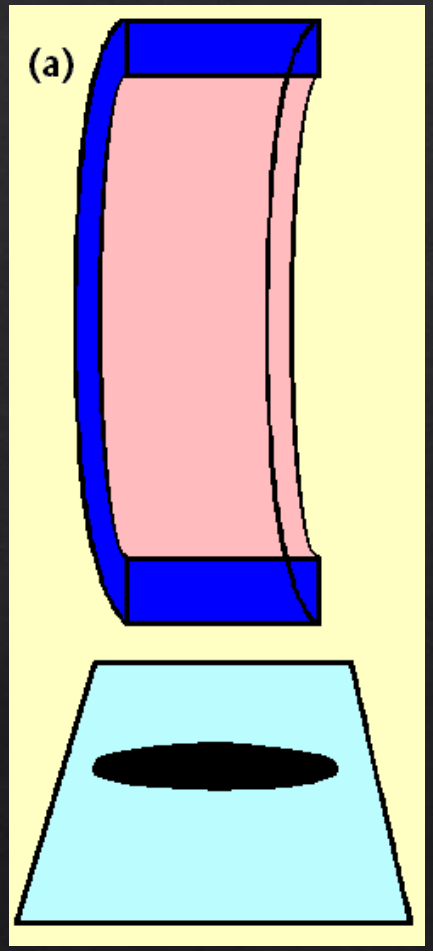

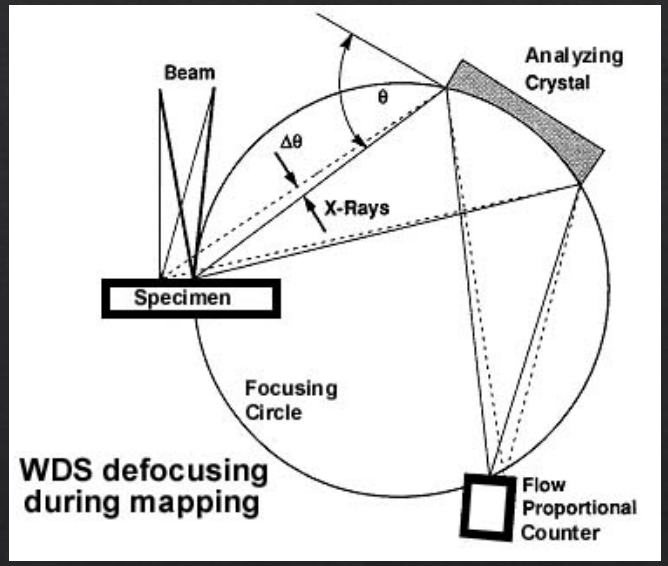

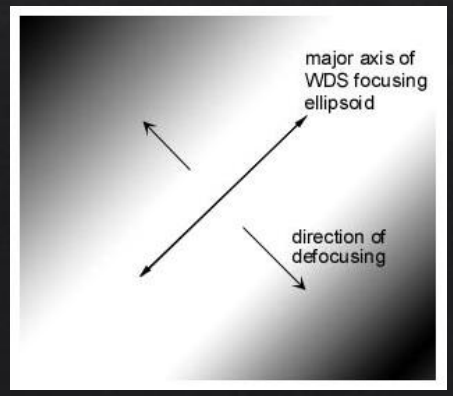

Image quality of X-ray maps

Two factors:

- Image resolution:

  number of points measured within the imaged area

- X-ray Signal:

  beam current and counting (dwell) time per point

Combined WDS and EDS X-ray mapping

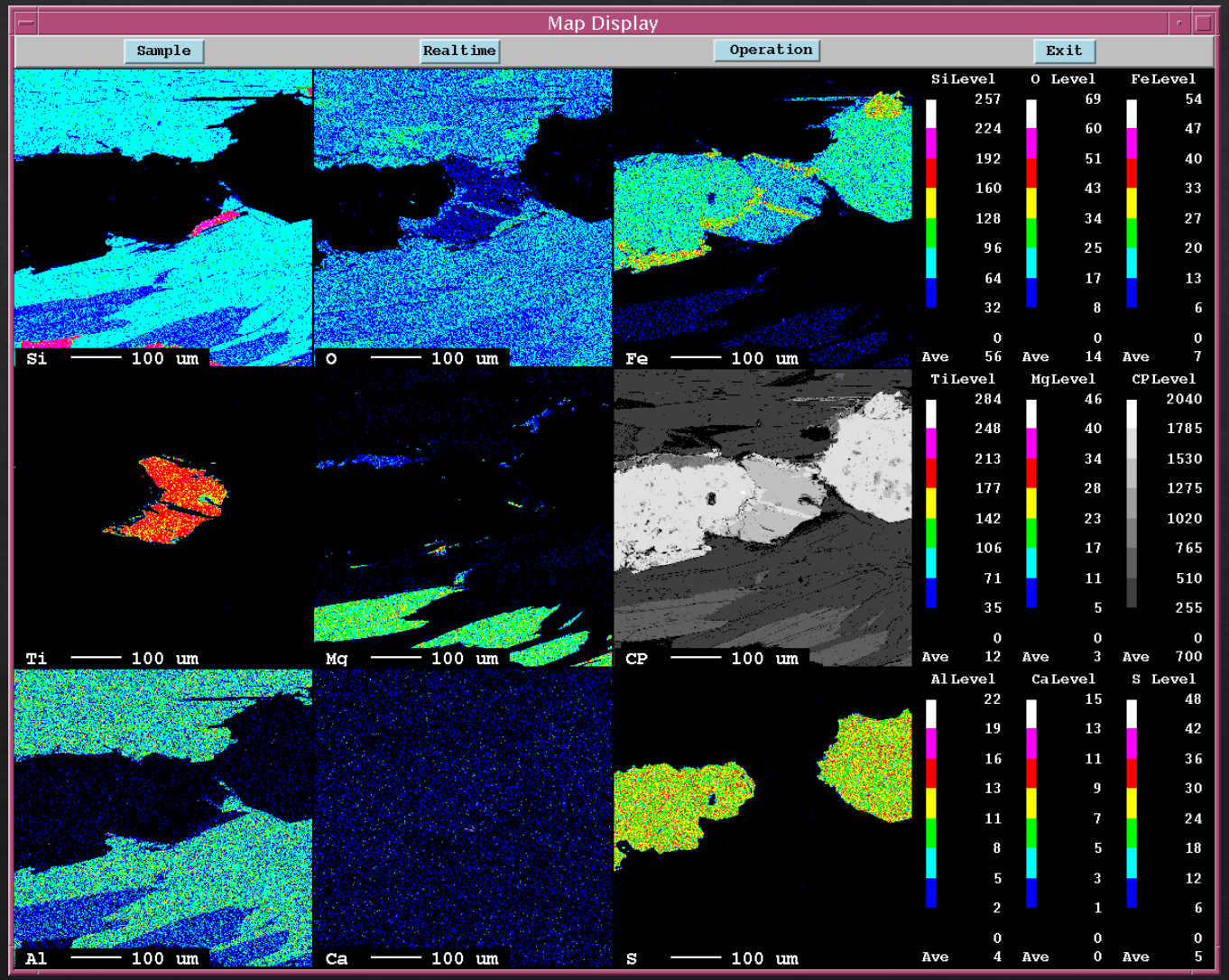

Combined BSE, CL and X-ray mapping